博士論文

Development of Novel mRNA Delivery Systems based on Flexible Biodegradable Block Copolymers

(効率的な mRNA 送達に向けた
柔軟な生分解性ブロック共重合体の設計)

宮崎　拓也

Preface

My results for three years in Cabral laboratory are summarized in this doctoral dissertation. In 2016, Prof. Cabral permitted me to join his laboratory and we developed mRNA delivery systems based on flexible biodegradable block copolymers to treat intractable diseases including pancreatic cancer by surface functionalization with ligand. We hope that all data in this thesis will be published in paper and after further development of our systems, it will be translated into clinical applications to treat patients with intractable diseases.

I would like to appreciate those who helped me to finish this Ph. D. dissertation. First, I appreciate Prof. Horacio Cabral for supervising me for three years and Prof. Satoshi Uchida for supervising and helping me with mRNA experiments. Second, I thank all staffs and students in Cabral laboratory for active discussion. Third, I appreciate my parents and friends for all their supports. Note that, without special helps from Prof. Kazunori Kataoka, Prof. Kouhei Tsumoto, Dr. Satoru Nagatoishi, Dr. Yu Matsumoto, Dr. Kazunori Igarashi, I was not able to complete this thesis.

<div align="right">

Takuya Miyazaki

Department of Bioengineering, Graduate School of Engineering

The University of Tokyo

March 2019

</div>

Table of contents

Chapter1

General introduction

1.1. Messenger RNA (mRNA) delivery

Messenger RNA (mRNA) is a candidate of therapeutic oligonucleotides because therapeutic protein is produced over several orders of magnitude [1, 2, 3] to treat gene diseases. Also, mRNA has several advantages over plasmid DNA (pDNA) and viral vector-based gene therapies, which is transcribed to mRNA to produce therapeutic protein, such as no need to enter the cell nucleis, which is issue in the case of non-deviding cells [4], and no concern to induce irreversible insertional mutagenesis [4]. However, because of its fragile nature to be degaraded by RNases and its immunogenicity to trigger tall-like receptors, resulting incresed cytokine level and associated side effects, the application of naked mRNA is limited though it has high potentials to cure intractable gene diseases.

To construct stable mRNA without immunogenicity, chemical modifications of mRNA [5], such as pseudouridine, 2-thiouridine, 5-methyluridine, 5-methylcytidine or N6-methyladenosine (**Figure 1**). By increasing biocompatibility of mRNA, gene expression in the cytoplasm was enhanced to show therapeutic effects against genetic diseases *in vivo* [6, 7]. In the case of gene related diseases where relatively small amount of protein shows therapeutic outcomes [8], this strategy with local injections seems to be promising. However, more intractable diseases which need a lot of protein to cure [9] or controlled biodistribution with targeting ability of specific cell population and organs [9] limit the broad application of mRNA with chemical modifications.
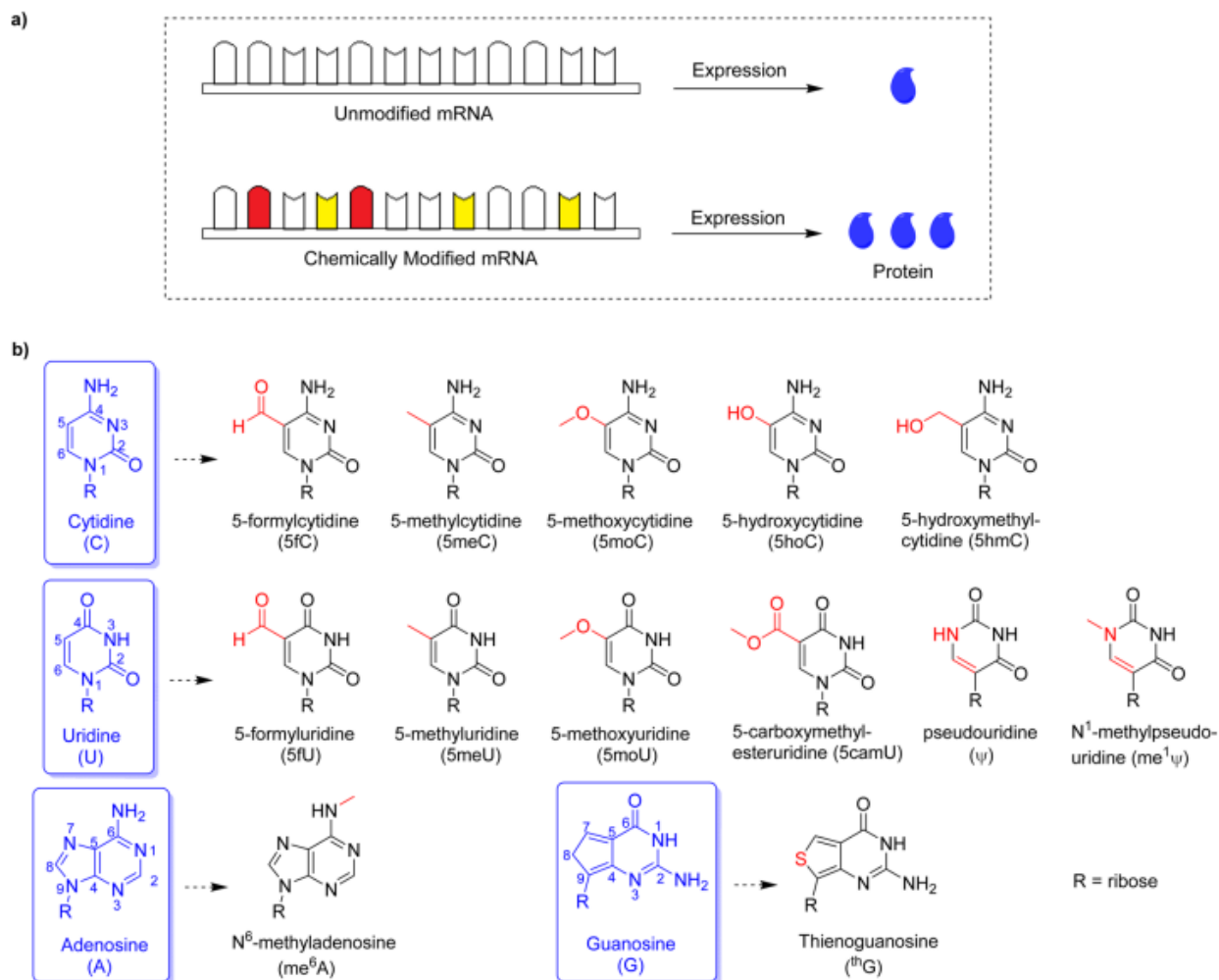
Figure 1. *The effect of chemical modifications of mRNA and chemical structure of modified bases in mRNA [5].*

Drug delivery system (DDS) is a promising way to control the accumulation with prefer biodistribution and timing of treatment [10]. To deliver mRNA, three strategies are being developed, including physical method to enhance the cellular uptake of mRNA in the cells of interest, viral-based nanocarrier to utilize its benefit promoting uptake of encapsulated gene, and non-viral based drug delivery system with lipid or synthetic polymers. Physical method in the case of mRNA, electropolation is suitable to floating cells like hematopoietic cells [11] to

collect from patient serum before the treatment of immune cells, resulting activated immune system [12]. However, electropolation is sometimes invasive to change the cell property or to disrupt cell membrane completely [13-15]. To develop non-invasive system, viral system was developed originally for pDNA and it was applied for mRNA delivery and effective therapies were reported previously [16-18]. Nevertheless, because of its inherent genes, which may be inserted to host genome or reversely transcribed to DNA to induce mutagenesis, and difficulties to control gene expression of loaded mRNA [19].

To develop the alternative system of novel viral-based DDS, lipid-based mRNA delivery has emerged (**Figure 2**) [20, 21]. As a nanocarrier with lipid, 1,2-dioleoyl-3-trimethylammonium-propane (DOTAP), commercially available liposomes and lipid nanoparticles (LNPs) with combinatorial chemistry have been developed. Before using DOTAP, its derivatives, N-[1-(2,3-dioleyloxy)propyl]-N,N,N-trimethylammonium chloride (DOTMA) was engineered to encapsulate mRNA by electrostatic interactions, resulting in high efficacy [22, 23], which would be compromised by the emergence of DOTAP [24]. As commercially available formulations, Lipofectamine and Dreamfect Gold were a candidate to load mRNA and showed higher gene expression than polymer-based formulations *in vitro* [25, 26]. Also, GL62A was originally developed for pDNA delivery [27-30], which is under the clinical trials, and it was studied to deliver mRNA with high efficacy [31]. LNPs are comprising phospholipid to form bilayer structures, PEG derivatives to avoid aggregation and non-specific interaction with cell surfaces, and ionized lipid to interact with mRNA by electrostatic interactions [32]. 1, 2-dilinoleyloxy-3-dimethylaminopropane (DLinDMA) [33, 34], C12-200 [35, 36] and 1,3,5-triazinane-2,4,6-trione (TNT) derivatives [37] were novel candidate of LNPs and though they were originally developed for siRNA delivery, efficient delivery of mRNA was achieved with

small modification of its chemical structure and composition [38]. However, though many formulations were coated with hydrophilic PEG, because of hydrophobic lipid or its relatively low stability in biological conditions, it seems to be difficult to control the biodistribution without any unfavorable accumulation in healthy tissues [39-41]. Therefore, polymer-based strategy would be one of the promising way to avoid non-specific interaction with healthy tissues.
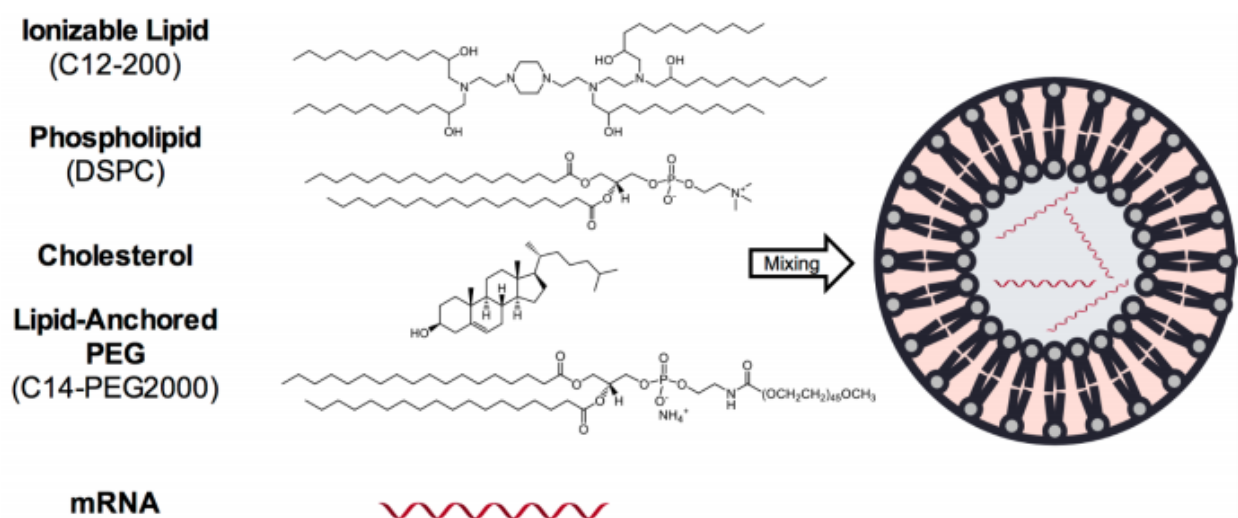
Figure 2. Preparation of lipid nanoparticles (LNPs) by ethanol dilution method [35].

1.2. Polyion complex (PIC) micelles

Polyion complex (PIC) micelles have been developed to deliver nucleic acids including antisense oligonucleotides [42], pDNA [43], siRNA [44] and mRNA [45]. To encapsulate negatively charged oligonucleotides, block copolymers comprising hydrophilic segments and polycation segments were engineered to form supramolecular nanoarchitecture (**Figure 3**) [46]. Nucleic acids with negative charges are recognized by oppositely charged polycation segments by electrostatic interactions [47] and hydrophilic segments prevent it from forming aggregation to

separate each PIC micelles. Many materials as hydrophilic coronas were extensively studied and PEG [48], poly(2-oxazoline)s [49], betain polymers [50] and poly(saccharides) [51] are the candidate for PIC-based DDS. As a cationic segment, poly(ethylene imine) (PEI) [52] have been developed and PEG-poly(L lysine) (PEG-PLL) is under the clinical trials for pDNA delivery. Like PEG-PLL, PEG-poly(amino acids) (PEG-PAA) is one of the novel carrier of nucleic acids because biodegradable segments of PAA fit in medical applications to increase biocompatibility [53]. For antisense oligonucleotides delivery, PEG-PLL was used to form spherical PIC micelles with sharp size distribution and showed significant gene expression *in vivo* [54]. In the case of pDNA with various topological shapes, PIC micelles showed several morphologies including spherical particles and lod-like micelles by changing salt concentrations to show outstanding transcriptional efficacy because of its circular shapes fitting the movement of transcriptional proteins [55]. For systemic siRNA delivery, PEG-PLL with chemical modifications was adapted to load siRNA before closs-linking to treat cancer with therapeutic siRNA [56]. Instead of PEG-PLL, PEG-poly(aspartate-diethlenetetramine) (PEG-PAsp(DET)) has emerged as a novel block ionomers with the ability of endosomal escape, termed proton sponge effects where P(Asp(DET) segments change its protonation states in acidic endosome from neutral physiological conditions [57]. For mRNA delivery, PEG-PAsp(DET) showed significant translation efficacy not only *in vitro* but also *in vivo* [45].

Note that PIC micelles are not only cargos for therapeutic agents but probes to trace the pharmacokinetics and pharmacodynamics by intravital conforcal laser scanning microscope (IV-CLSM). Instead of nucleic acids, block ionomers with polyanion segments were engineered to form PIC micelles by electrostatic interactions [46] before cross-linking of the core of micelles not to dissociate *in vivo* harsh environments. With this highly stabilized probes, glucose ligand

installed PIC micelles showed high penetration of brain blood barrier (BBB) to clarify the effect of glucose installation on receptors in BBB [58]. Moreover, by precise tunning of the length of hydrophilic segments, the formation of polymer version of liposome, named PICsome, was confirmed to check the size effect on the biodistribution of PICs [59].
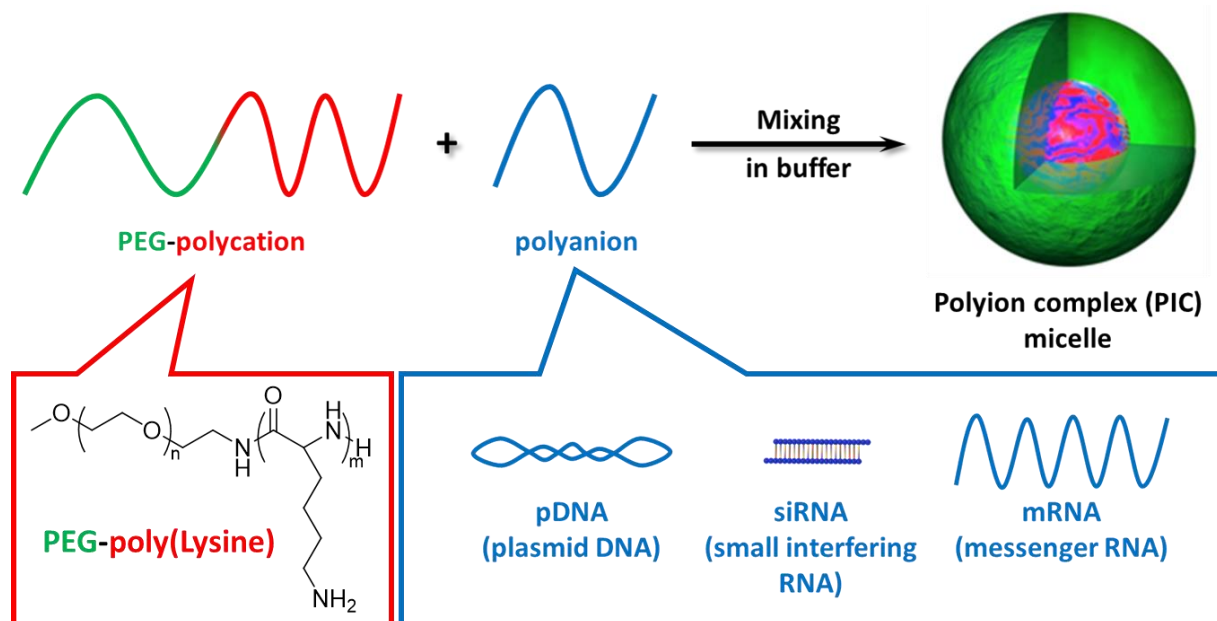
Figure 3. The formation of PIC micelles from block ionomers and therapeutic oligonucleotide.

1.3. Thermodynamics of PIC micelles

PIC formation can be explained by thermodynamical parameters including enthalpy and entropy (**Figure 4**) [46]. In the case of novel polymeric micelles like cisplatin-loaded micelles [60] and dichloro(1, 2-diaminocyclohexane)platinum(II) (DACHPt)-encapsulated micelles [61], the driving force of micelle formation is mainly decrease of surface area of block copolymers to decrease the formation enthalpy of micelles. In aquaous conditions, regarding mixing enthalpy of water phase and hydrophobic segments in block copolymers, hydrophilic segments appear on the surface of micelles to separate two phases. However, because of ionizable segments in block

ionomers, the driving force of PIC micelles is not only decrease of surface area but also the formation of ionic pairs between polycation and polyanion to release corresponding water, which may increase the entropy of free water, resulting quite low critical micelle concentration (CMC) for high coloidal stability.

The formation of unimodal PIC micelles without any aggregation of each PIC is explained by two factors to decrease the association number of block ionomers. After the increase of the association number of clock copolymers, the steric hyndrance between neiboring hydrophilic segments was increased to prevent it from aligning in proper way considering mixing enthalpy of water phase and hydrophobic segments. Also, the conformational enthalpy is a key to understand the adjustment of the association number of polymers. After increasing the association number, not only hydrophilic segments but also hydrophobic segments start to stretch because of excluded volume effects to increase the conformational entropy.

Once PIC micelles are formed by electrostatic interactions, loss of enthalpy and gain of entropy were observed by ITC measurements [62] and these thermodynamical parameters may be related to biological stability in vivo. Interestingly, though siRNA and mRNA are both similar RNA analogies, the conformational entropy of RNA strand played an important role in PIC micelle formations [63], which may involve in the gap of siRNA and mRNA formulations where we need further optimization of chemical structures and composition of carrier for mRNA delivery, which was originally designed for siRNA [64].
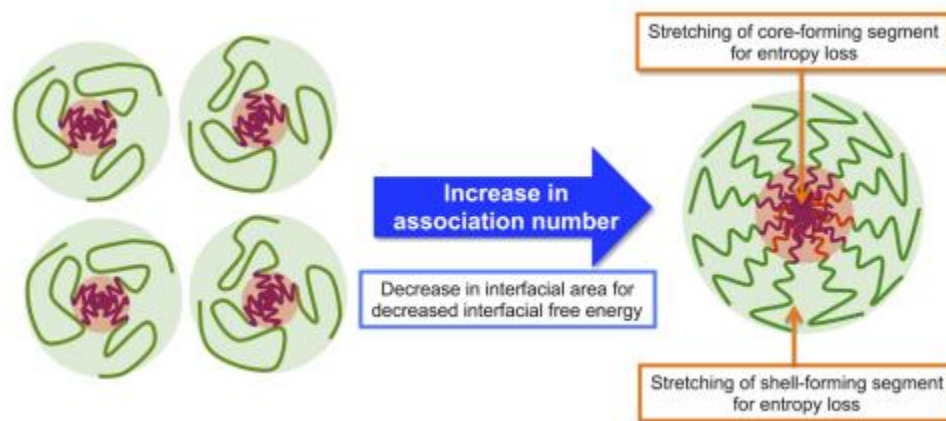
Figure 4. *The critical thermodynamical parameters to determine the association number of block copolymers [53].*

1.4. Protein-nucleic acids interaction

The interaction between nucleic acids and protein was found not only in prokaryotes but also in eukaryotes [65] and the protein was encoded by the genome to control tracscription of DNA and translation of RNA. The hydrogen bonding is a candidate to understand the interaction between nucleic acids and protein, followed by hydrophobic interactions and electrostatic interactions [66, 67].

As a hydrogen bond interaction, amino groups and hydroxyl groups play an important role to interact with oxygen, resulting in specific recognition of oligonucleotides by protein [68]. Such functional groups in the side chain of protein or bases in nucleic acid are essential for the interaction though amine and hydroxyl groups is the backbone or nucleic acids are important for the stability and the secondary structures of each component [68]. In addition to conventional hydrogen bonds, the interaction between alkyl chains and oxygen [69], and water-mediated interaction [70] have been shown as an important factor to understand the recognition of protein. Methylene chains in the sugar of DNA [69] and RNA [71] frequently appear in the interaction

with oxygen in amino acids. Water molecules involve in the interaction to reduce the electrostatic repulsion between phosphates in nucleic acids and ionic amino acid residues in protein to increase the contact area of two components [70]. The electrostatic interaction is also a key for deep understanding of the interaction between ionic residues and phosphate groups [70]. The ionic interactions enhanced the stability of complexes [72] and may be related to protein folding before the complexation [73].

For deep understanding of the interaction of protein and nucleic acids, bioinformatic approaches are helpful to clarify which residue or part of nucleic acids join the formation of complex [74]. Ionic residues (lysine, arginine, aspartate, aspartic acids, histidine, glutamic acids) formed electrostatic interactions with nucleic acids and as hydrophobic residues, tryptophan, tyrosine, serine and threonine also joined the complexation with nucleic acids (**Figure 5**). In the side of nucleic acids, regarding the 3D structure of complex from protein data bank (pdb), bases interact with arginine, histidine and aspartic acids, phosphates interact with lysine, threonine, serine, tryptophan and tyrosine by electrostatic interactions and hydrogen bonds.
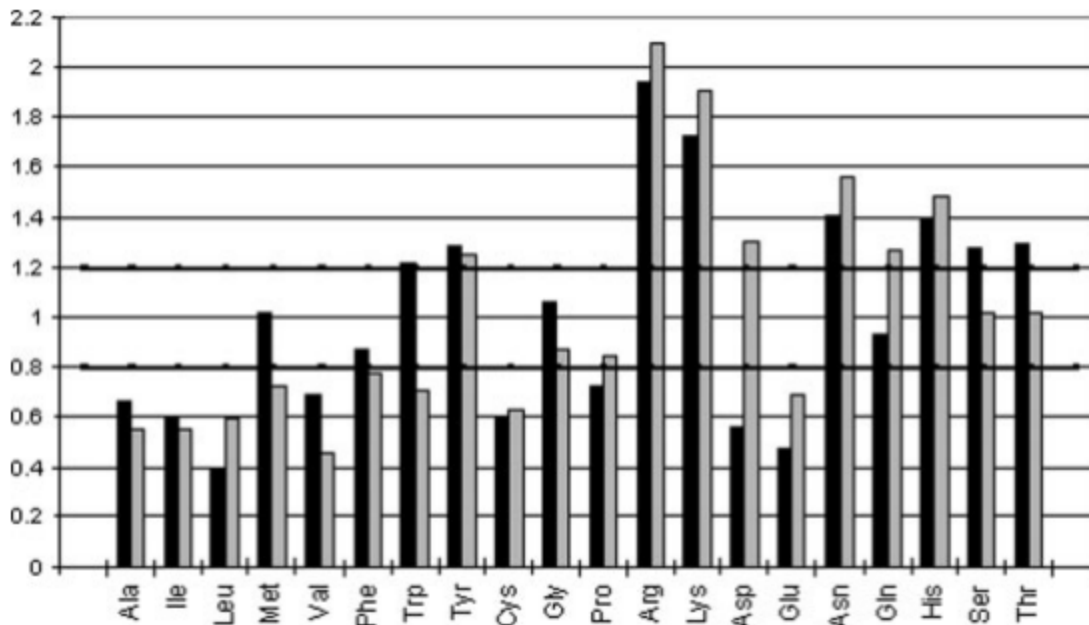
Figure 5. *The propensity of amino acid residues in the complex of protein and nucleotides.*

More than 1.2 means favor residues for the interaction with nucleic acids [74].

1.5. Active targeting with ligand installation

Active targeting is the strategy to enhance the accumulation of conjugated drugs or encapsulated therapeutic agents [75]. Diverse ligand molecules including antibodies, antibody derivatives, aptamers and small molecules have been developed (**Figure 6**) [75]. For active targeting, ligand molecules are conjugated to drugs *via* cleavable bonds with spacers not to decrease the activity of conjugated drugs and to increase the mobility of installed ligands. In the case of nanomedicine, ligands motifs are installed on the surface of the nanoparticles to guide it to targeted tissues with decreased accumulation in healthy tissues. To design ligand molecules, the distribution of receptor expression, receptor location and specificity of ligand to receptors are criteria for the development of ligand-based DDS.

The expression level of receptor is important to maximize the accumulation of drugs in targeted tissues and to minimize the accumulation of drugs in untargeted tissues. To avoid the accumulation in healthy tissues, at least 3 time higher expression in targeted tissues than healthy tissues is required [76] and when we use low cytotoxic agents, expression level of receptors can be compromised. In the case of relatively high cytotoxic drugs, the accumulation in healthy tissue should be decreased or completely inhibited to keep patients alive. However, comparing with conventional DDS or passive targeting system where drugs accumulate in targeted tissues and healthy tissue equally, active targeting always show reduced cytotoxicity against healthy organs because of relatively high ratio of the accumulation in targeted tissues and non-targeted tissues. In addition to relative expression level of receptors, absolute expression level and isoforms of targeted receptors should be considered to design ligand molecules.

After finding which receptor to target, the location of receptors should be considered to enhance the cellular uptake of conjugated therapeutic agents. In general, receptors are located not only on the surface of the cells but also inside the cells and to enhance the cellular uptake of therapeutic agents, receptors on the cell membrane seem to be proper target of ligand molecules [77]. Though receptors in cytoplasm are targetable to control the fate of the therapeutic agents after the cellular uptake, such a controlled distribution after the cellular internalization can be achieved with hydrophobic ligands and drugs, which may result in unspecific accumulation [78]. In the case of prodrug, which is activated only in targeted tissues, off-target release of therapeutic agents inside the cells is difficult to reduce and targeting of the cell surface is necessary to promote the internalization of drugs.

After identifying receptors on the cell membrane, the binding affinity of ligands to receptors should be considered to guide conjugated drugs from blood stream to targeted tissues.

Ligands with high binding constant is always better than ligands with low binding affinity to keep the therapeutic agents binding to cell receptors. For efficient delivery, nM orders of binding constant is preferable to maximize the therapeutic outcomes in general [79, 80]. However, by increasing the ratio of ligands and drugs, we can increase the binding affinity to aim the multivalent binding to one receptor. With this multi-binding strategy, the required binding constant is lowered from nM order to uM or mM order [81]. With these strategies, the proper set of ligands and receptors can be identified for efficient delivery of therapeutic agents by active targeting.
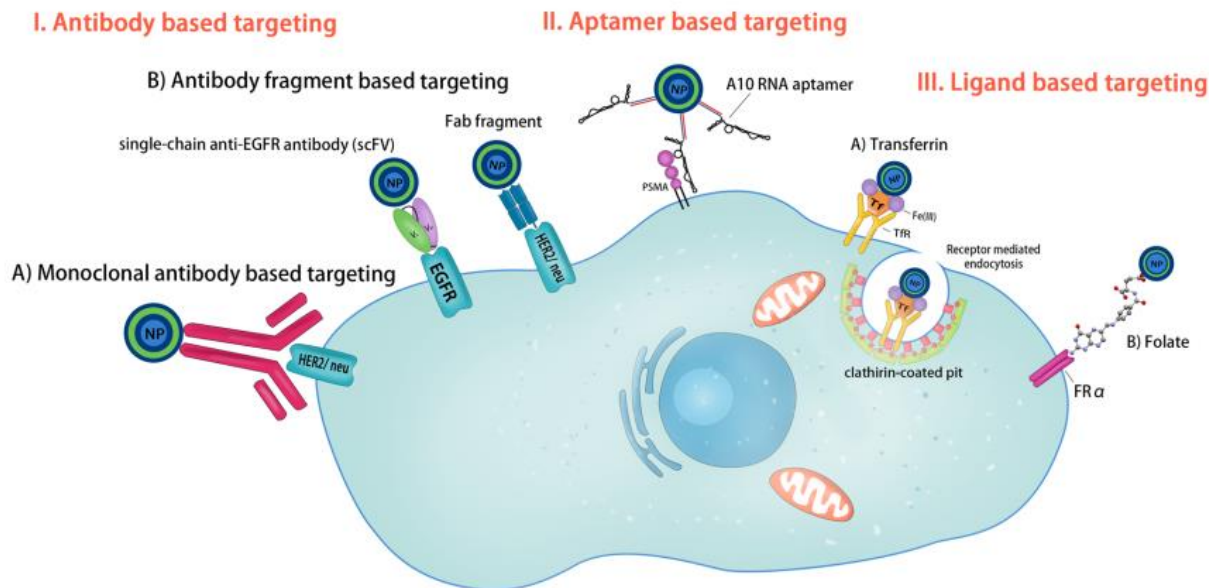
Figure 6. Active targeting of recptors on the cell surface

by antibody, aptamer and small molecules [75].

1.6. The aim of this doctoral dissertation

First, we developed an efficient way of synthesizing block copolymers, which are building blocks of PIC micelles. By optimizing the catalyst for polymerization of epoxides and N-

carboxylanhydride (NCA) based on its reactivity, we identified the proper set of catalyst and monomers to synthesize block polymers in one-pot reaction.

Next, with block copolymers with sharp molecular weight distributions, we synthesized block ionomers by the installation of primary amine in the side chain to form PIC micelles with mRNA. To develop efficient mRNA delivery system, we focused on the backbone structure of cationic segments, which has not been unexplored, to decrease the enthalpy and increase the entropy for improved thermodynamical stability, which was confirmed by isothermal calorimetry (ITC). To translate thermodynamical parameters to biological activities, both in vitro and in vivo experiments were conducted to examine the stability of encapsulated mRNA against enzymatic degradation and the gene expression.

After optimizing the backbone structure of block ionomers, we focused on the chemical structure in the side chain of cationic segments. To develop the mRNA delivery system with degradability and enhanced stability, functional amino acids were conjugated to flexible segments via degradable ester bonds, based on the interaction between protein and nucleic acids in physiological conditions. We confirmed both degradability of polymers and high stability of PIC micelles against enzymatic degradation to show high gene expression and prolonged half-life of intact mRNA *in vivo* harsh conditions.

Finally, we developed mRNA delivery system with surface functionalization of PIC micelles. We attempted to target pancreatic tumors, which are one of the most intractable diseases, with phosphocoline ligands. To investigate the activity of phosphocoline as a ligand, PIC micelles with high stability by cross linking were prepared as a platform for ligand installation. We confirmed the targeting ability of phosphocoline ligands in cultured pancreatic cancer cells and clarified the mechanism of internalization of ligand installed micelles. After the attachment of

ligands to mRNA-loaded PIC micelles, it showed high gene expression in cultured pancreatic cancer cells.

With these four strategies, we claimed the development of new synthetic route of block copolymers, new polymer structure for mRNA delivery, bio-inspired design with amino acids for nucleic acid delivery and ligand system to treat pancreatic cancer.

1.7. References

[1] K. Kariko, A. Kuo, E. Barnathan, Overexpression of urokinase receptor in mammalian cells following administration of the in vitro transcribed encoding mRNA. *Gene Therapy* **6** (1999) 1092-1100.

[2] S. Holtkamp, S. Kreiter, A. Selmi, P. Simon, M. Koslowski, C. Huber. Modification of antigen-encoding RNA increases stability, translational efficacy and T-cell stimulatory capacity of dendritic cells. *Blood* **108** (2006) 4009-4017.

[3] K-J. Kallen, A. Thefs, A development that may evolve into a revolution in medicine: mRNA as the basis for novel, nucleotide-based vaccines and drugs. *Ther. Adv. Vaccines* **2** (2014) 10-31.

[4] S. Guan and J. Rosenecker, Nanotechnologies in delivery of mRNA therapeutics using nonviral vector-based delivery systems. *Gene Ther.* **24** (2017) 133-143.

[5] B. Li, X. Luo and Y. Dong, Effects of chemical modified messenger RNA on protein expression. *Bioconjugate Chem.* **27** (2016) 849-853.

[6] M. S. D. Kormann, G. Hasenpusch, M. K. Aneja, G. Nica, A. W. Flemmer, S. Herber-Jonat et. al., Expression of therapeutic proteins after delivery of chemically modified mRNA in mice. *Nat. Biotechnol.* **29** (2011) 154–157.

[7] F. DeRosa, B. Guild, S. Karve, L. Smith, K. Love, J. R. Dorkin et. al., Therapeutic efficacy in a hemophilia B model using a biosynthetic mRNA liver depot system. *Gene Therapy* **23** (2016) 699–707.

[8] S. Kreiter, M. Diken, A. Selmi, Ö. Türeci and U. Sahin, Tumor vaccination using messenger RNA: prospects of a future therapy. *Curr. Opin. Immunol.* **23** (2013) 399–406.

[9] U. Sahin, K. Kakiko and Ö. Türeci, mRNA-based therapeutics — developing a new class of drugs. *Nat. Rev. Drug Discov.* **13** (2014) 759–780.

[10] A. Z. Wilczewska, K. Niemirowicz, K. H. Markiewicz and H. Car, Nanoparticles as drug delivery systems, *Phamacol. Rep.* **64** (2012) 1020-1037.

[11] V. F. V. Tendeloo, H. W. Snoeck, F. Lardon, G. L. Vanham, G. Nijs, M. Lenjou et. al., Nonviral transfection of distinct types of human dendritic cells: high-efficiency gene transfer by electroporation into hematopoietic progenitor- but not monocyte-derived dendritic cells. *Gene Therapy* **5** (1998) 700–707.

[12] T. Geng, Y. Zhan, J. Wang and C. Lu, Transfection of cells using flow-through electroporation based on constant voltage. *Nat. Protoc.* **6** (2011) 1192–1208.

[13] M-L. D. Temmerman, H. Dewitte, R. E. Vandenbroucke, B. Lucas, C. Libert, J. Demeester et. al., mRNA-Lipoplex loaded microbubble contrast agents for ultrasound-assisted transfection of dendritic cells. *Biomaterials* **32** (2011) 9128–9135.

[14] S. V. Meirvenne, L. Straetman, C. Heirman, M. Dullaers, C. D. Greef, V. V. Tendeloo et. al., Efficient genetic modification of murine dendritic cells by electroporation with mRNA. *Cancer Gene Ther.* **9** (2002) 787–797.

[15] H. Dewitte, S. V. Lint, C. Heirman, K. Thielemans, S. C. D. Smedt, K. Breckpot et. al., The potential of antigen and TriMix sonoporation using mRNA-loaded microbubbles for ultrasound-triggered cancer immunotherapy. *J. Control. Release* **194** (2014) 28–36.

[16] E. V. Agapov, I. Frolov, B. D. Lindenbach, B. M. Prágai, S. Schlesinger and C. M. Rice. Noncytopathic Sindbis virus RNA vectors for heterologous gene expression. *Proc. Natl. Acad. Sci. USA* **95** (1998) 12989–12994.

[17] S. Ferrari, U. Griesenbach, T. S. Iida, T. Shu, T. Hironaka, X. Hou et. al., A defective nontransmissible recombinant Sendai virus mediates efficient gene transfer to airway epithelium in vivo. *Gene Ther.* **11** (2004) 1659–1664.

[18] M. Bitzer, S. Armeanu, U. M. Lauer and W. J. Neubert, Sendai virus vectors as an emerging negative-strand RNA viral vector system. *J. Gene Med.* **5** (2003) 543–553.

[19] C. E. Thomas, A. Ehrhardt and M. A. Kay, Progress and problems with the use of viral vectors for gene therapy. *Nat. Rev. Genet.* **4** (2003) 346–358.

[20] S. Zou, K. Scarfo, M. H. Nantz and J. G. Hecker, Lipid-mediated delivery of RNA is more efficient than delivery of DNA in non-dividing cells. *Int, J. Pharm.* **389** (2010) 232–243.

[21] J. Rejman, G. Tavernier, N. Bavarsad, J. Demeester and S. C. D. Smedt, mRNA transfection of cervical carcinoma and mesenchymal stem cells mediated by cationic carriers. *J. Control. Release* **147** (2010) 385–391.

[22] R. W. Malone, P. L. Felgner and I. M. Verma, Cationic liposome-mediated RNA transfection. *Proc. Natl. Acad. Sci. USA* **86** (1989) 6077–6081.

[23] F. T. Zohra, E. H. Chowdhury, S. Tada, T. Hoshiba and T. Akaike, Effective delivery with enhanced translational activity synergistically accelerates mRNA-based transfection. *Biochem. Biophys. Res. Commun.* **358** (2007) 373–378.

[24] D. Lu, R. Benjamin, M. Kim, R. M. Conry and D. T. Curiel, Optimization of methods to achieve mRNA-mediated transfection of tumor cells in vitro and in vivo employing cationic liposome vectors. *Cancer Gene Ther.* **1** (1994) 245–252.

[25] E. R. Balmayor, J. P. Geiger, M. K. Aneja, T. Berezhanskyy, M. Utzinger, O. Mykhaylyk et. al., Chemically modified RNA induces osteogenesis of stem cells and human tissue explants as well as accelerates bone healing in rats. *Biomaterials* **87** (2016) 131–146.

[26] S. M. Johler, J. Rejman, S. Guan and J. Rosenecker, Nebulisation of IVT mRNA complexes for intrapulmonary administration. *PLoS ONE* **10** (2015) e0137504.

[27] U. Griesenbach and E. W. F. W. Alton, Gene transfer to the lung: lessons learned from more than 2 decades of CF gene therapy. *Adv. Drug Deliv. Rev.* **61** (2009) 128–139.

[28] U. Griesenbach, C. Meng, R. Farley, S. H. Cheng, R. K. Scheule, M. H. Davies et. al., In vivo imaging of gene transfer to the respiratory tract. *Biomaterials* **29** (2008) 1533–1540.

[29] E. W. F. W. Alton, D. K. Armstrong, D. Ashby, K. J. Bayfield, D. Bilton, E. V. Bloomfield et. al., Repeated nebulisation of non-viral CFTR gene therapy in patients with cystic fibrosis: a randomised, double-blind, placebo-controlled, phase 2b trial. *Lancet. Respir. Med.* **3** (2015) 684–691.

[30] F. E. Ruiz, J. P. Clancy, M. A. Perricone, Z. Bebok, J. S. Hong, S. H. Cheng et. al., A clinical inflammatory syndrome attributable to aerosolized lipid-DNA administration in cystic fibrosis. *Hum. Gene Ther.* **12** (2001) 751–761.

[31] O. Andries, M. D. Filette, S. C. D. Smedt, J. Demeester, M. Poucke, L. V. Peelman et. al., Innate immune response and programmed cell death following carrier mediated delivery of unmodified mRNA to respiratory cells. *J. Control. Release* **167** (2013) 157–166.

[32] R. Kanasty, J. R. Dorkin, A. Vegas and D. Anderson, Delivery materials for siRNA therapeutics. *Nat. Mater.* **12** (2013) 967–977.

[33] A. J. Geall, A. Verma, G. R. Otten, C. A. Shaw, A. Hekele, K. Banerjee et. al., Nonviral delivery of self-amplifying RNA vaccines. *Proc. Natl. Acad. Sci. USA* **109** (2012) 14604–14609.

[34] A. Hekele, S. Bertholet, J. Archer, D. G. Gibson, G. Palladino, L. A. Brito et. al., Rapidly produced SAM vaccine against H7N9 influenza is immunogenic in mice. *Emerg. Microbes Infect.* **2** (2013) e52.

[35] K. J. Kauffman, J. R. Dorkin, J. H. Yang, M. W. Heartlein, F. DeRosa, F. F. Mir et. al., Optimization of lipid nanoparticle formulations for mRNA delivery in vivo with fractional factorial and definitive screening designs. *Nano Lett.* **15** (2015) 7300–7306.

[36] H. Yin, C-Q. Song, J. R. Dorkin, L. J. Zhu, Y. Li, Q. Wu et. al., Therapeutic genome editing by combined viral and non-viral delivery of CRISPR system components in vivo. *Nat. Biotechnol.* **34** (2016) 328–333.

[37] B. Li, X. Luo, B. Deng, J. B. Giancola, D. W. McComb, T. D. Schmittgen et. al., Effects of local structural transformation of lipid-like compounds on delivery of messenger RNA. *Sci. Rep.* **6** (2016) 22137.

[38] Y. Dong, A. A. Eltoukhy, C. A. Alabi, O. F. Khan, O. Veiseh, J. R. Dorkin et. al., Lipid-like nanomaterials for simultaneous gene expression and silencing in vivo. Adv. Healthc. Mater. 3 (2014) 1392–1397.

[39] C.T. D. Ilarduya, M. A. Arangoa and N. Düzgüneş, Transferrin-lipoplexes with protamine-condensed DNA for serum-resistant gene delivery. *Methods Enzymol.* **373** (2003) 342–356.

[40] J. A. Wolff and D. B. Rozema, Breaking the bonds: non-viral vectors become chemically dynamic. *Mol. Ther.* **16** (2008) 8–15.

[41] K. J. Kauffman, M. J. Webber and D. G. Anderson, Materials for non-viral intracellular delivery of messenger RNA therapeutics. *J. Control. Release* **240** (2015) 227–234.

[42] K. Kataoka, H. Togawa, A. Harada, K. Yasugi, T. Matsumoto and S. Katayose, Spontaneous formation of polyion complex micelles with narrow distribution from antisense oligonucleotide and cationic block copolymer in physiological saline. *Macromolecules* **29** (1996) 8556-8557.

[43] K. Itaka, K. Yamauchi, A. Harada, K. Nakamura, H. Kawguchi and K. Kataoka, Polyion complex micelles from plasmid DNA and poly(ethylene glycol)-poly(L-lysine) block copolymer as serum-tolerable polyplex system: physiological properties of micelles relevant to gene transfection efficiency. *Biomaterials* **24** (2003) 4495-4506.

[44] M. Oishi, Y. Nagasaki, K. Itaka, N. Nishiyama and K. Kataoka, Lactosylated poly(ethylene glycol)-siRNA conjugate through acid-labile β-thioprotonate linkage to construct pH-sensitive polyion complex micelles achieving enhanced gene silencing in hepatoma cells. *J. Am. Chem. Soc.* **127** (2005) 1624-1625.

[45] S. Uchida, H. Kinoh, T. Ishii, A. Matsui, T. A. Tockary, K. M. Takeda, H. Uchida, K. Osada, K. Itaka and K. Kataoka, Systemic delivery of messenger RNA for the treatment of pancreatic cancer using polyplex nanomicelles with a cholesterol moiety. *Biomaterials* **82** (2016) 221-228.

[46] K. Kataoka, A. Harada and Y. Nagasaki, Block copolymer micelles for drug delivery: design, characterization and biological significance, *Adv. Drug Deliv. Rev.* **47** (2001) 113-131.

[47] A. Harada and K. Kataoka, Chain length recognition: core-shell supramolecular assembly from oppositely charged block copolymers. *Science* **283** (1999) 65-67.

[48] D. E. Owens and N. A. Peppas, Opsonization, Biodistribution, and Pharmacokinetics of Polymeric Nanoparticles. *Int. J. Pharm.* **307** (2006) 93−102.

[49] R. Hoogenboom, Poly(2-oxazoline)s: A Polymer Class with Numerous Potential Applications. *Angew. Chem. Int. Ed.* **48** (2009) 7978−7894.

[50] T. Konno, K. Kurita, Y. Iwasaki, N Nakabayashi and K. Ishihara, Preparation of Nanoparticles Composed with Bioinspired 2- Methacryloyloxyethyl Phosphorylcholine Polymer. *Biomaterials* **22** (2001) 1883−1889

[51] J. H. Park, G. Saravanakumar, K. Kim and I. C. Kwon, Targeted Delivery of Low Molecular Drugs Using Chitosan and its Derivatives. *Adv. Drug Delivery Rev.* **62** (2010) 28−41.

[52] O. Boussif, F. Lezoualc'h, M. A. Zanta, M. D. Mergny, D. Scherman, B. Demeneix and J. P. Behr, A Versatile Vector for Gene and Oligonucleotide Transfer into Cells in Culture and in vivo: Polyethylenimine. *Proc. Natl. Acad. Sci. U. S. A.* **92** (1995) 7297−7301.

[53] H. Cabral, K. Miyata, K. Osada and K. Kataoka, Block copolymer micelles in nanomedicine applications. *Chem. Rev.* **118** (2018) 6844-6892.

[54] Y. Kakizawa and K. Kataoka, Glutathione-sensitive stabilization of block copolymer micelles composed of antisense DNA and thiolated poly(ethylene glycol)-block poly(L-lysine): a potential carrier for systemic delivery of antisense DNA. *Biomacromolecules* **2** (2001) 491-497.

[55] Y. Li, K. Osada, Q. Chen, T. A. Tockary, A. Dirisala, K. M. Takeda, S. Uchida, K. Nagata, K. Itaka and Kataoka, K. Toroidal Packaging of pDNA into Block Ionomer Micelles Exerting Promoted in vivo Gene Expression. *Biomacromolecules* **16** (2015) 2664−2671.

[56] R. J. Christie, Y. Matsumoto, K. Miyata, T. Nomoto, S. Fukushima, K. Osada, J. Halnaut, F. Pittella, H. J. Kim, N. Nishiyama and K. Kataoka, Targeted polymeric micelles for siRNA treatment of experimental cancer by intravenous injection. *ACS nano* **6** (2012) 5174-5189.

[57] K. Miyat, M. Oba, M. Nakanishi, S. Fukushima, Y. Yamasaki, H. Koyama, N. Nishiyama and K. Kataoka, Polyplexs from poly(aspartamide) bearing 1, 2-diminoethane side chains induce pH-selective, endosomal membrane destabilization with amplified transfection and negligible cytotoxicity. *J. Am. Chem. Soc.* **130** (2008) 16287-16294.

[58] Y. Anraku, H. Kuwahara, Y. Fukusato, A. Mizoguchi, T. Ishii, K. Nitta, Y. Matsumoto, K. Toh, K. Miyata, S. Uchida et. al., Glycaemic Control Boosts Glucosylated Nanocarrier Crossing the BBB into the Brain. *Nat. Commun.* **8** (2017) 1001.

[59] Y. Anraku, A. Kishimura, A. Kobayashi, M. Oba and K. Kataoka, Size-Controlled Long-Circulating PICsome as a Ruler to Measure Critical Cut-Off Disposition Size into Normal and Tumor Tissues. *Chem. Commun.* **47** (2011) 6054−6056.

[60] N. Nishiyama, S. Okazaki, H. Cabral, M. Miyamoto, Y. Kato, Y. Sugiyama, K. Nishio, Y. Matsumura and K. Kataoka, Novel Cisplatin-Incorporated Polymeric Micelles Can Eradicate Solid Tumors Ii Mice. *Cancer Res.* **63** (2003) 8977−8983.

[61] H. Cabral, N. Nishiyama, S. Okazaki, H. Koyama and K. Kataoka, Preparation and biological property of dichloro(1, 2-diaminocyclohexane)platinum(II) (DACHPt)-loaded polymeric micelles. *J. Control. Release* **101** (2005) 223-232.

[62] W. Kim, Y. Yamasaki, W. D. Jang and K. Kataoka, Thermodynamics of DN condensation induced by poly(ethylene glycol)-block-polylysine through polyion complex micelle formation. *Biomacromolecules* **11** (2010) 1180-1186.

[63] K. Hayashi, H. Chaya, S. Fukushima, S. Watanabe, H. Takemoto, K. Osada, N. Nishiyama, K. Miyata and K. Kataoka, Influence of RNA strand rigidity on polyion complex formation with block catiomers, *Macromol. Rapid Commun.* **37** (2016) 486-493.

[64] S. Guan and J. Rosenecker, Nanotechnologies in delivery of mRNA therapeutics using nonviral vector based delivery systems. *Gene Ther.* **24** (2017) 133-143.

[65] N. M. Luscombe, S. E. Austin, H. M. Berman and J. M. Thornton, An overview of the structures of protein–DNA complexes. *Genome Biol.* **1** (2000)1–10.

[66] N. C. Seeman, J. M. Rosenberg and A. Rich, Sequence-specific recognition of double helical nucleic acids by proteins. Proc. Natl. Acad. Sci. U. S. A. 73 (1976) 804 – 808.

[67] Y. Mandel-Gutfreund, O. Schueler and H. Margalit, Comprehensive analysis of hydrogen bonds in regulatory protein DNA-complexes: in search of common principles. *J. Mol. Biol.* **253** (1995) 370 –382.

[68] C. O. Pabo and R. T. Sauer, Transcription factors: structural families and principles of DNA recognition. *Annu. Rev. Biochem.* **61** (1992) 1053– 1095.

[69] Y. Mandel-Gutfreund, H. Margalit, R. L. Jernigan and V. B. Zhurkin, A role for CH…O interactions in protein–DNA recognition. *J. Mol. Biol.* **277** (1998) 1129 –1140.

[70] K. Nadassy, S. J. Wodak and J. Janin, Structural features of protein– nucleic acid recognition sites. *Biochemistry* **38** (1999) 1999 –2017.

[71] M. Treger and E. Westhof, Statistical analysis of atomic contacts at RNA–protein interfaces. *J. Mol. Recognit.* **14** (2001) 199 –214.

[72] C. O. Pabo and R. T. Sauer, Protein–DNA recognition. *Annu. Rev. Biochem.* **53** (1984) 293– 321.

[73] L. N. Drozdov-Tikhomirov, D. M. Linde, V. V. Poroikov, A. A. Alexandrov and G. I. Skurida, Molecular mechanisms of protein–protein recognition: whether the surface placed charged residues determine the recognition process? *J. Biomol. Struct. Dyn.* **19** (2001) 279 –284.

[74] D. Lejeune, N. Delsaux, B. Charloteaux, A. Thomas and R. Brasseur, Protein-nucleic acid recognition: Statistical analysis of atomic interactions and influence of DNA structure. *Proteins Struct. Funct. Bioinf.* **61** (2005) 258-271.

[75] R. Bazak, M. Houri, S. E. Achy, S. Kamel and T. Rafaat, Cancer active targeting by nanoparticles: a comprehensive review of litarature, *J. Cancer Res. Clin. Oncol.* **141** (2015) 769-784.

[76] N. Parker, M. J. Turk, E. Westrick, J. D. Lewis, P. S. Low and C. P. Leamon, Folate receptor expression in carcinomas and normal tissues determined by a quantitative radioligand binding assay. *Anal. Biochem.* **338** (2005) 284−293.

[77] K. Sano, T. Takayama, K. Murakami, I Saiki and M. Makuuchi, Overexpression of retinoic acid receptor α in hepatocellular carcinoma. *Clin. Cancer Res.* **9** (2003) 3679−3683.

[78] L. Rajendran, H. J. Knolker and K. Simons, Subcellular targeting strategies for drug design and delivery. *Nat. Rev. Drug Discovery* **9** (2010) 29−42.

[79] A. K. Kanduluru, M. Srinivasarao and P. S. Low, Design, synthesis, and evaluation of a neurokinin-1 receptor-targeted near-IR dye for fluorescence-guided surgery of neuroendocrine cancers. *Bioconjugate Chem.* **27** (2016) 2157−2165.

[80] S. A. Kularatne, K. Wang, H. K. R. Santhapuram and P. S. Low, Prostate-specific membrane antigen targeted imaging and therapy of prostate cancer using a PSMA inhibitor as a homing ligand. *Mol. Pharmaceutics* **6** (2009) 780−789.

[81] C. Wayua and P. S. Low, Evaluation of a cholecystokinin 2 receptor-targeted near-infrared dye for fluorescence-guided surgery of cancer. *Mol. Pharmaceutics* **11** (2014) 468−476.

[82] V. M. Krishnamurthy, L. A. Estroff and G. M. Whitesides, Multivalency in ligand design. Fragment-based approaches in drug discovery **34** (2006) 11−53.

[83] B. Lepenies, J. Lee and S, Sonkaria Targeting C-type lectin receptors with multivalent carbohydrate ligands. *Adv. Drug Delivery Rev.* **65** (2013) 1271−1281.

Chapter2

Development of stabilized PIC micelles

with flexible block ionomers

2.1. Introduction

Messenger RNA (mRNA) is a promising therapeutic oligonucleotide, though its broad application as a therapeutic agent is confronted by several challenges, including its rapid degradation by nucleases [1]. Thus, the development of carrier systems protecting mRNA is essential for mRNA-based therapies. For systemic delivery of mRNA, nanomedicine such as viral vectors [2-4], lipid nanoparticles (LNPs) [5, 6] and polymeric micelles have been developed for gene therapy [7]. Among these novel mRNA delivery cargoes, polyion complex (PIC) micelles comprising block copolymers with polycation segments are promising nanocarriers for mRNA delivery [8]. These micelles can load mRNA in their core *via* electrostatic interaction with the polycation blocks, protecting it from the harsh biological environments [9]. Recent observations have suggested that the rigidity of the charged blocks is critical in the association and stability of the polyion complexes between block ionomers and nucleic acids [10]. Nevertheless, the effects of the flexibility of the block ionomers on the assembly and performance of mRNA-loaded micelles remains unexplored.

Herein, we focused on the rigidity of the backbone of the polycation segment, and developed novel mRNA-loaded micelles by using a block copolymer consisting of PEG and the flexible poly(glycidyl butylamine) segments (PEG-PGBA) (**Figure 1**). We hypothesized the stability of mRNA-loaded PIC micelles would be enhanced by increased contact area between cationic segments and mRNA and by promoted release of free water during the formation of ionic pairs. We synthesized PEG-PGBA from PEG-PGB by Brown hydroboration and amination. With this block ionomers, we attempted to prepare PIC micelles with mRNA by electrostatic interactions and characterized its physicochemical properties including thermodynamical parameters. To examine its *in vitro* performance, micelles stability against enzymatic degradation in serum and the translation efficacy of loaded mRNA in cultured cells were evaluated and compared to mRNA-loaded micelles prepared from the relatively more rigid PEG-poly(L-Lysine) (PEG-PLL).. Furthermore, for in vivo applications, the efficacy of mRNA transfection in lung and

its bioavailability in mice were investigated. Our results indicate the high potential of our strategy of engineer flexible polyether backbone in block ionomers to overcome intractable diseases by gene therapies based on mRNA.
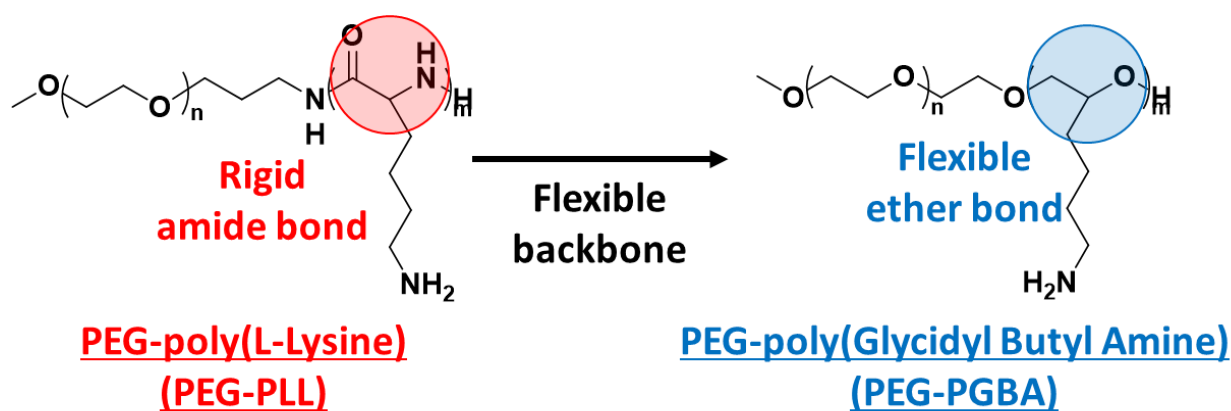
Figure 1. *Chemical structure of PEG-PGBA and PEG-PLL.*

2.2. Materials and Method

2.2.1. Materials

Diethyl ether (purity >99.5%) was bought from Showa ether (Tokyo, Japan). Borane tetrahydrofuran complex, hydroxylamine-O-sulfonic acid (purity >90.0%) were bought from Tokyo Chemical Industry Co., Ltd. (Tokyo, Japan). Lithium chloride (purity >99.0%) was bought from Nakalai Tesque Co., Inc. (Kyoto, Japan). Methanol (purity >99.5%) and sodium hydroxide (purity >97.0%) was bought from Sigma-Aldrich (St. Louis, MO, USA). Tetrahydrofuran (THF) as dehydrated solvent were bought from Kanto Chemical, Co., Inc., (Tokyo, Japan).

2.2.2. Measurements

Gel permeation chromatography (GPC) measurements were conducted with a Tosoh HLC-8220. The GPC system was equipped with a TSKgel G4000H$_{HR}$ column (linear, 7.8 mm × 300 mm; pore size, 20 nm; bead size, 5 µm; exclusion limit, 4×10^5 g/mol), a TSKgel G3000H$_{HR}$ column (linear, 7.8 mm × 300 mm; pore size, 7.5 nm; bead size, 5 µm; exclusion limit, 6×10^4 g/mol), a TSKgel guard column H$_{HR}$-L and a detector for refractive index (RI). DMF containing 10 mM lithium chloride was used as the eluent at a flow rate of 0.5 mL/min at 40 °C. GPC measurements using aqueous eluent were performed by using a Jasco HPLC system equipped with a Superdex^{TM} 200 10/300 GL column (linear, 10 mm × 300 mm; bead size, 13 µm; bead volume, 24 mL; exclusion limit, 1.3×10^6 g/mol), an internal RI detector and UV detector. The eluent was 10 mM phosphate buffer (pH 7.4) containing 500 mM sodium chloride and 10 mM acetic acids and the flow rate was 0.75 mL/min at 25 °C. The ^{1}H-NMR spectra were obtained with a JEOL EX400 spectrometer (JEOL, Tokyo, Japan) at 400 MHz. Molecular weight of polymers was measured by GPC using a sstandard PEGs with different molecular weight (Polymer Laboratories, Ltd., U.K.).

2.2.3. Hydroboration and hydroamination for MeO-PEG-*b*-poly(glycidyl butyl amine) copolymer (PEG-PGBA) preparation

Borane tetrahydrofuran complex (1.4 mmol, 1.6 mL) was added to PEG-PGB (2.4 µmol, 50 mg) in 3.4 mL of THF. The mixture was allowed to react for 3 h at room temperature and added to hydroxylamine-O-sulfonic acid (1.4 mmol, 160 mg). The mixture was allowed to react for 3 h at 66 °C. Then, the ether precipitation was performed by adding the reaction solution to the excess amount of diethyl ether (300 mL). The recovered polymer was dried under the reduced pressure

to obtain PEG-PGBA. The yield of PEG-PGBA was calculated to be 84%; number-averaged molecular weight (Mn) = 22,622, molecular weight distribution (MWD) = 1.05. ^{1}H-NMR (D$_2$O): δ (ppm) = 1.25-1.53 (-CH_2-CH_2-CH_2-PGBA side chain), 2.69 (-CH_2-NH$_2$-PGBA side chain) 3.39 (-O-CH_3), 3.42-3.80 (-CH_2-CH_2-O-PEG backbone, -CH_2-CH-O-PGBA backbone).

2.2.4. Deprotection of TFA groups in PEG-PLL-TFA for MeO-PEG-*block*-poly(L-Lysine) copolymer (PEG-PLL) synthesis

A 0.5 M solution of NaOH (0.25 mmol, 0.5 mL) was added to PEG-PLL(TFA) (1.7 µmol, 50 mg) in 5 mL of MeOH. The mixture was allowed to react for 1 day at room temperature. Then, the reaction solution was dialyzed with a dialysis membrane (Spectra/Pro 6 Membrane: MWCO, 6,000-8,000) against 0.01 M HClaq 3 times and pure water 3 times. The residue was freeze-dried to obtain PEG-PLL. The yield of PEG-PLL was determined to be 60%; number-averaged molecular weight (Mn) = 22,541, molecular weight distribution (MWD) = 1.09. ^{1}H-NMR (D$_2$O): δ (ppm) = 1.25-1.77 (-CH_2-CH_2-CH_2-PLL side chain), 2.69 (-CH_2-NH$_2$-PLL side chain), 3.21 (-CH-PLL backbone), 3.39 (-O-CH_3), 3.42-3.80 (-CH_2-CH_2-O-PEG backbone).

2.2.5. Preparation of polyion complex (PIC) micelles with mRNA

mRNA was prepared as previously described [9]. PEG-PGBA, PEG-PLL and mRNA were dissolved in 10 mM HEPES buffer (pH 7.3), and polymers and mRNA solutions were mixed at a molar ratio of primary amines in polymers to phosphate groups in mRNA (N/P) of 3. The size and polydispersity index (PDI) of PIC were measured by DLS measurement at 25°C.

2.2.6. Characterization of PIC micelles with thermodynamical parameters

The binding of polymers to mRNA was investigated by iTC200 instrument (GE Healthcare). The cell in ITC instrument was full of mRNA solution (11 μM) in 10 mM HEPES buffer (pH 7.3) and titrated with a polymer solution (110 μM) in 10 mM HEPES buffer (pH 7.3) at 25 °C every 120 s at 750 rpm. The fitting was performed with ORIGIN7 software by using sigmoid curve [11].

2.2.7. PIC stability against polyanion exchange

PIC micelles loaded with Cy5-labelled mRNA at a mRNA concentration of 15 nM were incubated with heparin solution (FUJIFILM Wako Pure Chemical Co., Tokyo, Japan) for 6 h at a various molar ratio of sulfo groups in heparin to phosphate groups in mRNA (S/P). Fluorescence correlation spectroscopy (FCS) was performed using LSM 780 (Carl Zeiss, Germny) with a Cy5 dye (Lumiprobe Co., USA) as a standard to calculate diffusion coefficient.

2.2.8. Quantification of intact mRNA after serum incubation

PIC micelles loaded with gaussia luciferase (GLuc) at a mRNA concentration of 50 μg/mL were incubated in 50% fetal bovine serum (FBS, Thermo Scientific Fisher Inc., USA) for 15 min at 37 °C. After mRNA purification with the RNeasy Mini Preparation Kit (Qiagen, Hilden, Germany), quantitative real-time PCR (qRT-PCR) was performed using an ABI Prism 7,500 Detector (Applied Biosystems, Foster City, CA, USA) and a primer pair for GLuc (Forward: TGCAAAAGATCCTCAACGTG, Reverse: AATGGGAAGTCACGAAGGTG). For

normalization, mRNA quantifications were also obtained for each PIC micelles with serum incubation at room temperature.

2.2.9. *In vitro* gene expression of mRNA introduced by PIC micelles

HuH-7 cells were cultured with Dulbecco's modified Eagle's medium (DMEM, Sigma-Aldrich, St. Louis, MO, USA) with 10% FBS and 1% penicillin/streptomycin (Sigma-Aldrich, St. Louis, MO, USA). The cells were seeded onto 96-well plates at a density of 5,000 cells/well. After 24 h incubation, the culture medium was exchanged and 2 μg of GLuc mRNA was added to the medium. After 24 h incubation, the medium was collected to quantify the GLuc secretion between 0 h and 24 h. The GLuc expression levels in the medium were measured using the Renilla Luciferase Assay System (Promega) and the GloMax 96 microplate luminometer (Promega).

2.2.10. *In vivo* evaluation of bioavailability of PIC micelles

All animal studies described below were conducted with the approval of the Animal Care and Use Committee of the University of Tokyo (Tokyo, Japan) and Innovation Center of NanoMedicine, Kawasaki Institute of Industrial Promotion (Kawasaki, Japan). Balb/c mice (7 weeks-old, female) were purchased from Charles River Laboratories (Yokohama, Japan). The PIC micelles (200 μL) containing 40 μg of mRNA were injected in the tail vein. Then, blood was collected from the tail vein, and the mRNA was purified with the RNeasy Mini Preparation Kit to quantify the mRNA levels by qRT-PCR.

2.2.11. *In vivo* gene expression of GLuc mRNA in lung tissues

PIC micelles (200 μL) containing 67 μg of mRNA were administered to Balb/c mice (7 weeks-old, female) by pulmonary infusion. Twenty-four hours after administration, the lung was excised and lysed with Passive Lysis Buffer. The GLuc amount in the lysate was quantified with the Renilla Luciferase Assay System (Promega) and the GloMax 96 microplate luminometer (Promega). For normalization, the protein levels in the excised tissues were measured by using the BCA Protein Assay Kit (TaKaRa, Tokyo, Japan).

2.3. Results and Discussion

First, we synthesized PEG-PGBA by Brown hydroboration-amination with boran-tetrahydrofuran (BH_3-THF) complex and hydroxylamine-o-suldonic acid (HOSA) [12] to obtain PEG-PGBA (**Scheme 1**). For PEG-PGBA synthesis, to the PEG-PGB, BH_3-THF was added at 10 equivalents to butene pendants to convert butene to butyl borane and the reaction was allowed to proceed for 1 overnight. After obtaining PEG-poly(glycidyl butyl butene) (PEG-PGB), HOSA was added at 10 equivalents to butyl borane in the side chains, aiming to produce PEG-PGBA with 80 DP of PGBA segments and the reaction solution was stirred for additional 1 overnight. The degree of polymerization of PGBA segments were caluculated to be 93 units by ^{1}H-NMR (**Figure 2**), while the narrow molecular weight distribution was observed by GPC (**Figure 3**), indicating that the butene in PEG-PGB was reacted with brane and HOSA to show primary amines in the side chain of PGBA pendants without any unfavorable side reactions to shorten polymer backbones.
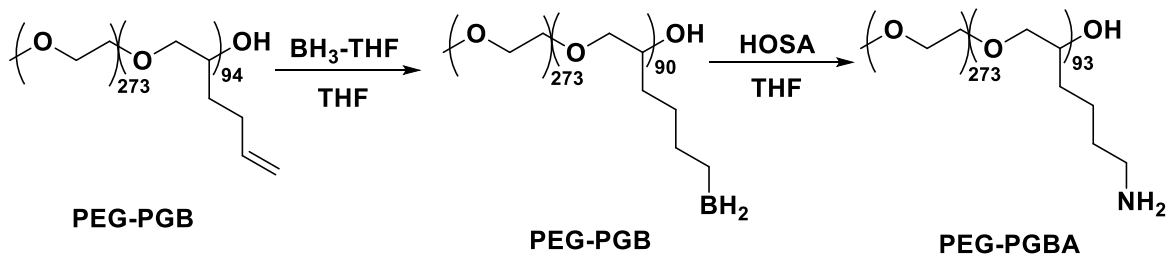
Scheme. 1. *Synthesis scheme of PEG-PGBA.*
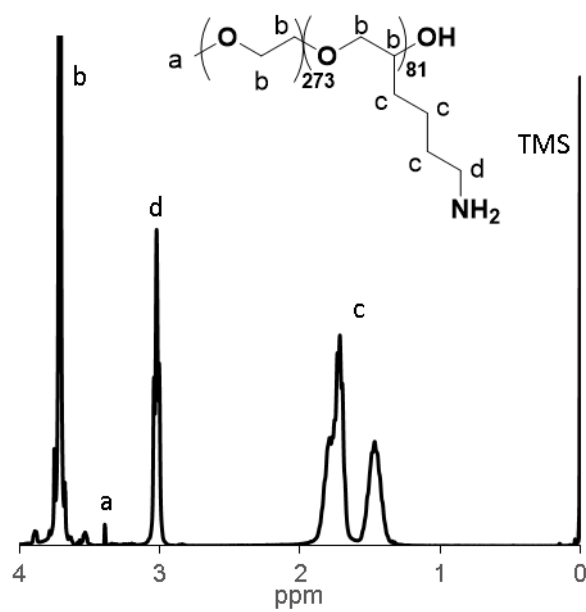
Figure. 2. *^{1}H-NMR spectrum of PEG-PGBA.*
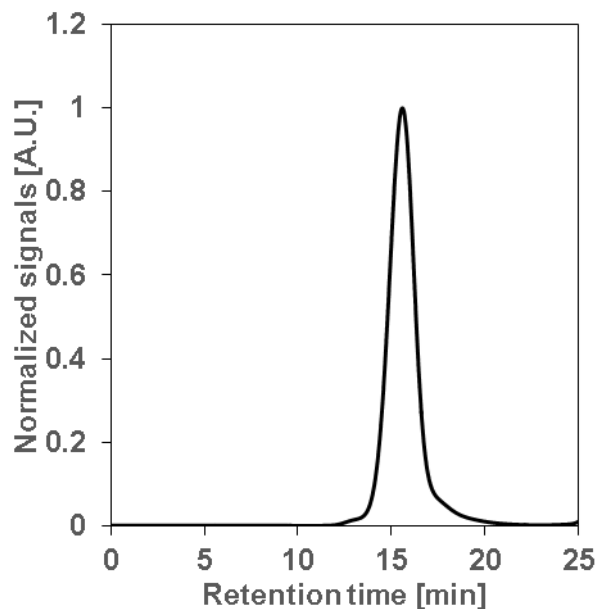
Figure. 3. *GPC spectrum of PEG-PGBA.*

To check the effect the rigidity of cationic segments on PIC stability, we synthesized control block ionomers, PEG-PLL by deprotection of TFA groups in the side chain of PEG-PLL(TFA) with sodium hydroxide (**Scheme 2**). For PEG-PLL synthesis, to the PEG-PLL(TFA), 1 M NaOH*aq* was added at 10 equivalents to TFA groups to obtain primary amine and the reaction was allowed to proceed for 1 overnight. The degree of polymerization of PLL segments were determined to be 83 units by ^{1}H-NMR, which was comparable with the number of primary amines in PEG-PGBA (**Figure 4**), while the narrow molecular weight distribution was observed by GPC (**Figure 5**), indicating that the TFA groups in PEG-PLL(TFA) was effectively deprotected to obtain primary amines in the side chain without any unfavorable side reactions to shorten polymer backbones.
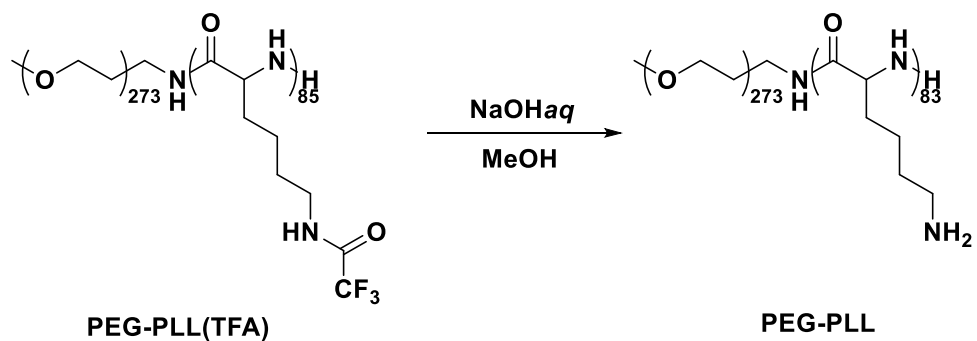
Scheme 2. *Synthesis scheme of PEG-PLL.*
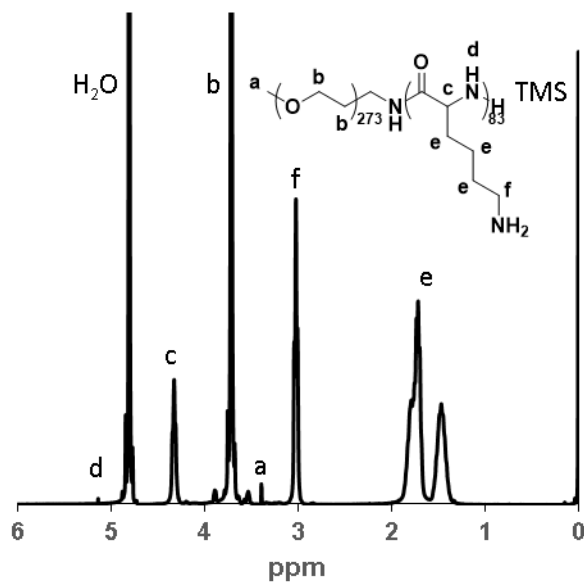
Figure 4. *^{1}H-NMR spectrum of PEG-PLL.*
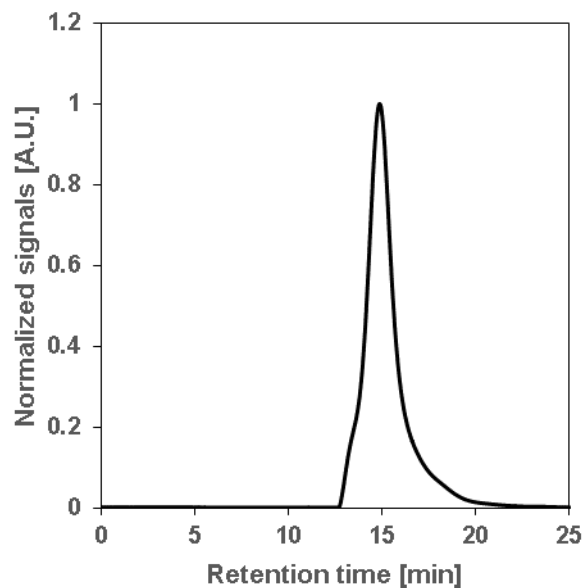
Figure 5. *GPC chromatogram of PEG-PLL.*

Next, we assembled PIC micelles with PEG-PGBA and mRNA in aqueous solutions and characterized its physicochemical and thermodynamical properties. PEG-PGBA and mRNA were mixed in 10 mM Hepes buffer (pH 7.4) to prepare PIC micelles *via* electrostatic interactions. The size and PDI were measured by dynamic light scattering (DLS). The PIC micelles formation with the sharp size distribution and the size of 56 nm, which was comparable with PIC micelles with PEG-PLL, was confirmed (**Table 1**). According to previous research, this size of PIC micelles is large enough to avoid renal clearance during blood circulation and accumulation in tumor with effective extravasation [13-15]. To check the effect of polyether backbone on the thermodynamical properties of assembled PIC, the thermodynamical parameters, including the formation enthalpy, the formation entropy and the binding constant were measured by isothermal calorimetry (ITC). The polymer solution was added to the mRNA solution and the emition of heat during complexation was measured and the obtained ITC curve was analyzed with fitting to calculate

thermodynamical parameters. Lower formation enthalpy and higher formation entropy after complexation of PEG-PGBA and mRNA than that of PEG-PLL and mRNA were observed, indicating polyether backbone decreased the contact area between cationic segments in polymers and mRNA and promoted the water release during ionic pairs formation because of its flexibility to increase the binding affinity between block ionomers and mRNA (**Table 1**).

Table. 1. *Characterization of mRNA-loaded PIC micelles.*

	Size [nm]	PDI	$\Delta_f H$ [cal/mol]	$\Delta_f S$ [cal/(mol·K)]	K [M^{-1}]
PEG-PGBA/mRNA	56	0.16	6.10	57.0	1.4×10^{-8}
PEG-PLL/mRNA	52	0.18	7.00	52.8	2.6×10^{-6}

These results of enhanced thermodynamical stabilities promoted us to investigate its biological availabilities including mRNA protection against polyanion exchange and enzymatic degradation, and translation in cultured cells. For *in vivo* application, it seems to be important to examine the stability of PIC against polyanion because it can dissociate by polyanion attacks at the kidney glomerular basement membrane [16]. To check the stability against polyanion, heparin as polyanion was added to PIC micelles with fluorescence-labelled mRNA. After 6 h incubation, the diffusion coefficient of fluorescence-labelled mRNA was measured by fluorescence correlation spectroscopy (FCS). In the case of PEG-PLL micelles, the increase of the diffusion coefficient of mRNA, which was corresponding to the release of free mRNA, was observed at the low S/P ratio (**Figure 6**). However, the diffusion coefficient of mRNA in PEG-PGBA micelles was kept constant at the low S/P ratio (**Figure 6**), indicating the binding of PEG-PGBA to mRNA

was enhanced by flexible PGBA segments, which is consistent with ITC experiments. At the high S/P ratio, the increase of the diffusion coefficient of mRNA in PEG-PGBA micelles was observed (**Figure 6**), suggesting the binding affinity between PEG-PGBA and mRNA was not too high to release the encapsulated mRNA, which is necessary for translation in cytosol. High stability against polyanion exchange is a key for PIC with nucleic acids but in the case of mRNA, high stability against enzymatic degradation is also important for high translation efficacy. To examine the stability of mRNA-loaded PIC micelles, serum with nucleases was added to mRNA-loaded PIC micelles and after 15 min incubation, the intact mRNA level was measured by qRT-PCR. Both PIC micelles showed better protection of mRNA against nucleases attack than fragile naked mRNA [9] and PIC micelles with PEG-PGBA protected more intact mRNA than PIC micelles prepared from PEG-PLL (**Figure 7**), indicating high binding affinities of PEG-PGBA to mRNA prevented the dissociation of micelles in nucleases enriched conditions. We encapsulated gaussia luciferase (GLuc) mRNA in the core of PIC micelles and transfected cultured Huh-7 cells to check luminescence produced by GLuc mRNA. Higher intensity of luminescence was observed by introduction of GLuc mRNA-loaded PIC micelles with PEG-PGBA than PIC micelles with PEG-PLL (**Figure 8**), indicating the cellular uptake of intact mRNA was promoted by PEG-PGBA micelles because of its high stability to show high gene expression in cultured cells.
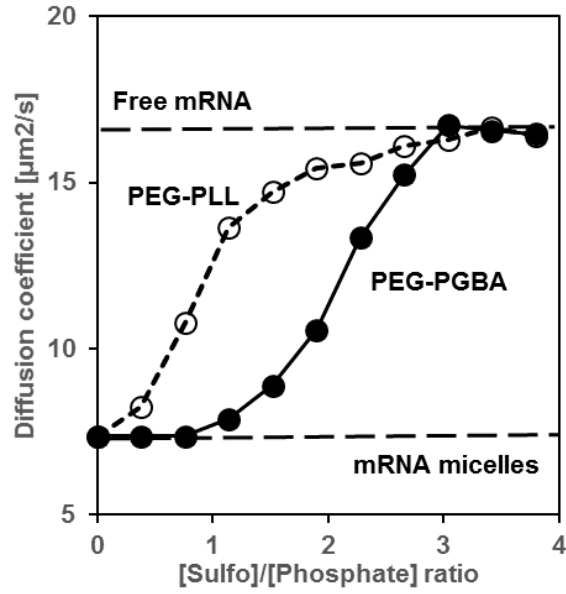
Figure 6. *The change of the diffusion coefficient of mRNA after 6 h incubation with heparin.*
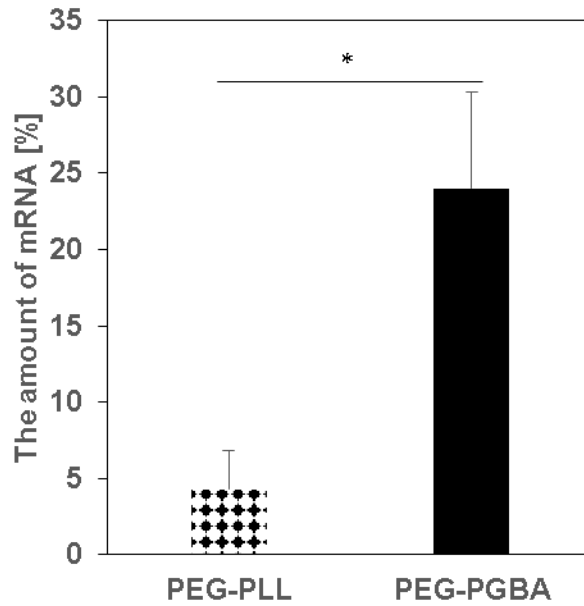
Figure 7. *The amount of intact mRNA after 15 min incubation with serum at 37 ºC (*P<0.05).*
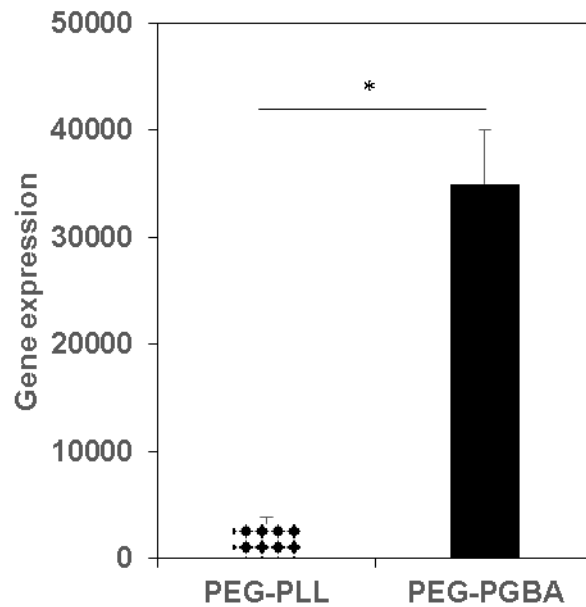
Figure 8. _Gene expression of Gluc mRNA after 24 h incubation in Huh-7 cells (*P<0.05)._

Finally, we explored the utility of mRNA-loaded PIC micelles _in vivo_ conditions by pulmonary administration and intravenous injection (i.v. injection). To examine the gene expression level derived from mRNA in lung, we encapsulated GLuc mRNA in the core of PIC micelles and it was allowed to produce luciferase protein for 24 h before collecting and homogenizing lung to check its expression level by luminometer. Both PIC micelles showed higher expression of GLuc in lung than naked mRNA and the luminescence intensity of PEG-PGBA micelles was higher than that of PEG-PLL micelles (**Figure 9**), indicating encapsulated mRNA was protected against enzymatic degradation and exchange of polyanion, which is abundant in pulmonary tissues. To check the bioavailability of mRNA-loaded PIC micelles, GLuc mRNA-loaded PIC micelles were allowed to circulate blood stream in mice after i.v. injection, followed by collecting blood from tail vain before RNA extraction and qRT-PCR, which is suitable to detect intact mRNA before degradation [9]. Although naked mRNA showed rapid degradation

[9], mRNA in both PIC micelles showed long bioavailability, and PEG-PGBA micelles circulated longer than PEG-PLL micelles (**Figure 10**), indicating high binding constant and high serum stability resulted in the protection *in vivo* harsh environment. These results indicate the utility of mRNA-loaded PIC micelles on mRNA-based therapeutics not only by local administration but systemic injections.
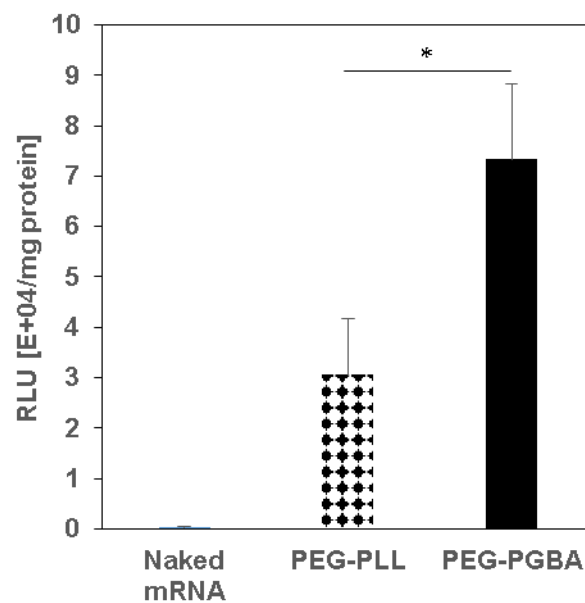
Figure 9. *Gene expression of GLuc mRNA in lung after pulmonary administration (*P<0.05).*
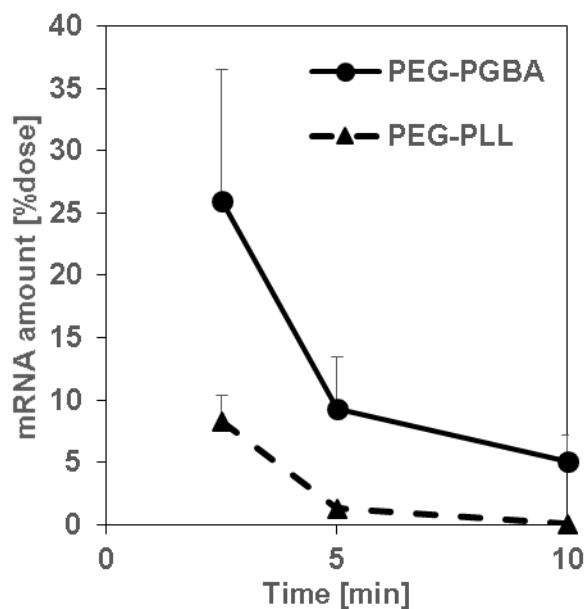
Figure 10. *Blood circulation profile of intact mRNA in PIC micelles after i.v. injection in mice.*

2.4. Conclusion

We have developed mRNA-loaded PIC micelles by engineering flexible polyether backbone in polycation segments. PEG-PGBA was synthesized by Brown hydroboration-amination of PEG-PGB and PEG-PGBA with sharp molecular weight distribution and the comparable length of cation segments with PEG-PLL were confirmed. The assembled mRNA-loaded PIC micelles showed narrow size distribution and the comparable size with PIC micelles prepared from PEG-PLL. Because of flexible nature of polyether backbone in PEG-PGBA, it decreased the contact area and increased water release during ionic pair formation to show higher binding affinity with mRNA. This high stability resulted in high protection of encapsulated mRNA against enzymatic degradation to enhance the translation of GLuc mRNA in cultured cells. Furthermore, these results may increase the versatility of polyether-based nanostructure to show high gene expression in lung and prolonged blood circulation time in mice. Our results indicate

that the backbone structure is a key for mRNA survival *in vivo* harsh environment and with further engineering of stability and biodegradability in nanomedicine, mRNA-based therapeutics will be a candidate to treat intractable diseases related to gene malfunctions.

2.5. References

[1] N. B. Tsui, K. O. Enders and Y. M. Dennis, Stability of endogenous and added RNA in blood specimens, serum and plasma, *Clin. Chem.* **48** (2002) 1647-1653.

[2] E. V. Agapov, I. Frolov, B. D. Lindenbach, B. M. Prágai, S. Schlesinger and C. M. Rice. Noncytopathic Sindbis virus RNA vectors for heterologous gene expression. *Proc. Natl. Acad. Sci. USA* **95** (1998) 12989–12994.

[3] S. Ferrari, U. Griesenbach, T. S. Iida, T. Shu, T. Hironaka, X. Hou et. al., A defective nontransmissible recombinant Sendai virus mediates efficient gene transfer to airway epithelium in vivo. *Gene Ther.* **11** (2004) 1659–1664.

[4] M. Bitzer, S. Armeanu, U. M. Lauer and W. J. Neubert, Sendai virus vectors as an emerging negative-strand RNA viral vector system. *J. Gene Med.* **5** (2003) 543–553.

[5] S. Zou, K. Scarfo, M. H. Nantz and J. G. Hecker, Lipid-mediated delivery of RNA is more efficient than delivery of DNA in non-dividing cells. *Int, J. Pharm.* **389** (2010) 232–243.

[6] J. Rejman, G. Tavernier, N. Bavarsad, J. Demeester and S. C. D. Smedt, mRNA transfection of cervical carcinoma and mesenchymal stem cells mediated by cationic carriers. *J. Control. Release* **147** (2010) 385–391.

[7] S. Guan and J. Rosenecker, Nanotechnologies in delivery of mRNA therapeutics using nonviral vector based delivery systems. *Gene Ther.* **24** (2017) 133-143.

[8] K. Kataoka, A. Harada and Y. Nagasaki, Block copolymer micelles for drug delivery: design, characterization and biological significance, *Adv. Drug Deliv. Rev.* **47** (2001) 113-131.

[9] S. Uchida, H. Kinoh, T. Ishii, A. Matsui, T. A. Tockary, K. M. Takeda, H. Uchida, K. Osada, K. Itaka and K. Kataoka, Systemic delivery of messenger RNA for the treatment of pancreatic cancer using polyplex nanomicelles with a cholesterol moiety. *Biomaterials* **82** (2016) 221-228.

[10] K. Hayashi, H. Chaya, S. Fukushima, S. Watanabe, H. Takemoto, K. Osada, N. Nishiyama, K. Miyata and K. Kataoka, Influence of RNA strand rigidity on polyion complex formation with block catiomers, *Macromol. Rapid Commun.* **37** (2016) 486-493.

[11] J. E. Labdury and M. L. Doyle, Biocalorimetry 2. Applications of calorimetry in the biological sciences. (2004) 2nd ed., John Wiley and Sons, Chichester, England.

[12] H. C. Brown, W. R. Heydkamp, E. Breuer and W. S. Murphy, The reaction of organoboranes with chloramine and with hydroxylamine-O-sulfonic acid. A. conversion synthesis of amines from olefins via hydroboration. *J. Am. Chem. Soc.* **86** (1964) 3565-3566.

[13] O. Ishida, K. Maruyama, K. Sasaki and M. Iwatsuru, Size-dependent extravasation and

interstitial localization of polyethyleneglycol liposomes in solid tumor-bearing mice. *Int. J. Pharm.* **190** (1999) 49-56.

[14] Y. Anraku, A. Kishimura, A. Kobayashi, M. Oba and K. Kataoka, Size-controlled long-circulating PICsome as a ruler to measure critical cut-off disposition size into normal and tumor tissues. *Chem. Commun. Camb.* **47** (2011) 6054-6056.

[15] H. S. Choi, W. Liu, P. Misra, E. Tanaka, J. P. Zimmer, B. I. Ipr, M. G. Bawendi and J. V. Frangioni, Renal clearance of quantum dots. *Nat. Biotechnol.* **25** (2007) 1165-1170.

[16] J. E. Zucherman, C. H. J. Choi, H. Han and M. E. Davis, Polycation-siRNA nanoparticles can disassemble at the kidney glomerular basement membrane. *Proc. Natl. Acad. Sci. USA* **109** (2012) 3137-3142.

Chapter3

Stabilization of PIC micelles with biodegradable block ionomers with functional amino acids

3.1. Introduction

The interaction between protein and nucleic acids was found not only in prokaryotes but also in eukaryotes [1] and the protein was encoded by the genome to control tracscription of DNA and translation of RNA. The hydrogen bonding is a candidate to understand the interaction between nucleic acids and protein, followed by hydrophobic interactions and electrostatic interactions [2, 3]. To form the hydrogen bonding, specific amino acids were adapted in the contact area of protein and nucleic acids, and previous report identified tryptophan, tyrosine, serine and threonine increased the stability of the complex by informatics of protein-RNA and protein-DNA interactions. Though ionic residue like lysine and histidine was found in the field of DDS because of cationic charges which can form the complex with the therapeutic oligonucleotides, hydrophobic amino acids with strong hydrogen bonding were unexplored.

In last chapter, we have reported the development of mRNA-loaded PIC micelles by engineering flexible polyether backbone in polycation segments. The assembled mRNA-loaded PIC micelles showed narrow size distribution, approximately 50 nm size, high binding affinity with mRNA. This high stability resulted in high protection of encapsulated mRNA against enzymatic degradation to enhance the translation of GLuc mRNA in cultured cells. Furthermore, these results may increase the versatility of polyether-based nanostructure to show high gene expression in lung and prolonged blood circulation time in mice. However, cytotoxicity of polycation segments in block ionomers against healthy tissue is issue for medical applications and the development of mRNA delivery system with biodegradability is important for safe and effective *in vivo* applications.

Herein, we focused on the ester bonds, which seem to be degraded in physiological conditions [4-7], and developed novel mRNA-loaded micelles by engineering the ester bonds

between polymer backbone and amino acids with primary amine and functional groups to enhance the stability of mRNA-loaded PIC micelles. Regarding the interaction between amino acids and nucleic acids in biological conditions [8], tryptophan for π-π stacking interaction with purine bases in mRNA, tyrosine for π-π interaction with pyrimidine bases in mRNA, leucine for hydrophobic interactions and glycine as a control were assumed to enhance the binding affinity of block ionomers and mRNA (**Figure 1**). We synthesized a block copolymer consisting of PEG and the flexible poly(glycidyl) segments, where amino acids were conjugated via degradable ester bonds. We examined the hydrolysis of ester bonds in physiological conditions and the polymer cytotoxicity against cultured cells. With this degradable block ionomers, we attempted to prepare PIC micelles with mRNA by electrostatic interactions and characterized its physicochemical properties. To examine its *in vitro* performance, micelles stability against enzymatic degradation in serum and the translation efficacy of loaded mRNA in cultured cells were evaluated. Furthermore, for *in vivo* applications, the efficacy of mRNA transfection in lung and its bioavailability in mice were investigated. Our results indicate the high potential of our strategy of engineering the biodegradable ester bonds between flexible polymer backbone and functional amino acids to increase biocompatibility and stability of mRNA delivery system simultaneously for mRNA-based gene therapies.
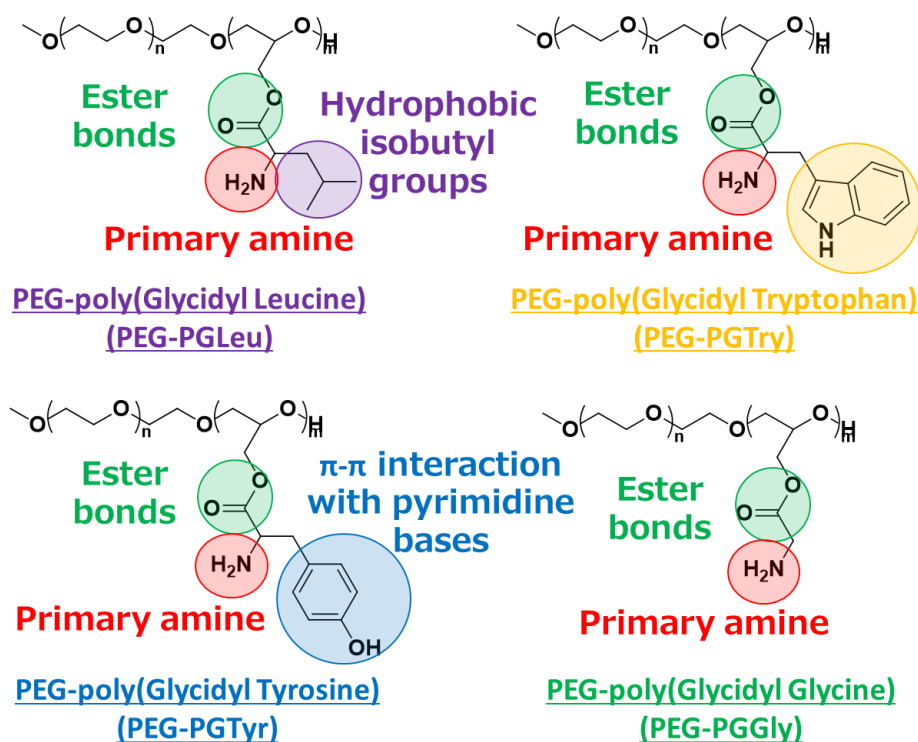
Figure 1. *Design of degradable block copolymers with functional amino acids.*

3.2. Materials and Method

3.2.1. Materials

4-dimethylaminopyridine (purity >99.0%), piperidine (purity >99.0%), N-[(9H-fluoren-9-ylmethoxy)carbonyl]glycine (purity >98.0%), N-[(9H-fluoren-9-ylmethoxy)carbonyl]leucine (purity >98.0%) N-[(9H-fluoren-9-ylmethoxy)carbonyl]tryptophan (purity >98.0%) N-[(9H-fluoren-9-ylmethoxy)carbonyl]tyrosine (purity >98.0%), EDC hydrochloride (purity >98.0%) and N, N-dimethylformamide (purity >99.5%) were bought from Tokyo Chemical Industry Co., Ltd. (Tokyo, Japan). Lithium chloride (purity >99.0%), sodium hydroxide (purity >97.0) was bought from Nakalai Tesque Co., Inc. (Kyoto, Japan). Methanol (purity >99.5%) was purchased from Sigma-Aldrich (St. Louis, MO, USA).

3.2.2. Measurements

Gel permeation chromatography (GPC) measurements were conducted with a Tosoh HLC-8220. The GPC system was equipped with a TSKgel G4000H$_{HR}$ column (linear, 7.8 mm × 300 mm; pore size, 20 nm; bead size, 5 µm; exclusion limit, 4×10^5 g/mol), a TSKgel G3000H$_{HR}$ column (linear, 7.8 mm × 300 mm; pore size, 7.5 nm; bead size, 5 µm; exclusion limit, 6×10^4 g/mol), a TSKgel guard column H$_{HR}$-L and a detector for refractive index (RI). DMF containing 10 mM lithium chloride was used as the eluent at a flow rate of 0.5 mL/min at 40 °C. GPC measurements using aqueous eluent were performed by using a Jasco HPLC system equipped with a Superdex^{TM} 200 10/300 GL column (linear, 10 mm × 300 mm; bead size, 13 µm; bead volume, 24 mL; exclusion limit, 1.3×10^6 g/mol), an internal RI detector and UV detector. The eluent was 10 mM phosphate buffer (pH 7.4) containing 500 mM sodium chloride and 10 mM acetic acids and the flow rate was 0.75 mL/min at 25 °C. The ^{1}H-NMR spectra were obtained with a JEOL EX400 spectrometer (JEOL, Tokyo, Japan) at 400 MHz. Molecular weight of polymers was measured by GPC using a sstandard PEGs with different molecular weight (Polymer Laboratories, Ltd., U.K.).

3.2.3. Preparation of MeO-PEG-*b*-poly(glycidol) copolymer (PEG-PGlycidol)

PEG-PECH (5.0 µmol,100 mg) was dissolved in 5 mL of methanol before the addition of 5 mL of 1 M NaOHaq and the solution was stirred for 1 day. It was dialyzed with a dialysis membrane (Spectra/Pro 6 Membrane: MWCO, 6,000-8,000) against 0.01 M HClaq 3 times and pure water 3 times. The residue was freeze-dried to obtain PEG-PGlycidol. The yield of PEG-

PGlycidol was determined to be 91% based on the elemental analysis of chlorine in PGlycidol segments; number-averaged molecular weight (Mn) = 18,036, molecular weight distribution (MWD) = 1.05.

3.2.4. Preparation of MeO-PEG-b-poly(glycidyl amino acids (Fmoc)) copolymer (PEG-PGTrp(Fmoc), PEG-PGTyr(Fmoc), PEG-PGLeu(Fmoc) and PEG-PGGly(Fmoc))

PEG-PGlycidol (5.0 µmol,100 mg) was dissolved in 10 mL of N, N-dimethylformamide (DMF) before the addition of 4-dimethylaminopyridine (4.1 mmol, 501 mg), 1-(3-dimethylaminopropyl)-3-ethylcordiimide hydrochloride (4.1 mmol, 637 mg) followed by N-[(9H-fluoren-9-ylmethoxy)carbonyl]glycine (4.1 mmol, 1.6 g), N-[(9H-fluoren-9-ylmethoxy)carbonyl]leucine (4.1 mmol, 1.6 g), N-[(9H-fluoren-9-ylmethoxy)carbonyl]tryptophan (4.1 mmol, 1.6 g), or N-[(9H-fluoren-9-ylmethoxy)carbonyl]tyrosine (4.1 mmol, 1.6 g) and the solution was stirred for 1 day. It was added to the excess amount of diethyl ether (200 mL) to perform ether precipitation The polymer was dried under the reduced pressure to obtain PEG-PGTrp(Fmoc), PEG-PGTyr(Fmoc), PEG-PGLeu(Fmoc) and PEG-PGGly(Fmoc). The yield of obtained polymer after purification was 88%, 92%, 98% 91% for each polymers based on the elemental analysis of nitrogen; number-averaged molecular weight (Mn) = 55, 524, 50,582, 42, 760, 44,679, molecular weight distribution (MWD) = 1.07, 1.08, 1.03, 1.05.

3.2.5. Preparation of MeO-PEG-b-poly(glycidyl amino acids) copolymer (PEG-PGTrp, PEG-PGTyr, PEG-PGLeu and PEG-PGGly)

PEG-PGTrp(Fmoc), PEG-PGTyr(Fmoc), PEG-PGLeu(Fmoc) and PEG-PGGly(Fmoc) (100 mg) were dissolved in 10 mL of mixing solution of piperidine and DMF (v/v = 1) and the solution was stirred for 1 day. It was added to the excess amount of diethyl ether (200 mL) to precipitate the polymer. The recovered polymer was dried *in vacuo* to obtain PEG-PGTrp, PEG-PGTyr, PEG-PGLeu and PEG-PGGly. The yield of obtained polymer after purification was 100%; number-averaged molecular weight (Mn) = 34, 626, 29,684, 21, 862, 23,781.

3.2.6. Polymer degradation in physiological conditions

PEG-PGTrp, PEG-PGTyr, PEG-PGLeu and PEG-PGGly (10 mg) were dissolved in 10 mL of 10 mM phosphate buffer (pH 7.4) with 150 mM saline (PBS) and the solution was allowed to stir for different time points. Then, the solution was purified by ultrafiltration (MWCO, 3,000) and the polymer was collected for freezing dry. The obtained polymer was dissolved in 10 mL of DMF and fluorescamine in DMF was added to the solution before the measurement of fluorescence with calibration curve prepared by n-buthylamine.

3.2.7. Polymer cytotoxicity in cultured cells

HEK293 cells (5,000 cells/well) were seeded on the 96-well plate and incubated for 24 h. Then, PEG-PGTrp, PEG-PGTyr, PEG-PGLeu, PEG-PGGly and PEG-PLL (10 mg) in 10 mL of PBS was added to the cell culture media. After 24 h incubation, the cells were washed with PBS 3 times and cell-counting kit-8 (CCK-8, 10 µL/well) was added to the media. After 30 min incubation, the absorbance was measured and the cell viability was calculated based on the absorbance of blank and PBS treatment.

3.2.8. Preparation of polyion complex (PIC) micelles with mRNA

PEG-PGBA, PEG-PLL and mRNA were dissolved in 10 mM HEPES buffer (pH 7.3), and polymers and mRNA solutions were mixed at a molar ratio of primary amines in polymers to phosphate groups in mRNA (N/P) of 3. The size and PDI of prepared PIC were examined by DLS measurement at 25°C.

3.2.9. PIC stability against polyanion exchange

PIC micelles loaded with Cy5-labelled mRNA at a mRNA concentration of 15 nM were incubated with heparin solution (FUJIFILM Wako Pure Chemical Co., Tokyo, Japan) for 6 h at a various molar ratio of sulfo groups in heparin to phosphate groups in mRNA (S/P). Fluorescence correlation spectroscopy (FCS) was performed using LSM 780 (Carl Zeiss, Germny) with a Cy5 dye (Lumiprobe Co., USA) as a standard to calculate diffusion coefficient.

3.2.10. Quantification of intact mRNA after serum incubation

PIC micelles loaded with gaussia luciferase (GLuc) at a mRNA concentration of 50 μg/mL were incubated in 50% fetal bovine serum (FBS, Thermo Scientific Fisher Inc., USA) for 15 min at 37 °C. After mRNA purification with the RNeasy Mini Preparation Kit (Qiagen, Hilden, Germany), quantitative real-time PCR (qRT-PCR) was performed using an ABI Prism 7,500 Detector (Applied Biosystems, Foster City, CA, USA) and a primer pair for GLuc (Forward: TGCAAAAGATCCTCAACGTG, Reverse: AATGGGAAGTCACGAAGGTG). For

normalization, mRNA quantifications were also obtained for each PIC micelles with serum incubation at room temperature.

3.2.11. *In vitro* gene expression of mRNA introduced by PIC micelles

HuH-7 cells were cultured with Dulbecco's modified Eagle's medium (DMEM, Sigma-Aldrich, St. Louis, MO, USA) with 10% FBS and 1% penicillin/streptomycin (Sigma-Aldrich, St. Louis, MO, USA). The cells were seeded onto 96-well plates at a density of 5,000 cells/well. After 24 h incubation, the culture medium was exchanged and 2 μg of GLuc mRNA was added to the medium. After 24 h incubation, the medium was collected to quantify the GLuc secretion between 0 h and 24 h. The GLuc expression levels in the medium were measured using the Renilla Luciferase Assay System (Promega) and the GloMax 96 microplate luminometer (Promega).

3.2.12. *In vivo* evaluation of bioavailability of PIC micelles

All animal studies described below were conducted with the approval of the Animal Care and Use Committee of the University of Tokyo (Tokyo, Japan) and Innovation Center of NanoMedicine, Kawasaki Institute of Industrial Promotion (Kawasaki, Japan). Balb/c mice (7 weeks-old, female) were purchased from Charles River Laboratories (Yokohama, Japan). The PIC micelles (200 μL) containing 40 μg of mRNA were injected in the tail vein. Then, blood was collected from the tail vein, and the mRNA was purified with the RNeasy Mini Preparation Kit to quantify the mRNA levels by qRT-PCR.

3.2.13. *In vivo* gene expression of GLuc mRNA in lung tissues

PIC micelles (200 µL) containing 67 µg of mRNA were administered to Balb/c mice (7 weeks-old, female) by pulmonary infusion. Twenty-four hours after administration, the lung was excised and lysed with Passive Lysis Buffer. The GLuc amount in the lysate was quantified with the Renilla Luciferase Assay System (Promega) and the GloMax 96 microplate luminometer (Promega). For normalization, the protein levels in the excised tissues were measured by using the BCA Protein Assay Kit (TaKaRa, Tokyo, Japan).

3.3. Results and Discussion

First, we constructed poly(glycidol) segments by using the PEG-PECH and NaOH (**Scheme 1**). To convert chlorine in PECH segments to hydroxyl groups, the NaOH was added at 10 equivalents to the PECH and the reaction solution was stirred for 24 h. The yield of the reaction introducing hydroxyl groups to PECH segments were determined to be 100 % by elemental analysis of chlorine in polymers and obtained products showed a narrow molecular weight distribution (**Figure 1**).
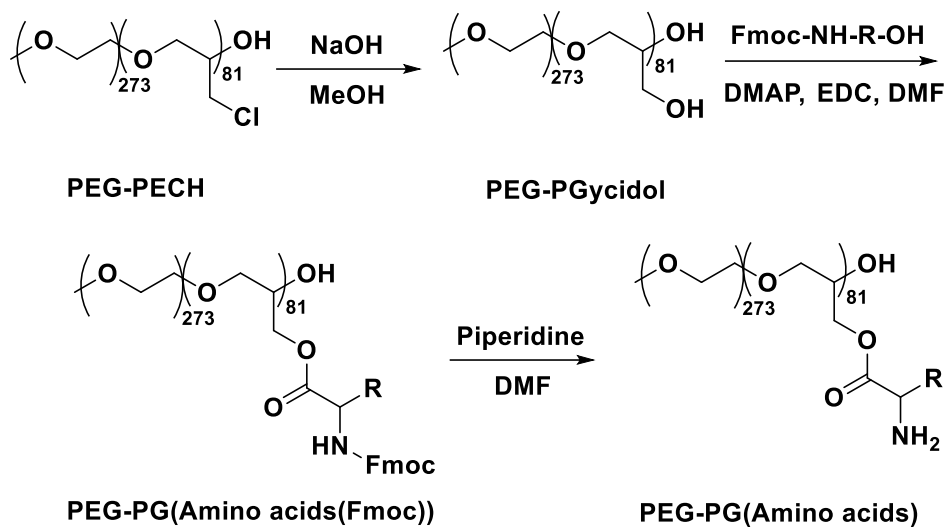
Scheme 1. *Synthesis scheme of PEG-PG(Amino acids).*
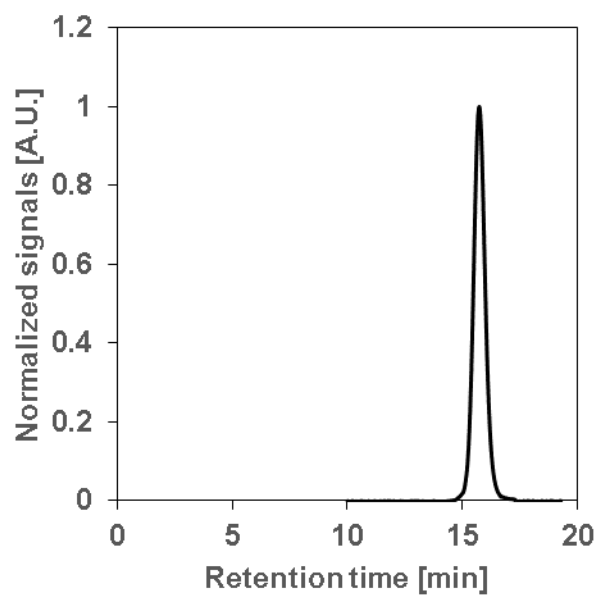
Figure 2. *GPC chromatogram of PEG-PGlycidol.*

After preparing PEG-poly(glycidol), Fmoc-NH-leucine-OH, Fmoc-NH-triptophan-OH, Fmoc-NH-tyrosine-OH or Fmoc-NH-glycine-OH with DMAP and EDC·HCl were added at 10 equivalents to hydroxyl groups in poly(glycidol) segments and the reaction was allowed to proceed for 1 overnight. After obtaining polymers, piperidine in DMF was added to deprotect fmoc groups in amino acids pendants, and the reaction was allowed to proceed further 1 overnight. The introduction ratio of leucine, tryptophan, tyrosine, glycine in were calculated to be 98, 88, 92, 91 % by ^{1}H-NMR (**Table 1**), while the narrow molecular weight distribution was observed by GPC (**Table 1**), indicating that the functional amino acids were effectively introduced to polymers *via* ester bonds without any unfavorable side reactions to shorten polymer backbones or crosslinking of polymers.

Table 1. Characterization of amino acids conjugated polymers

(Determined by Elemental analysis[1], GPC[2] and ^{1}H-NMR[3]).

Polymer	DP[1]	Mw/Mn[2]	Introduction ratio (%)[3]
PEG-poly(Glycidyl Glycine)	81	1.05	91
PEG-poly(Glycidyl Leucine)	81	1.03	98
PEG-poly(Glycidyl Tryptophan)	81	1.07	88
PEG-poly(Glycidyl Tyrosine)	81	1.08	92

Next, we examined the degradation of ester bonds between polymer backbone and amino acids in physiological conditions. PEG-PGLeu, PEG-PGTrp, PEG-PGTyr and PEG-PGGly were dissolved in 10 mM Hepes buffer (pH 7.4) to prepare polymer solutions and the solutions were

allowed to incubate for different time points at 37°C. After purification with ultrafiltration to remove free amino acids, the amount of primary amine in polymers was determined by fluorescamine, which was reacted with primary amine to produce fluorescence, with standard carve prepared by n-butylamine. Although PEG-PLL without ester bonds showed no change in the amount of primary amine, PEG-PGLeu, PEG-PGTrp, PEG-PGTyr and PEG-PGGly with ester bonds between amino acids and polymer backbone showed the decrease of the amount of primary amine (**Figure 3**), indicating the ester bonds were cleaved in physiological conditions to release free amino acids, resulting in low amount of primary amine in the side chain of polymers. These results motivated us to examine the polymers cytotoxicity against cultured cells *in vitro*. PEG-PGLeu, PEG-PGTrp, PEG-PGTyr and PEG-PGGly were added to cultured HEK293 cells and the system was allowed to incubate for 24 h before CCK-8 assay was conducted to measure the cell viability of cultured cells with polycation co-incubation. Though PEG-PLL without cleavable ester bonds showed cytotoxicity in high polymer concentration, PEG-PGLeu, PEG-PGTrp, PEG-PGTyr and PEG-PGGly showed low cytotoxicity against cultured HEK293 cells (**Figure 4**), indicating the ester bonds in polymers were degraded in cell culture media to reduce primary amine, which may induce the cell death because of electrostatic interactions with negatively charged cell membranes.
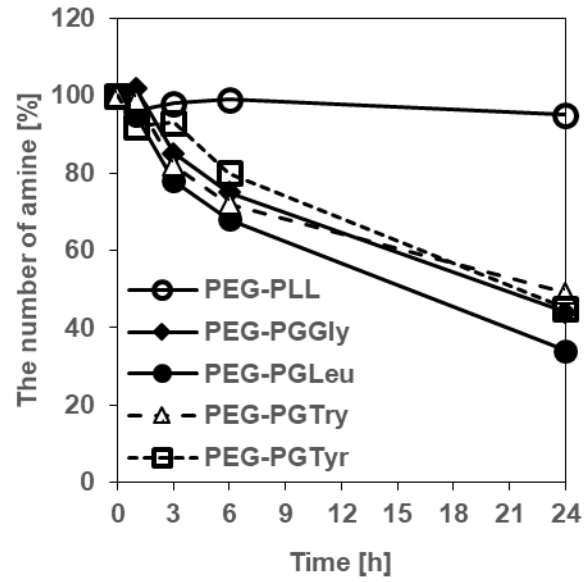
Figure 3. *The number of primary amine in degradable polymers.*
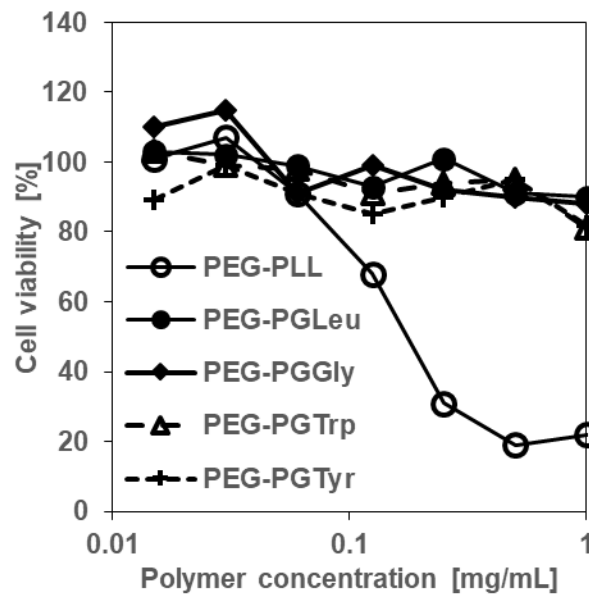
Figure 4. *Polymer cytotoxicity against cultured HEK293 cells.*

Next, we assembled PIC micelles with PEG-PGLeu, PEG-PGTrp, PEG-PGTyr and PEG-PGGly and mRNA in aqueous solutions and characterized its physicochemical properties. PEG-PGLeu, PEG-PGTrp, PEG-PGTyr or PEG-PGGly, and mRNA were mixed in 10 mM Hepes buffer (pH 7.4) to prepare PIC micelles *via* electrostatic interactions. The size and the PDI were checked by DLS measurement. The formation of PIC micelles with the sharp size distribution and the size of approximately 60 nm, which was comparable with PIC micelles with PEG-PLL, was confirmed (**Table 2**). According to previous research, this size of PIC micelles is large enough to avoid renal clearance during blood circulation and accumulation in tumor with effective extravasation [9-11].

Table. 2. Characterization of mRNA-loaded PIC micelles.

Sample	Size [nm]	Polydispersity index
PEG-PLL/mRNA	52	0.18
PEG-PGLeu/mRNA	60	0.15
PEG-PGTrp/mRNA	59	0.18
PEG-PGTyr/mRNA	55	0.19
PEG-PGGly/mRNA	58	0.19

To check the effect of functional groups in amino acids on the biological stability of mRNA-loaded PIC micelles, mRNA protection against polyanion exchange and enzymatic degradation was examined. For *in vivo* application, it is supposed to be important to examine the stability of PIC against polyanion because it can dissociate by polyanion attacks at the kidney glomerular basement membrane [12]. To check the stability against polyanion, heparin as polyanion was added to PIC micelles with fluorescence-labelled mRNA. After 6 h incubation, the

diffusion coefficient of fluorescence-labelled mRNA was measured by fluorescence correlation spectroscopy (FCS). In the case of PEG-PGGly micelles, the increase of the diffusion coefficient of mRNA, which was corresponding to the release of free mRNA, was observed at the relatively low S/P ratio (**Figure 5**). However, the diffusion coefficient of mRNA in PEG-PGLeu, PEG-PGTrp and PEG-PGTyr micelles was kept constant at the low S/P ratio (**Figure 5-7**), indicating the binding of block ionomers to mRNA was enhanced by hydrophobic interactions in the case of PEG-PGLeu, π-π stacking interactions with bases in mRNA in the case of PEG-PGTrp and PEG-PGTyr. At the high S/P ratio, the increase of the diffusion coefficient of mRNA in PEG-PGLeu, PEG-PGTrp and PEG-PGTyr micelles was observed (**Figure 5-7**), suggesting the binding affinity between block ionomers and mRNA was not too high to release the encapsulated mRNA, which is necessary for translation in cytosol. High stability against polyanion exchange is a key for PIC with nucleic acids but in the case of mRNA, high stability against enzymatic degradation is also important for high translation efficacy. Serum with nucleases was added to mRNA-loaded PIC micelles prepared with PEG-PGLeu, PEG-PGTrp, PEG-PGTyr and PEG-PGGly and the intact mRNA level was measured by qRT-PCR. PIC micelles with PEG-PGLeu, PEG-PGTrp or PEG-PGTyr showed protection of more intact mRNA than PIC micelles prepared from PEG-PGGly (**Figure 8**), indicating the binding affinity of polymers and mRNA was enhanced by hydrophobic isobutyl groups in the case of PEG-PGLeu, indole groups in PGTrp segments and phenolic groups in PEG-PGTyr. To confirm the release of mRNA from highly stabilized mRNA-loaded PIC micelles inside the cells, we examined the expression level of transfected mRNA in cultured cells. We encapsulated gaussia luciferase (GLuc) mRNA in the core of PIC micelles and added to cultured Huh-7 cells to check luminescence produced by GLuc mRNA. Higher intensity of luminescence was observed by introduction of GLuc mRNA-loaded PIC micelles with PEG-

PGLeu, PEG-PGTrp or PEG-PGTyr than PIC micelles with PEG-PGGly (**Figure 9**), indicating

the intactness was preserved in cell cultured media with serum to enhance the cellular uptake of

intact mRNA, resulting in high gene expression in cultured cells.

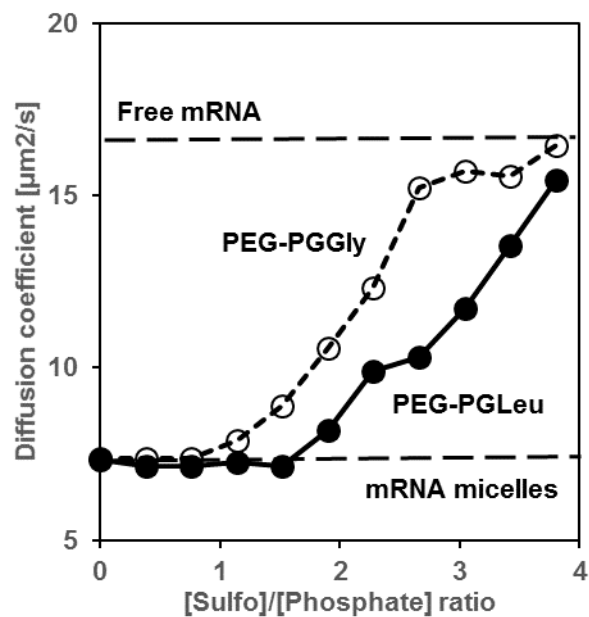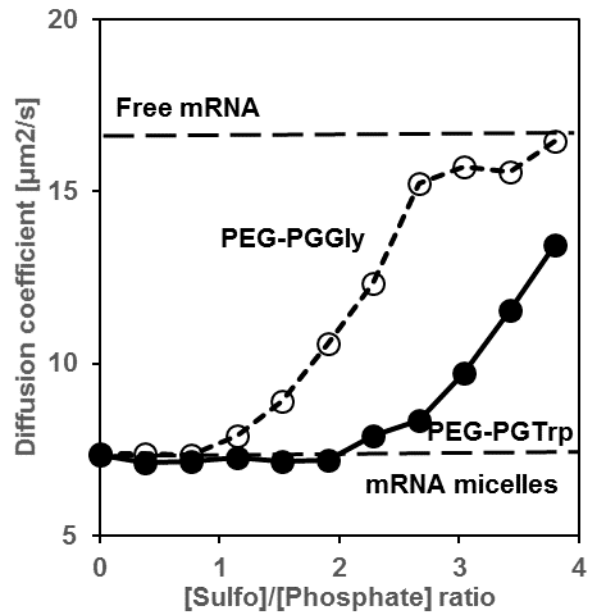*Figure 5. The change of the diffusion coefficient of mRNA in PEG-PGLeu micelles.*

Figure 6. The change of the diffusion coefficient of mRNA in PEG-PGTrp micelles.
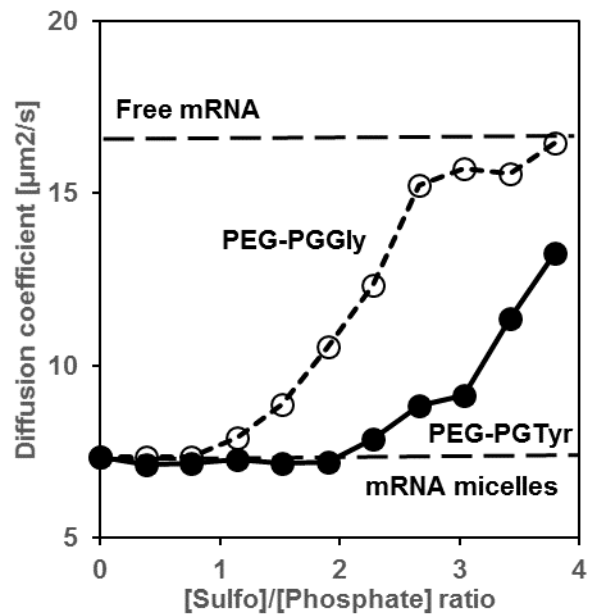
Figure 7. The change of the diffusion coefficient of mRNA in PEG-PGTyr micelles.
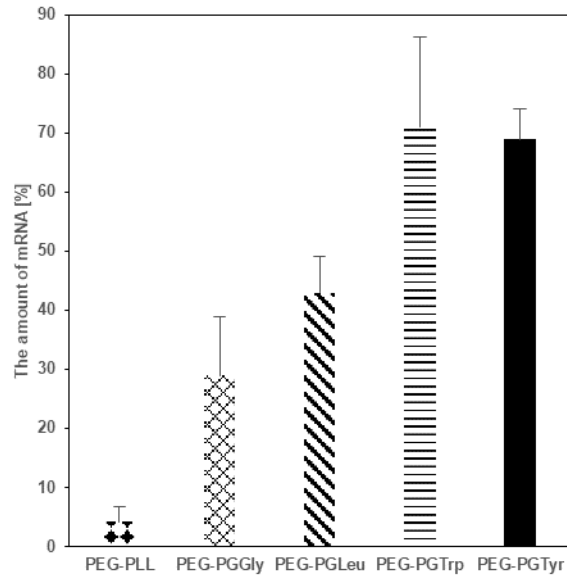
Figure 8. *The amount of intact mRNA after 15 min incubation with serum at 37 ºC.*
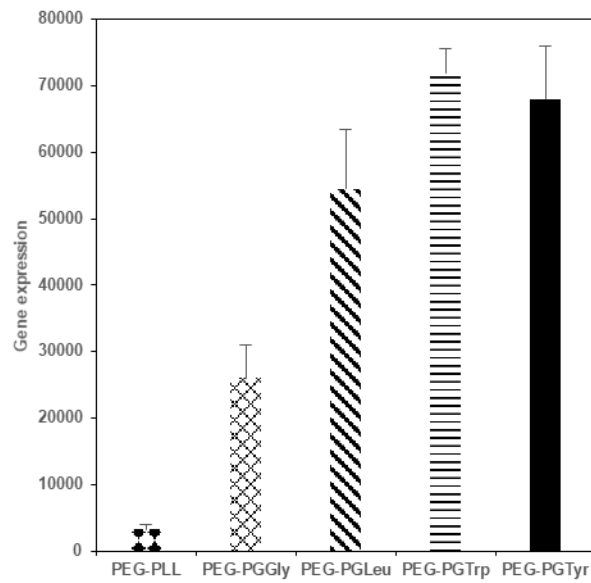
Figure 9. *Gene expression of Gluc mRNA after 24 h incubation in Huh-7 cells.*

Finally, we explored the availability of mRNA-loaded PIC micelles *in vivo* conditions by pulmonary administration and intravenous injection (i.v. injection). To examine the gene expression level derived from mRNA in lung, we chose PEG-PGTrp micelles, which showed highest stability against enzymatic degradation and highest gene expression *in vitro* and encapsulated GLuc mRNA in the core of PIC micelles and it was allowed to produce luciferase protein for 24 h before collecting and homogenizing lung to check its expression level by luminometer. PIC micelles prepared by PEG-PGTrp showed higher expression of GLuc mRNA in lung than PIC micelles prepared by PEG-PGGly (**Figure 10**), indicating encapsulated mRNA was protected against enzymatic degradation before the cellular uptake to show the gene expression of loaded GLuc mRNA. To check the bioavailability of mRNA-loaded PIC micelles, GLuc mRNA-loaded PIC micelles were allowed to circulate blood stream in mice after i.v. injection, followed by collecting blood from tail vain before RNA extraction and qRT-PCR. Comparing with PEG-PGGly micelles, mRNA in PEG-PGLeu, PEG-PGTrp or PEG-PGTyr micelles showed longer blood circulation time (**Figure 11**), indicating high nuclease stability resulted in the protection of encapsulated mRNA *in vivo* harsh environment. These results indicate the installation of tryptophan, which may interact with mRNA by π-π stacking, broadened the utility of mRNA-loaded PIC micelles on mRNA-based therapeutics not only by local administration but systemic injections.
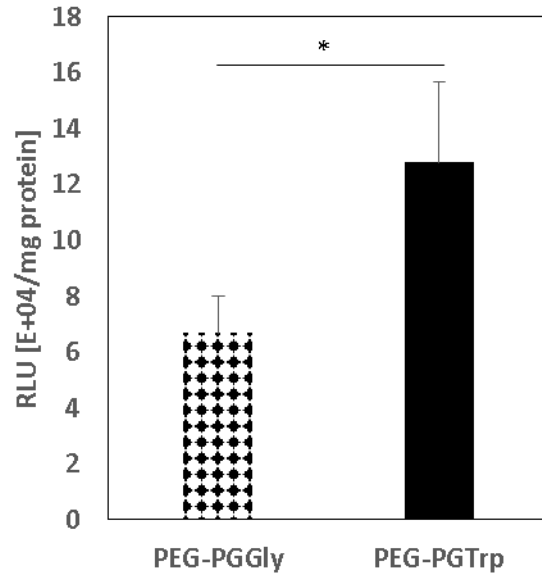
Figure 10. *Gene expression of GLuc mRNA in lung after pulmonary administration (*P<0.05).*
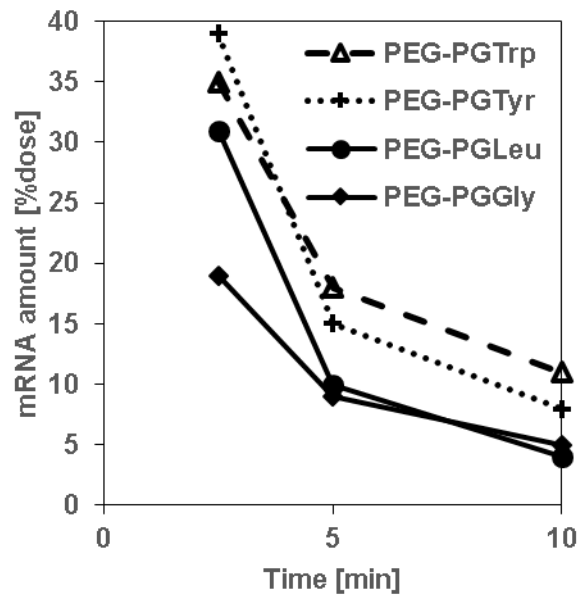
Figure 11. *Blood circulation profile of intact mRNA in PIC micelles after i.v. injection in mice.*

3.4. Conclusion

We have developed biodegradable block copolymers with functional amino acids for efficient mRNA delivery by PIC micelles. Amino acids in this case, leucine, tryptophan, tyrosine and glycine, were conjugated to flexible poly(glycidyl) chains via degradable ester bonds, which showed relatively rapid degradation in physiological conditions to reduce its polymer cytotoxicity against cultured cells. The assembled mRNA-loaded PIC micelles prepared by biodegradable polymers showed sharp size distribution and the comparable size with PIC micelles prepared from PEG-PLL or PEG-PGBA. We assumed hydrophobic leucine, tryptophan with indole groups and tyrosine with phenolic alcohols which may interact with RNA bases via π-π stacking interaction and this hypothesis was supported by high protection of encapsulated mRNA against enzymatic degradation. Though these PIC micelles had high affinities with mRNA, loaded-mRNA was released inside cells to promote the translation of GLuc mRNA in cultured cells. Furthermore, these results may increase the versatility of amino acid conjugated nanostructure to show high gene expression in lung and prolonged blood circulation time in mice. Our results indicate that the bio-inspired design based on in vivo interaction of protein and RNA is a key for prolonged halflife of mRNA *in vivo* harsh environment and because of the nature of amino acids having carboxylate, the ester bonds were successfully introduced between flexible polymer backbone to degrade itself after the release of therapeutic agents in this case, mRNA. This system has space to functionalize mRNA delivery system by engineering other kind of amino acids to construct peptides pendants including cysteine for crosslinking, histidine for endosomal escape and synthetic amino acids for the development of multi-function mRNA delivery system.

3.5. References

[1] N. M. Luscombe, S. E. Austin, H. M. Berman and J. M. Thornton, An overview of the structures of protein–DNA complexes. *Genome Biol.* **1** (2000)1–10.

[2] N. C. Seeman, J. M. Rosenberg and A. Rich, Sequence-specific recognition of double helical nucleic acids by proteins. Proc. Natl. Acad. Sci. U. S. A. 73 (1976) 804 – 808.

[3] Y. Mandel-Gutfreund, O. Schueler and H. Margalit, Comprehensive analysis of hydrogen bonds in regulatory protein DNA-complexes: in search of common principles. *J. Mol. Biol.* **253** (1995) 370 –382.

[4] X. J. Loh, The effect of pH on the hydrolytic degradation of poly(ε-caprolactone)-block-poly(ethylene glycol) copolymers. *J. Appl. Polym. Sci.* **127** (2013) 2046-2056.

[5] A. R. Webb, J. Yang and G. A. Ameer, Biodegradable polyester elastomers in tissue engineering. *Expert Opin. Biol. Ther.* **4** (2004) 801-812.

[6] D. Cohn and A. H. Salomon, Designing biodegradable multiblock PCL/PLA thermoplastic elastomers. *Biomaterials* **26** (2005) 2297-2305.

[7] Y. Hong, J. Guan, K. L. Fujimoto, R. Hashizume, A. L. Pelinescu and W. R. Wagner, Tailoring the degradation kinetics of poly(ester carbonate urethane)urea thermoplastic elastomers for tissue engineering scaffolds. *Biomaterials* **31** (2010) 4249-4258.

[8] D. Lejeune, N. Delsaux, B. Charloteaux, A. Thomas and R. Brasseur, Protein-nucleic acid recognition: Statistical analysis of atomic interactions and influence of DNA structure. *Proteins Struct. Funct. Bioinf.* **61** (2005) 258-271.

[9] O. Ishida, K. Maruyama, K. Sasaki and M. Iwatsuru, Size-dependent extravasation and

interstitial localization of polyethyleneglycol liposomes in solid tumor-bearing mice. *Int. J. Pharm.* **190** (1999) 49-56.

[10] Y. Anraku, A. Kishimura, A. Kobayashi, M. Oba and K. Kataoka, Size-controlled long-circulating PICsome as a ruler to measure critical cut-off disposition size into normal and tumor tissues. *Chem. Commun. Camb.* **47** (2011) 6054-6056.

[11] H. S. Choi, W. Liu, P. Misra, E. Tanaka, J. P. Zimmer, B. I. Ipr, M. G. Bawendi and J. V. Frangioni, Renal clearance of quantum dots. *Nat. Biotechnol.* **25** (2007) 1165-1170.

[12] J. E. Zucherman, C. H. J. Choi, H. Han and M. E. Davis, Polycation-siRNA nanoparticles can disassemble at the kidney glomerular basement membrane. *Proc. Natl. Acad. Sci. USA* **109** (2012) 3137-3142.

[13] S. Uchida, H. Kinoh, T. Ishii, A. Matsui, T. A. Tockary, K. M. Takeda, H. Uchida, K. Osada, K. Itaka and K. Kataoka, Systemic delivery of messenger RNA for the treatment of pancreatic cancer using polyplex nanomicelles with a cholesterol moiety. *Biomaterials* **82** (2016) 221-228.

Chapter4

Surface functionalization with phosphocoline of PIC micelles for active targeting

4.1. Introduction

Messenger RNA (mRNA) is a candidate of therapeutic oligonucleotides and short half-life in blood stream and poor cellular uptake limit the application of mRNA as therapeutic agents. To protect it from *in vivo* harsh environments and promote the cellular internalization, delivery cargo such as viral vector [1], lipid nanoparticles (LNPs) [2] and polyplex [3] has been extensively studied and they showed protection of mRNA against enzymatic degradation and enhanced the cellular uptake. However, the short life of such mRNA-loaded nanomedicine is still compromised by that of other formulations, for example, long-circulating liposomes [4]. Therefore, mRNA delivery system which prolongs blood circulation time of intact mRNA and shows rapid cellular uptake by targeted cells is important to treat intractable gene diseases.

Surface functionalization of nanomedicine is promising way to promote the cellular uptake by targeted cells [5]. To target the cells, ligand molecules including small molecules, aptamer and antibody are adapted and the conjugated materials are guided to the target before the release of therapeutic agents. To develop the new ligand system, the expression profile of receptors and the property of ligand molecules are important to accumulate the targeted tissues and to keep the property of conjugated therapeutic agents.

Herein, we focus on phosphocoline (PC) molecules as a ligand and phospholipid transfer protein (PLTP) as a target. PLTP is a protein to uptake phospholipid from blood stream to construct cell membrane and overexpressed in various kinds of cancer, e.g. pancreatic cancers [6]. PLTP recognize the betain structure of PC to uptake phosphatidylcoline, which is the building block of cell membrane [7]. Regarding the interaction between PC and PLTP, we hypothesized we can target the pancreatic tumors by engineering PC with hydrophilic structure, which may keep the surface property of PIC micelles. We developed PIC micelles probe with high stability as a platform to examine the effect of ligands on the cellular uptake in cultured cells. We synthesized the polymers and prepared the ligand-installed PIC micelles before the EDC coupling of primary amine and carboxylate in the core of micelles not to dissociate in the cell culture conditions. Then,

we investigated the effect of the installation of PC ligands on the cellular uptake in cultured pancreatic cancer BxPC3 cells. To examine the mechanism of the cellular uptake, the completive assay with free PC molecules and the inhibition assay with PLTP inhibitors, thiomersal were conducted. Moreover, we attached the PC ligands on the surface of the mRNA-loaded PIC micelles by preparing PC-PEG-PGTrp (**Figure 1**) and examined the gene expression in cultured cells. Our results indicated that newly developed PC ligand system is a promising way to target intractable pancreatic cancer cells without unfavorable change of surface properties.
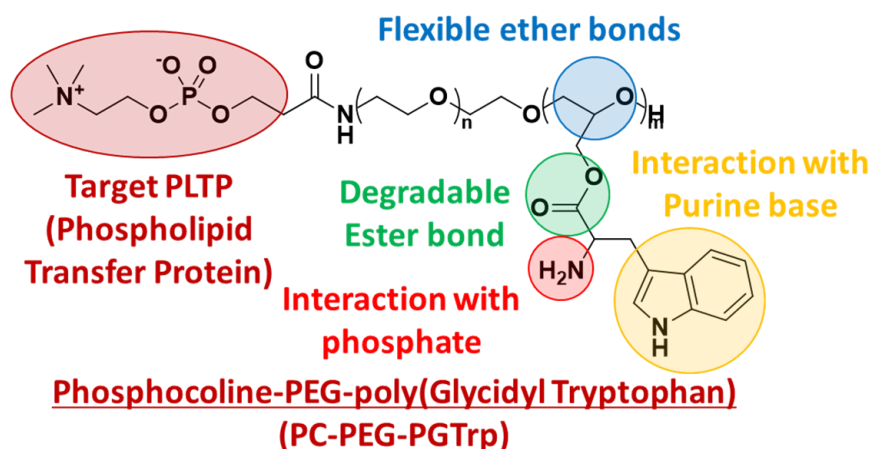
Figure 1. *Chemical structure of PC-PEG-PGTrp.*

4.2. Materials and Method

4.2.1. Materials

2-methacryloyloxyethyl phosphorylcholine (purity >96.0%), 1, 5-diaminopentane (purity >98.0%), triphenylphosphine (purity >95.0%), diisopropylamine (purity >99.0%), EDC hydrochloride (purity >98.0%) were bought from Tokyo Chemical Industry Co., Ltd. (Tokyo, Japan). N-methyl-2-pyroridone (purity >99.0%) and benzene (purity >95.0%) were purchased

from Sigma-Aldrich (St. Louis, MO, USA). Lithium chloride (purity >99.0%), sodium hydroxide (purity >97.0) was bought from Nakalai Tesque Co., Inc. (Kyoto, Japan). β-benzyl-L-aspartate N-carboxyanhydride (BLA-NCA) was purchased from Chuo Kaseihin Co. Inc. (Tokyo, Japan) and used as received. N, N-dimethylformamide (DMF) and dichloromethane (DCM) as dehydrated solvents were bought from Kanto Chemical, Co., Inc., (Tokyo, Japan). Hexane (purity >96.0%), toluene (purity >99.0%) and ethyl acetate (purity >96.0%) were bought from FUJIFILM Wako Pure Chemical Co. (Tokyo, Japan).

4.2.2. Measurements

Gel permeation chromatography (GPC) measurements were conducted with a Tosoh HLC-8220. The GPC system was equipped with a TSKgel G4000H$_{HR}$ column (linear, 7.8 mm × 300 mm; pore size, 20 nm; bead size, 5 µm; exclusion limit, 4×10^5 g/mol), a TSKgel G3000H$_{HR}$ column (linear, 7.8 mm × 300 mm; pore size, 7.5 nm; bead size, 5 µm; exclusion limit, 6×10^4 g/mol), a TSKgel guard column H$_{HR}$-L and a detector for refractive index (RI). DMF containing 10 mM lithium chloride was used as the eluent at a flow rate of 0.5 mL/min at 40 °C. GPC measurements using aqueous eluent were performed by using a Jasco HPLC system equipped with a Superdex^{TM} 200 10/300 GL column (linear, 10 mm × 300 mm; bead size, 13 µm; bead volume, 24 mL; exclusion limit, 1.3×10^6 g/mol), an internal RI detector and UV detector. The eluent was 10 mM phosphate buffer (pH 7.4) containing 500 mM sodium chloride and 10 mM acetic acids and the flow rate was 0.75 mL/min at 25 °C. The ^{1}H-NMR spectra were obtained with a JEOL EX400 spectrometer (JEOL, Tokyo, Japan) at 400 MHz. Molecular weight of polymers was measured by GPC using a sstandard PEGs with different molecular weight (Polymer Laboratories, Ltd., U.K.).

4.2.3. Preparation of α-phosphocoline-ω-amino-PEG (PC-PEG-NH$_2$)

PC-PEG-NH$_2$ was synthesized following previous report [8]. SH-PEG-NH$_2$ (100 mg, 10 μmol) and 2-methacryloyloxyethyl phosphorylcholine (MPC, 0.10 mmol) were dissolved in 10 mL of ethanol before the Ar bubbling and diisopropylamine (DIPA, 0.10 mmol) was added to catalyze the reaction. After 48 h reaction, ethanol was removed under the reduced pressure and the polymer solution in pure water was dialyzed with a dialysis membrane (Spectra/Pro 6 Membrane: MWCO, 6,000-8,000) against pure water 6 times. The residue was freeze-dried to obtain PC-PEG-NH$_2$. The yield of obtained polymer after purification was 98%; number-averaged molecular weight (Mn) = 10,295. ^{1}H-NMR (CDCl$_3$): δ (ppm) = 1.21-1.24 (-CH-(C$\underline{H}_3$)-C(=O)), 2.50-2.82 (-C$\underline{H}_2$-CH$_2$-S-CH$_2$-CH(CH$_3$)-), 3.22 (-N(C$\underline{H}_3$)$_3$-), 3.39 (-O-C$\underline{H}_3$), 3.42-3.80 (-C$\underline{H}_2$-C$\underline{H}_2$-O-PEG backbone, -C$\underline{H}_2$N-), 4.04-4.09 (-POC$\underline{H}_2$-), 4.25-4.30 (-O-CH$_2$-CH$_2$-OP).

4.2.4. Preparation of phosphocoline-PEG-b-poly(β-benzyl-L-aspartate) copolymer (SH-PEG-PBLA)

PC-PEG-NH$_2$ (5.0 μmol, 100 mg) was dissolved in 1.5 mL of dichloromethane (DCM) before the addition of β-benzyl-L-aspartate N-carboxyanhydride (BLA-NCA) (0.50 mmol, 125 mg) in 2 mL of mixing solvent of DCM and DMF (v/v = 10) and the solution was stirred for 3 days at 35 ºC. It was added to the excess amount of mixing solvent of hexane and ethyl acetate (v/v = 1) to perform ether precipitation. The polymer was dried under the reduced pressure to obtain PC-PEG-PBLA. The yield of PC-PEG-PBLA was calculated to be 88%; number-averaged molecular weight (Mn) = 31,931, molecular weight distribution (MWD) = 1.09. ^{1}H-NMR (D$_2$O):

δ (ppm) = 1.21-1.24 (-CH-(C$\underline{H}_3$)-C(=O)), 1.70-2.70 (-C$\underline{H}_2$-PBLA side chain), 2.50-2.82 (-C$\underline{H}_2$-C$\underline{H}_2$-S-C$\underline{H}_2$-C$\underline{H}$(CH$_3$)-), 3.22 (-N(C$\underline{H}_3$)$_3$-), 3.39 (-O-C$\underline{H}_3$), 3.42-3.80 (-C$\underline{H}_2$-C$\underline{H}_2$-O-PEG backbone, -C$\underline{H}_2$N-), 3.80-4.13 (-C$\underline{H}$-PBLA backbone), 4.04-4.09 (-POC$\underline{H}_2$-), 4.25-4.30 (-O-CH$_2$-CH$_2$-OP) 4.80-5.30 (-C$\underline{H}_2$-(CH$_2$)$_6$-PBLA side chain), 7.02-7.50 (-CH$_2$-(C$\underline{H}_2$)$_6$-PBLA side chain).

4.2.5. Preparation of phosphocoline-PEG-*b*-poly(L-aspartate) copolymer (SH-PEG-PAsp)

PBLA groups in PC-PEG-PBLA (3.1 µmol, 100 mg) were deprotected with 10 mL of 1 M NaOH*aq* and the solution was stirred for 1 h at 4 ℃. It was dialyzed with a dialysis membrane (Spectra/Pro 6 Membrane: MWCO, 6,000-8,000) against pure water 6 times. The residue was freeze-dried to obtain PC-PEG-NH$_2$. The yield of obtained polymer after purification was 100%; number-averaged molecular weight (*Mn*) = 23,923. ^{1}H-NMR (D$_2$O): δ (ppm) = 1.21-1.24 (-CH-(C$\underline{H}_3$)-C(=O)), 2.50-2.82 (-C$\underline{H}_2$-C$\underline{H}_2$-S-C$\underline{H}_2$-C$\underline{H}$(CH$_3$)-), 3.22 (-N(C$\underline{H}_3$)$_3$-), 3.39 (-O-C$\underline{H}_3$), 3.42-3.80 (-C$\underline{H}_2$-C$\underline{H}_2$-O-PEG backbone, -C$\underline{H}_2$N-), 4.04-4.09 (-POC$\underline{H}_2$-), 4.25-4.30 (-O-CH$_2$-CH$_2$-OP).

4.2.6. Synthesis of poly(β-benzyl-L-aspartate) homopolymer (Homo-PBLA)

n-butylamine (0.10 mmol,73 µL) was diluted with DCM before the addition of BLA-NCA (5.0 mmol, 1.3 g), which was dissolved in 20 mL of mixing solvent of DCM and DMF (v/v = 10) and the solution was stirred for 3 days at 35 ℃. It was added to the excess amount of mixing solvent of hexane and ethyl acetate (v/v = 1) to precipitate the polymer. The polymer was dried under the reduced pressure to obtain Homo-PBLA. The yield of Homo-PBLA was determined to be 55%; number-averaged molecular weight (*Mn*) = 11,275. ^{1}H-NMR (D$_2$O): δ (ppm) = 1.70-2.70

(-C$\underline{H_2}$-PBLA side chain), 3.80-4.13 (-C$\underline{H}$-PBLA backbone), (-C$\underline{H_2}$-(CH$_2$)$_6$-PBLA side chain), 7.02-7.50 (-CH$_2$-(C$\underline{H_2}$)$_6$-PBLA side chain).

4.2.7. Synthesis of poly(aspartate-amino-pentane) homopolymer (Homo-P(Asp-AP))

Homo-PBLA (55 µmol, 500 mg) was dissolved in N-methyl-2-pyroridone (NMP, 10 mL) before the addition of benzene (50 mL) and the solution was frozen to dry polymers. NMP (10 mL) was added to the dried polymer and 1, 5-diaminopentane (5.5 mmol, 0.64 mL) was added to the polymer solution on the water bath at 13 ºC. After 1 h reaction, the solution was neutralized with 5 M HClaq and the solution was dialyzed with a dialysis membrane (Spectra/Pro 6 Membrane: MWCO, 6,000-8,000) against pure water 6 times. The residue was freeze-dried to obtain PC-PEG-NH$_2$. The yield of obtained polymer after purification was 100%; number-averaged molecular weight (Mn) = 10,890.

4.2.8. Preparation of azido-PEG-b-PECH copolymer (N$_3$-PEG-PECH)

α-azido-ω-amino-poly(ethylene glycol) (N$_3$-PEG-NH$_2$) with 12,000 Da was synthesized as previous report [9]. N$_3$-PEG-NH$_2$ (8.3 µmol, 100 mg) was dissolved in 100 mL of toluene and the solution was dried under the reduced pressure with heating at 180 ºC. The dried polymer was dissolved in 4.2 mL of toluene and triisobutylaluminum (8.3 µmol) and epichlorohydrin (0.83 mmol) were added to the solution to initiate the polymerization. After 2 days reaction, ethanol was added to the reaction solution and ether precipitation was performed by adding the reaction solution to the excess amount of ether (100 mL) before removal of residual ether to obtain N$_3$-PEG-PECH. The yield of obtained polymer after purification was 80% based on the elemental

analysis of chlorine in PECH segments; number-averaged molecular weight (Mn) = 19,402, molecular weight distribution (MWD) = 1.05.

4.2.9. Preparation of azido-PEG-*b*-poly(glycidol) copolymer (N_3-PEG-PGlycidol)

N_3-PEG-PECH (5.2 µmol, 100 mg) was dissolved in 5 mL of methanol before the addition of 5 mL of 1 M NaOHaq and the solution was stirred for 1 day. It was dialyzed with a dialysis membrane (Spectra/Pro 6 Membrane: MWCO, 6,000-8,000) against 0.01 M HClaq 3 times and pure water 3 times. The residue was freeze-dried to obtain PEG-PGlycidol. The yield of the reaction was determined to be 88% based on the elemental analysis of chlorine in PGlycidol segments; number-averaged molecular weight (Mn) = 17,922, molecular weight distribution (MWD) = 1.05.

4.2.10. Preparation of amino-PEG-*b*-poly(glycidol) copolymer (NH_2-PEG-PGlycidol)

N_3-PEG-PGlycidol (5.6 µmol, 100 mg) was dissolved in 10 mL of DMF and triphenylphosphine (56 µmol) was added to the solution and the solution was stirred for 1 day. Ether precipitation was performed by the addition to the excess amount of water (1 L) and the solution was stirred for extra 1 day. After the filtration to remove the precipitation, the solution was dialyzed with a dialysis membrane (Spectra/Pro 6 Membrane: MWCO, 6,000-8,000) against pure water 6 times. The residue was freeze-dried to get NH_2-PEG-PGlycidol. The yield of amination was calculated to be 90% by fluorescamine with the standard curve prepared by n-butylamine; number-averaged molecular weight (Mn) = 17,922, molecular weight distribution (MWD) = 1.05.

4.2.11. Preparation of PC-PEG-*b*-poly(glycidol) copolymer (PC-PEG-PGlycidol)

NH₂-PEG-PGlycidol (5.6 µmol, 100 mg) was dissolved in 10 mL of DMF before the Ar bubbling, followed by the addition of DIPA (56µmol) and MPC (56µmol), and the solution was stirred for 48 h at 100 °C. It was dialyzed with a dialysis membrane (Spectra/Pro 6 Membrane: MWCO, 6,000-8,000) against pure water 6 times. The residue was freeze-dried to get PC-PEG-PGlycidol. The yield of the reaction to install PC was determined to be 90% by fluorescamine with the standard curve prepared by n-butylamine; number-averaged molecular weight (Mn) = 18,106.

4.2.12. Preparation of PC-PEG-*b*-poly(glycidyl tryptophan (Fmoc)) copolymer (PC-PEG-PGTrp(Fmoc))

PC-PEG-PGlycidol (5.5 µmol,100 mg) was dissolved in 10 mL of DMF before the addition of 4-dimethylaminopyridine (4.4 mmol, 538 mg), 1-(3-dimethylaminopropyl)-3-ethylcordiimide hydrochloride (4.4 mmol, 684 mg) followed by N-[(9H-fluoren-9-ylmethoxy)carbonyl]tryptophan (4.4 mmol, 1.7 g), and the solution was stirred for 1 day. Ether precipitation was performed by adding the reaction siolution to the excess amount of diethyl ether (200 mL). The polymer was dried to get PC-PEG-PGTrp(Fmoc). The yield of amino acid installation was determined to be 98%; number-averaged molecular weight (Mn) = 42, 760, molecular weight distribution (MWD) = 1.05.

4.2.13. Preparation of PC-PEG-*b*-poly(glycidyl tryptophan) copolymer (PC-PEG-PGTrp)

PEG-PGTrp (100 mg) were dissolved in 10 mL of mixing solution of piperidine and DMF (v/v = 1) and the solution was stirred for 1 day. Ether precipitation was performed by the addtion

to the excess amount of diethyl ether (200 mL). The purification by drying under the reduced pressure was performed to get PEG-PGTrp. The yield of obtained polymer after purification was 100%; number-averaged molecular weight (Mn) = 21, 862.

4.2.14. PC ligand installed PIC micelle preparation

PC-PEG-PAsp and Homo-P(Asp-AP) were mixed in 10 mM phosphate buffer (pH 7.4) at the stoichiometric N/P ([COOH in PAsp]/[NH$_2$ in P(Asp-AP)]). 1-(3-dimethylaminopropyl)-3-ethylcordiimide hydrochloride (EDC, 10 mg/mL) in 10 mM phosphate buffer (pH 7.4) was added to the PIC solution and the solution was allowed to react for 1 overnight. After ultrafiltration of PIC, the size and the PDI were checked by DLS measurement. Also, the zeta potential was measured by electrophoretic light scattering (ELS).

4.2.15. Cellular uptake study of PC micelles

BxPC3 cells were cultured with Roswel Park Memorial Institute medium (RPMI1640) with 10% FBS and 1% penicillin/streptomycin (Sigma-Aldrich, St. Louis, MO, USA). The cells were seeded on the 96-well plate and cultured for 24 h. Then, micelle solution with Cy3 or Cy5 fluorescence (fluorescence intensity: 1,000) was added to the medium. For competitive assay with free PC molecules, PC (100 nM) was also added to the medium. For inhibition assay with PLTP inhibitor, thimerosal [10 nM] was added to the cell medium. In the case of the investigation of uptake pathway, endocytosis was inhibited at 4 °C. After different time points, the cell was washed with PBS 3 times and Hoechst33342 (10 uL/well) was added to the medium and after 15 min incubation, the cells were washed with PBS once before the addition of fresh cell culture medium.

Fluorescence derived from Hoechst33342, Cy3 and Cy5 was observed by conforcal laser scanning microscopy (CLSM, LSM780, Car Zeiss, Germany).

4.2.16. mRNA-loaded micelle preparation

PC-PEG-PGTrp, polymers with no ligand (MeO-PEG-PGTrp), PEG-PLL and mRNA were dissolved in 10 mM HEPES buffer (pH 7.3), and polymers and mRNA solutions were mixed at a molar ratio of primary amines in polymers to phosphate groups in mRNA (N/P) of 3. The hydrodynamic diameter and PDI were measured by DLS measurement.

4.2.17. *In vitro* gene expression of mRNA introduced by PIC micelles

The BxPC3 cells were seeded onto 96-well plates at a density of 5,000 cells/well. After 24 h incubation, the culture medium was exchanged and 2 μg of GLuc mRNA was added to the medium. After 24 h incubation, the medium was collected to quantify the GLuc secretion between 0 h and 24 h. The GLuc expression levels in the medium were measured using the Renilla Luciferase Assay System (Promega) and the GloMax 96 microplate luminometer (Promega).

4.3. Results and Discussion

First, we synthesized PC-PEG-NH2 by Michael addition reaction [8], followed by the polymerization of PBLA segments and the deprotection of the benzyl groups in the side chains to obtain PC-PEG-PAsp (**Scheme 1**). For PC-PEG-NH$_2$, the MPC was added to the SH-PEG-NH$_2$ in

the presence of the catalyst, DIPA, and the reaction was stirred for 48 h. The introduction ratio of

phosphocoline to PEG was determined to be 98 % by ¹H-NMR analysis (**Figure 1**).
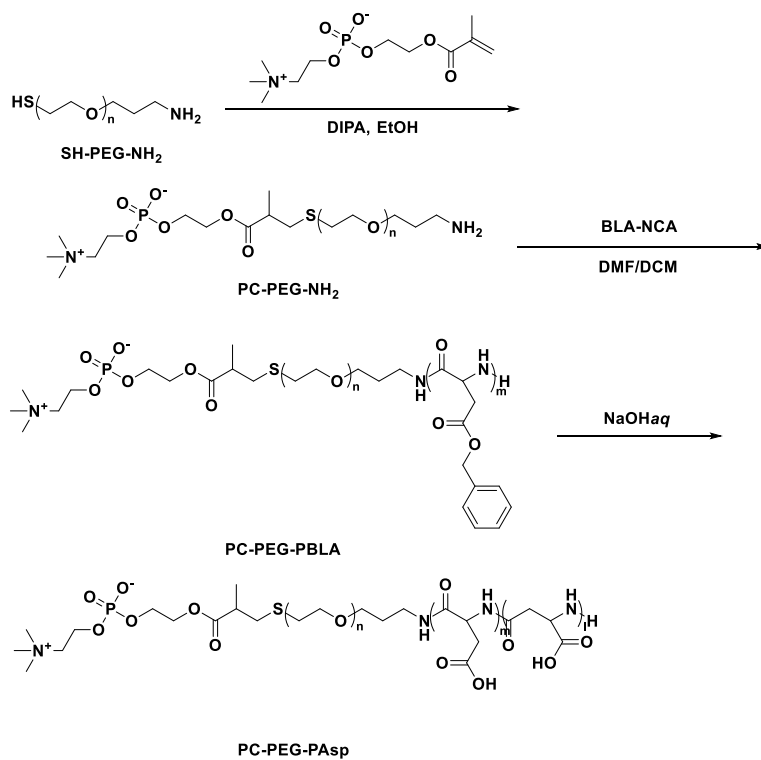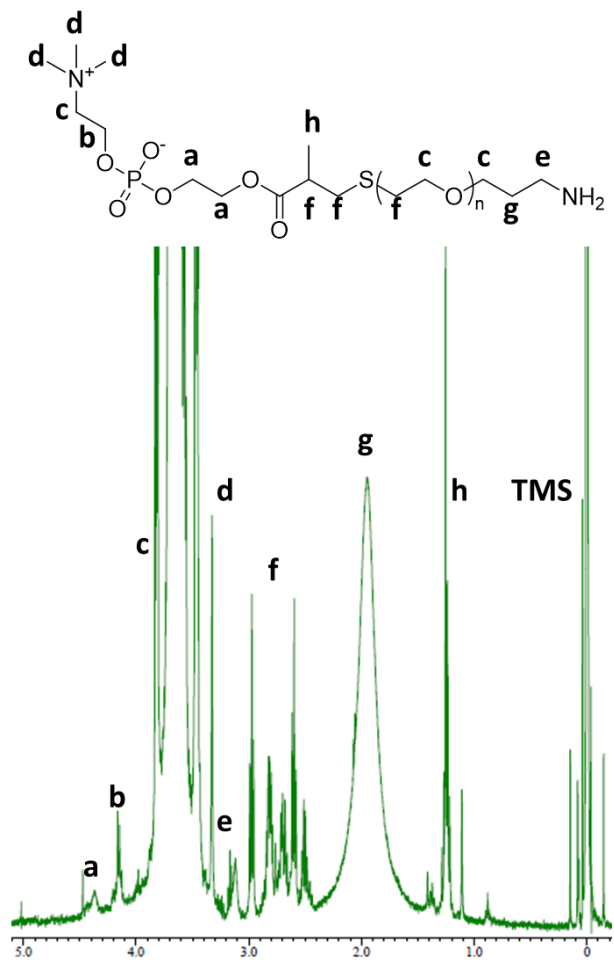

Scheme 1. *Synthesis scheme of PC-PEG-PAsp.*

Figure 1. ^{1}*H-NMR spectrum of PC-PEG-NH$_2$.*

After preparing PC-PEG-NH$_2$, PBLA-NCA was added to primary amine to obtain PBLA chains with 80 DP, and the solution was stirred at 35 ℃. The DP of PBLA segments was calculated to be 88 by ^{1}H-NMR analysis (**Figure 2**), indicating PC molecules did not interfere with the polymerization of BLA-NCA.
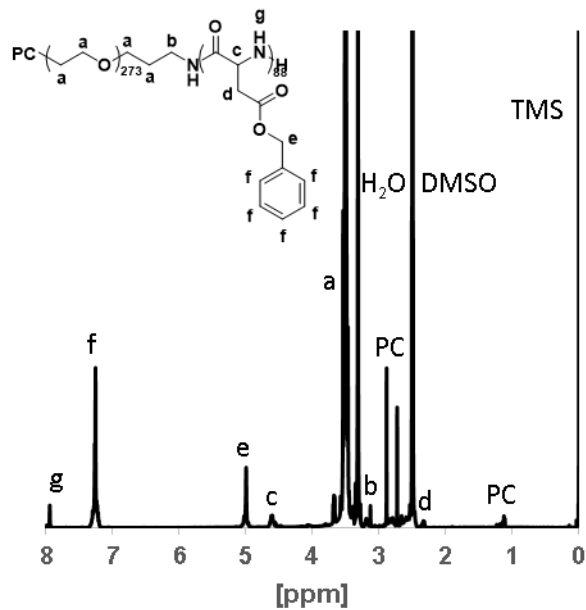
Figure 2. *^{1}H-NMR of PC-PEG-PBLA.*

After preparing PC-PEG-PBLA, the solution of 1 M NaOHaq was added at 10 equivalent to BLA units and the solution was allowed to stir for 1 h to obtain PC-PEG-PAsp. The detachment of benzyl ester in the side chain of PBLA segments was confirmed by ^{1}H-NMR analysis and sharp molecular weight distribution was confirmed by GPC measumrent (**Figure 3**).
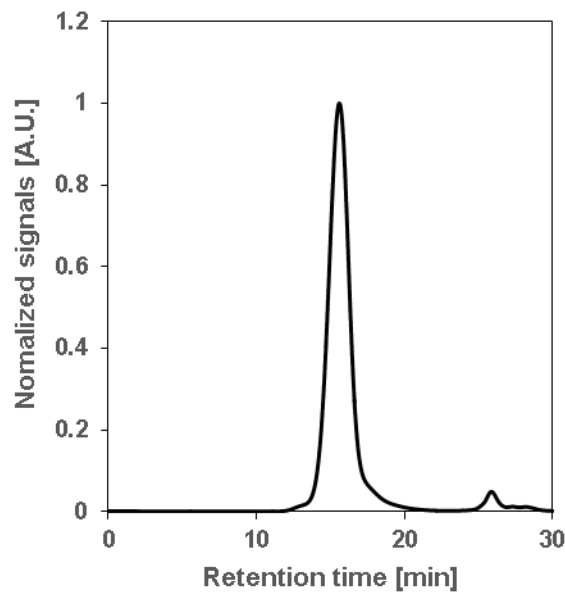
Figure 3. *GPC spectrum of PC-PEG-PAsp.*

Next, we synthesized polycation, Homo-P(Asp-AP) by NCA polymerization with n-buthyl amine as an initiator and BLA-NCA, followed by the aminolysis of PBLA segments by 1, 5-diaminopentane (DAP) with primary amine (**Scheme 2**). For Homo-PBLA synthesis, BLA-NCA was added at 100 equivalent to the initiator , in this case, n-buthylamine. After 3 days reaction, hexane precipitation was perfomed to obtain Homo-PBLA. The DP of PBLA segments was calculated to be 55 by ^{1}H-NMR analysis (**Figure 4**). Then, the aminolysis of the benzyl ester of PBLA segments was performed in the presence of primary amine, DAP. DAP was added at 100 equivalent to PBLA units because DAP has 2 primary amines, which may induce the cross linking of polymers or PBLA units in one polymer, and the reaction was performed at low temperature for the same purpose. The detachment of benzyl ester in the side chain of PBLA segments was confirmed by ^{1}H-NMR analysis (**Figure 5**), indicating the aminolysis was completely proceeded. The obtained product showed narrow molecular weight distribution in GPC chromatogram

(**Figure 6**), indicating no cross-linking was induced during aminolysis because of low temperature and polymer concentration.
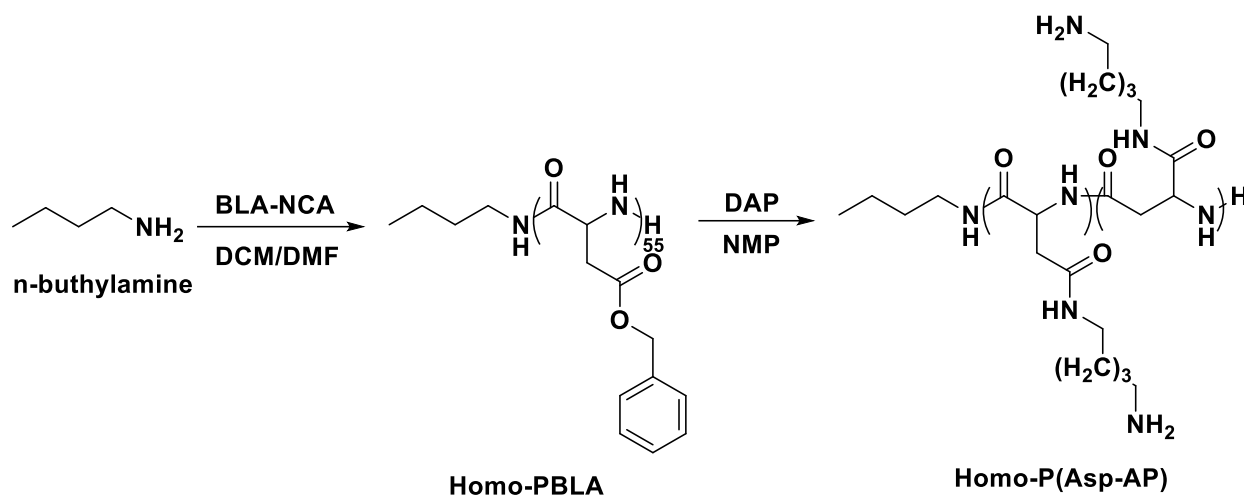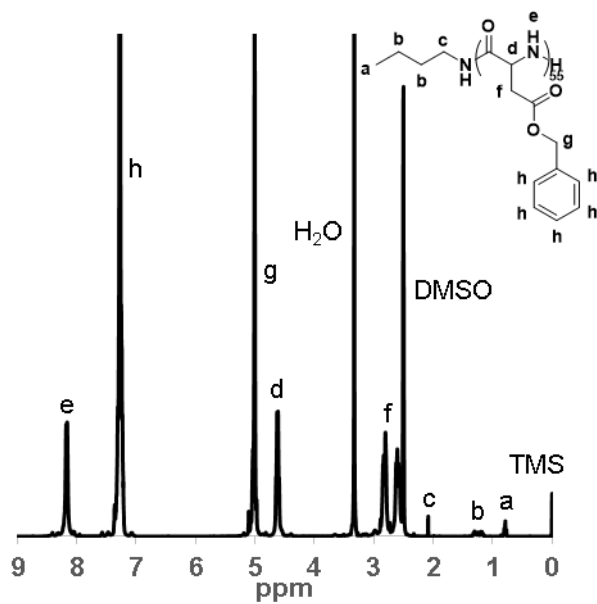

Scheme 2. *Synthesis scheme of Homo-P(Asp-AP).*
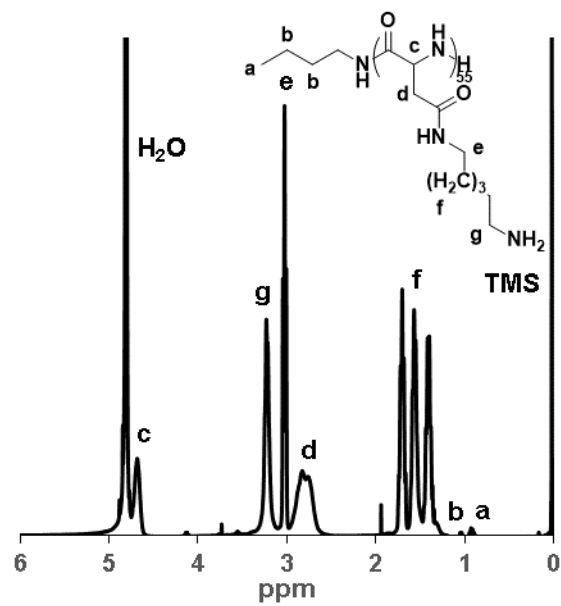

Figure 4. *^{1}H-NMR spectrum of Homo-PBLA.*

Figure 5. *¹H-NMR spectrum of Homo-P(Asp-AP).*

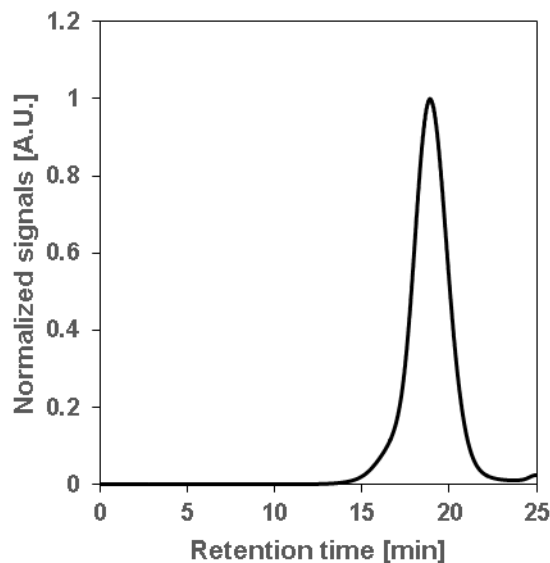*The chemical structure shows only α-aspartate.*

Figure 6. GPC chromatogram of Homo-P(Asp-AP).

Next, we attemeted to prepare the PIC micelles by mixing PC-PEG-PAsp and Homo-P(Asp-AP). Note that by engineering no ligand ionomers, in this case, MeO-PEG-PAsp, we can control the density of the ligand on the surface of PIC micelles. Regarding previpus report [11], we assumed that PIC micelles with 25 % density of PC ligands may keep the stealth effect of PEG. Therefore, for polyanion, we mixed the MeO-PEG-PAsp and PC-PEG-PAsp at the ratio of 3, and we mixed with Homo-P(Asp-AP) as polycation to form PIC micelles. After preparation, primary amine and carboxylate in the core of micelles were cross linked by EDC not to dissociate the complex both *in vitro* and *in vivo* conditions. If PIC micelles dissociate before passing cell membrane, polycation segments promote the cellular uptake by interacting with negatively charged phopholipids. After EDC cross linking, PIC micelles were characterized by both DLS and ELS (**Table 1**). PC micelles with sharp size distribution showed comparable size with MeO micelles, indicating PC ligands had no effect on the complexation of oppositely charged polymers.

ELS measurements showed PC micelles showed similar zeta potential with MeO micelles, indicating PC molecules with betain structure had no effect on the surface propeties.

Table 1. *Characterization of PC ligands installed PIC micelles.*

Polymer	Cumulant diameter [nm]	Polydispersity index	Zeta potential [mV]
PC-PEG-PAsp	46	0.06	0.71
MeO-PEG-PAsp	42	0.06	-0.12

After preparing proves to investigate the ligand effect, the cellular uptake study was performed. We hypothesized PC ligands may inteact with PLTP receptors on the surface of the pancreatic cancer cells so we cultured BxPC3 cells and PC micelles with fluorescence were added to trace the kinetics of the cellular uptake . PC micelles showed rapid cellular uptake comparing with micelles with no ligand, indicating the cellular uptake in cultured pancreatic cancer cells was promoted by PC ligands (**Figure 7, 8**). To confirm the effect of the PC ligands, we performed the competitive assay with free PC molecules and PC micelles were compromised by free PC molecules (**Figure 7, 8**), indicating PC ligands on the surface of the PIC micelles played an important role in cellular uptake.
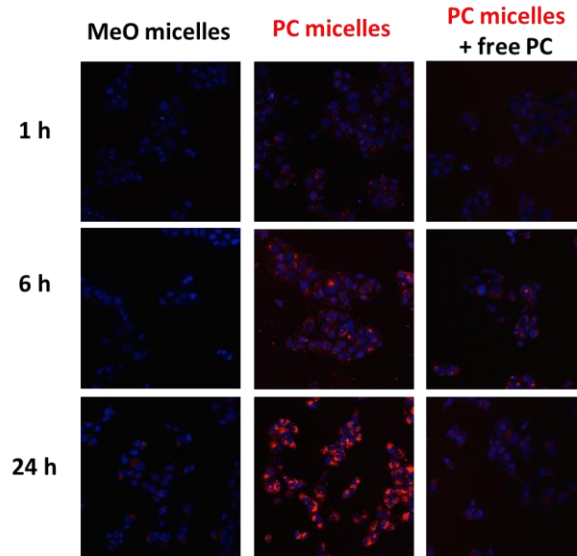
Figure 7. *The cellular uptake of PC micelles in cultured pancreatic cancer BxPC3 cells.*
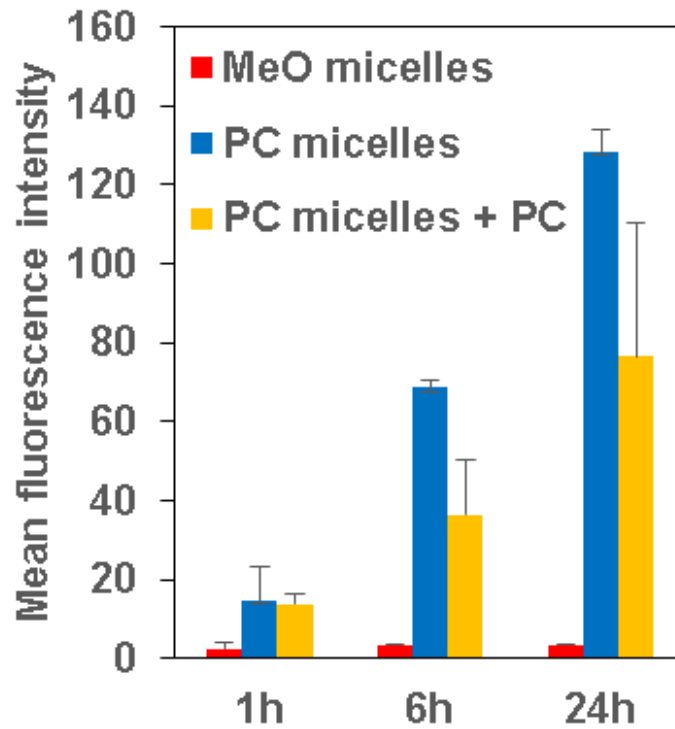
Figure 8. *Quantification of fluorescence signals in **Figure** 7.*

Moreover, we conducted the inhibition assay with PLTP inhibitor, thiomersal [11] to clarify the interaction of PC ligands with PLTP. After the inhibition of PLTP, the fluoresence signals corresponding to PC micelles were significantly decreased (**Figure 9, 10**), indicating the cellular uptake of PC micelles was promoted by the interaction between PC ligands and PLTP on the cell surface. To investigate the mechanism of the internalization of PC micelles, we decreased the temperature during the cellular uptake of PC micelles. Endocytosis is known as a passway to uptake nanoparticle and it depends on the thermodynamical energy in phyological conditions. After decreasing the temperature, the cellular uptake of PC micelles was inhibited (Figure 5, 6), indicating that PC micelles interact with PLTP on the cell surface to increase the chance of uptake by endocytosis.

1 h

PC micelles

PC micelles
+ thiomersal

PC micelles
at 4°C
inhibiting
endocytosis

Figure 9. *The mechanism study of PC micelles with thiomersal and decreased temperature.*
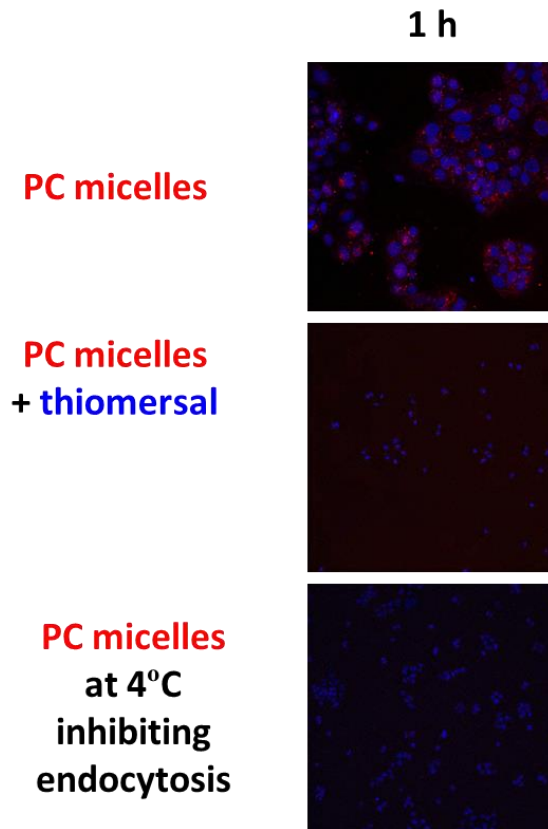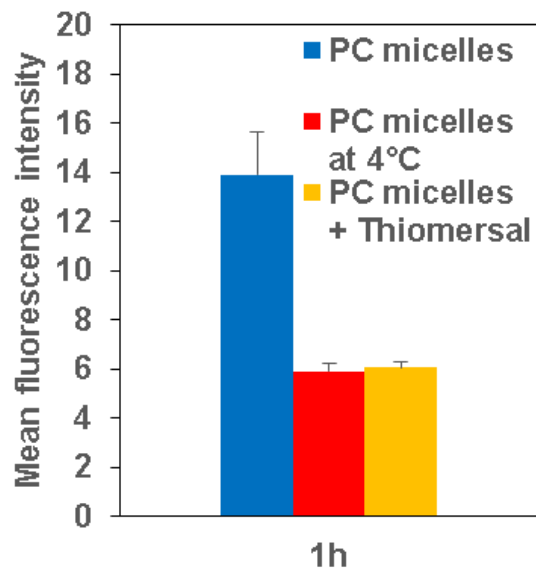
Figure 10. *Quantification of fluorescence signals in* *Figure 9*.

These observations promoted us to attach PC ligands to our mRNA system or PEG-PGTrp block ionomers. To functionalize the surface of the PIC micelles, we engineered azide froups in α-end of PEG for orthogonal chemistry. We synthesized N_3-PEG-PECH with a macroinitiator of N_3-PEG-OH before converting azide groups to primary amine for Michael addition reaction with MPC and converting clorine to hydroxyl groups for the attachment of tryptophan (**Scheme 3**). Water molecules in PEG may affect the ROPs of epichlorohydrin so N_3-PEG-OH was dried in toluene solution with heating at 180 ℃ before the addition of epichlorohydrin at 100 equivalent to the initiator. The 80 segments of PECH segments were confirmed by the elemental analysis of chlorine. Next, to convert chlorine to hydroxyl groups, the solution of 1M NaOH*aq* was added and the reaction solution was allowed to react for 1 day. The conversion of chlorine groups to hydroxyl groups was confirmed by the disapparance of chlorine in PECH segments. For PC conjugation, azide groups in in α-end of PEG were converted to primary amine by triphenylphosphine (TPP). TPP was added at 10 equivalent to the polymer solution in DMF, followed by the hydrolysis of TPP molecules, which were attached to the polymer to reduce the azide groups. The conversion of azide groups to primary amine was confirmed by fluorescamine, which produces the fluoresence to detect the primary amine. Primary amine is known as hard nucleophile, which is difficult to react with electrophile, in this case, MPC, comparing with thiol groups, which are known as soft nucleophile. Thus, after the addition of MPC at 10 equivalent to polymer solution, the solution was allowed to react at higher temperature, 100 ℃. The introduction ratio of PC molecules to polymers was calculated to be 90 % from the decrease of the primary amine, which was confirmed by fluorescamine with standard carves prepared by n-buthylamine. After the preparation of PC-PEG-PGlycidol, tryptophan was introduced as before.

Scheme 3. *Synthesis scheme of PC-PEG-PGTrp.*
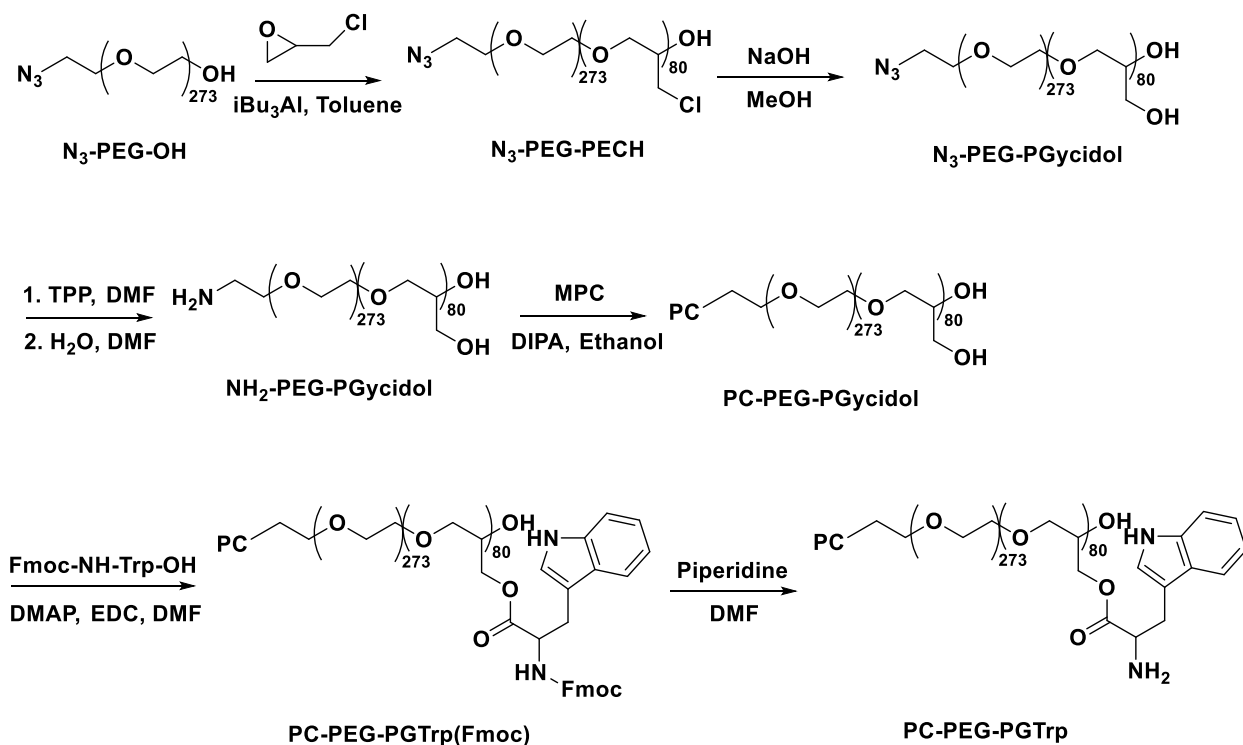
Next, we attempted to prepare the mRNA-loaded PIC micelles with PC ligands by mixing the PC-PEG-PGTrp and mRNA in 10 mM Hepes buffer (pH 7.3) and characterized by DLS (**Table 2**). PC micelles showed the narrow size distribution and comparable size with MeO micelles, indicating PC molecules had no impact on the formation of PIC micelles.

Table 2. *Characterization of mRNA-loaded PIC micelles with PC ligands.*

Sample	Cumulant diameter [nm]	Polydispersity index	Association number of mRNA
PEG-PLL/mRNA	52	0.18	1.6
MeO-PEG-PGTrp/mRNA	59	0.18	1.9
PC-PEG-PGTrp/mRNA	54	0.17	1.9

Finally, we investigated the effect of PC ligands on the gene expression in pancreatic cancer BxPC3 cells. GLuc mRNA was encapsulated to PC micelles before the transfection of BxPC3 cells. After 24 h incubation, the luminescence intensity of supernatant was measured by luminometer. Comparing with MeO micelles, PC-PEG-PGTrp micelles showed higher gene expression in BxPC3 cells (**Figure 11**), indicating the cellular uptake of highly stabilized PEG-PGTrp micelles was promoted, resulting in high efficacy of intact mRNA internarization.

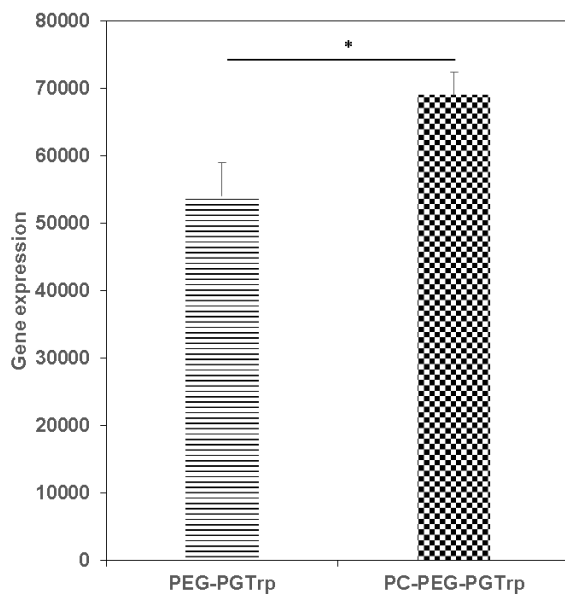***Figure 11.*** *The gene expression of PC-PEG-PGTrp micelles in cultured BxPC3 cells (*P<0.05).*

4.4. Conclusion

We developed a platform to investigate the ligand effect on targeting ability by engineering PIC micelles highly stabilized by EDC cross linking. PC formulations showed significant cellular uptake in cultured pancreatic cancer cells and competitive assay with free molecules confirmed

the effect of PC ligands on the surface of PIC micelles. Our hypothesis of the interaction between PC ligands and PLTP receptors was supported by the inhibition assay of PLTP by thiomersal, which significantly inhibited the cellular uptake of PC micelles. The cellular uptake passway of PC micelles was also clarified by low temperature incubation, indicating endocytosis played an important role in the cellular uptake of PC micelles. After the installation of PC ligands to our mRNA-loaded PIC micelles, PC ligands had no effects on the phycochemical properties of PIC micelles and PC formulations showed high transfection in cultured pancreatic cancer cells. Our results indicated that PC ligand is the promising way to target intractable pancreatic tumors and by incorporating with therapeutic mRNA, PC installation will enhance the ability of active targeting to show the therapeutic outcomes *in vivo* conditions.

4.5. References

[1] C. E. Thomas, A. Ehrhardt and M. A. Kay, Progress and problems with the use of viral vectors for gene therapy. *Nat. Rev. Genet.* **4** (2003) 346–358.

[2] K. J. Kauffman, J. R. Dorkin, J. H. Yang, M. W. Heartlein, F. DeRosa, F. F. Mir et. al., Optimization of lipid nanoparticle formulations for mRNA delivery in vivo with fractional factorial and definitive screening designs. *Nano Lett.* **15** (2015) 7300–7306.

[3] S. Uchida, H. Kinoh, T. Ishii, A. Matsui, T. A. Tockary, K. M. Takeda, H. Uchida, K. Osada, K. Itaka and K. Kataoka, Systemic delivery of messenger RNA for the treatment of pancreatic cancer using polyplex nanomicelles with a cholesterol moiety. *Biomaterials* **82** (2016) 221-228.

[4] A. Gabizon, H. Shmeeda and Y. Barenholz, Phamacokinetics of pygylated liposomal doxorubicin. *Clin. Phrmacokinet.* **42** (2003) 419-436.

[5] R. Bazak, M. Houri, S. E. Achy, S. Kamel and T. Rafaat, Cancer active targeting by nanoparticles: a comprehensive review of litarature, *J. Cancer Res. Clin. Oncol.* **141** (2015) 769-784.

[6] S. Nie, A. Lo, J. Wu, J. Zhu, Z. Tan, D. D. Simeone et. al., Glycoprotein biomarker panel for pancreatic cancer discovered by quantitative proteomics analysis. *J. Proteome Res.* **13** (2014) 1873-1884.

[7] I. Filipuzzi, S. Catesta, F. Perruccio, B. Knapp, Y. Fu, C. Studer et. al., High-resolution genetics identifies the lipid transfer protein as target for antifungal ergolines. *PLoS Genet.* **12** (2016) 1-19.

[8] R. Matsuno, K. Takami and K. Ishihara, Simple synthesis of a library of zwitterionic surfactants via Michael-type addition of methacrylate and alkane thiol compounds. *Langmuir* **26** (2010) 13028-13032.

[9] S. Hiki and K. Kataoka, Versatile and selective synthesis of "click chemistry compatible heterobifunctional poly(ethylene glycol)s possessing azide and alkyne functionalities. *Bioconjugate Chem.* **21** (2010) 248-254.

[10] Y. Miura, T. Takenaka, K. Toh, S. Wu, H. Nishihara, M. R. Kano, Y. Ino, T. Nomoto, Y. Matsumoto, H. Koyama, H. Cabral, N. Nishiyama and K. Kataoka. Cyclic RGD-linked polymeric micelles for targeted delivery of platinum anticancer drugs to glioblastoma through the blood-brain tumor barrier. *ACS nano* **7** (2013) 8583-8592.

[11] B. Marchi, B. Burlando, M. N. Moore and A. Viarengo, Mercury- and copper-induced lysosomal membrane destabilization depends on [Ca2+] dependent phospholidase as activation. *Aquatic Toxicology* **66** (2004) 197-204.

Chapter5

Development of one-pot preparation of

PEG-poly(amino acid) and PEG-poly(glycidyl ether)

5.1. Introduction

Block copolymers have been studied to make a progression in both basic research and its application in the field of physics, chemistry, materials, biology and medicine [1, 2]. In the field of biology and medicine, block copolymers comprising PEG and PAA segments have been considered as a novel candidate of building units of biocompatible 3D structure (e.g. polymeric micelles) to encapsulate several kinds of therapeutic agents [3, 4]. For example, PEG-poly(L-glutamic acid) (PEG-P(Glu)) block copolymer can encapsulate platinum-based anti-cancer drug to prepare polymeric micelles, which is under the clinical trials for solid tumors treatment [5], and PEG-poly(L-lysine) (PEG-P(Lys)) can load therapeutic oligonucleotides, such as plasmid DNA (pDNA), small interfering RNA (siRNA) and messenger RNA (mRNA), *via* electrostatic interactions to form polyion complex (PIC) micelles [6, 7]. There are several reaction and purification steps in conventional method to prepare PEG-PAA, including synthesis of PEG-segment by ring-opening polymerization (ROP), amination of hydroxyl groups in the end of PEG and ROP of N-carboxyanhydride (NCA) to elongate the PAA segments [8]. Because of several steps in PEG-PAA preparation, high cost and long-time preparation have limited the design of PEG-PAA. On the other hand, the development of one-pot preparation of PEG-PAA is a promising way to reduce cost, time and commercial burden.

To prepare PEG-PAA in one-pot reaction, we propose a new method to elongate PAA segments by ROP with alcohol initiators, in this case PEG with hydroxyl terminus. For alcohol initiated NCA polymerization, we focus on the organo-base, which is known as a catalyst to activate alcohol groups in initiators and monomers, including epoxides and NCAs [9, 10]. Previous paper showed the efficient activation of alcohol initiators by neutral organo-catalyst or 1, 1, 3, 3-tetramethylguanidine (TMG) to elongate polypeptoid by NCA polymerization [11]. However, the

utility of TMG for activation of alcohol groups to elongate polyether by ROP of epoxides Thus, in this study, we investigated the possibility of TMG for proceeding the polymerization of epoxides including ethylene oxide, epichlorohydrin and 1, 2-epoxy-5-hexene by using TMG as the catalyst and developed a one pot approaches to synthesize PEG-polyether (**Scheme 1, 2, 3**). Then, we examined the utility of TMG to elongate both PEG and PAA in one-pot manner, in this time BLG-NCA for PEG-PBLG preparation and Lys-TFA-NCA for PEG-PLL synthesis (**Scheme 5, 6**). The obtained polymer showed not only controlled the degree of polymerization (DP) and molecular weight distribution but also degradable ester bonds between PEG and PAA segments, which cannot be found in block copolymers prepared by conventional method. This spontaneous formation of ester bonds promoted us to investigate the possibility of hydrolysis of ester bonds in physiological conditions to reduce the cytotoxicity and enhance the cellular uptake in cells, which is an issue of PEG dilemma. For *in vivo* applications, we also examined the effect of this hydrolysable ester bonds on pharmacokinetics of polymeric micelles prepared with block copolymers in one-pot reaction. These observation will broaden the applicability of block copolymers by reducing the industrial burden and functionalizing supramolecular architectures for medical applications.
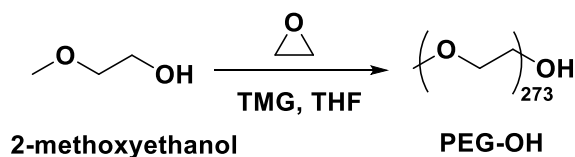
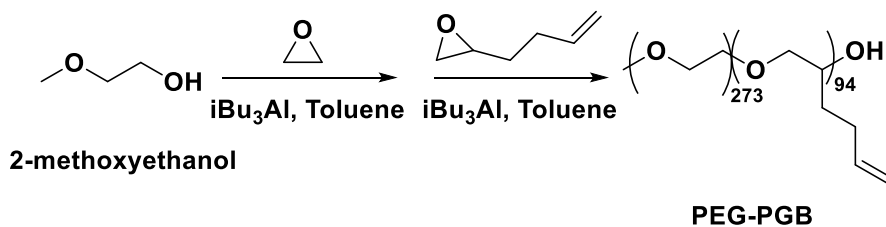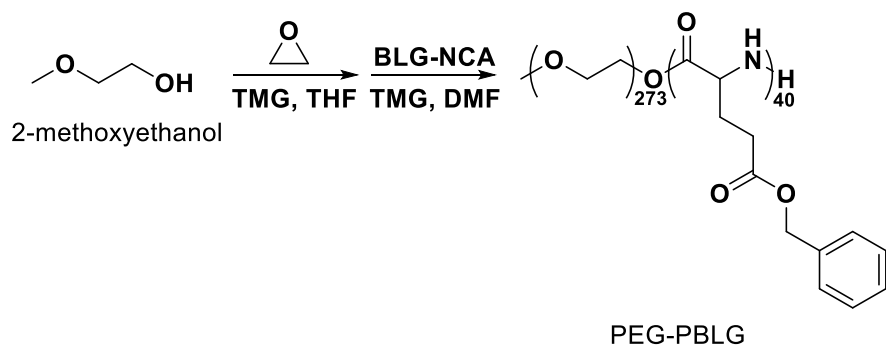**Scheme 1.** *Synthesis scheme of PEG-OH*
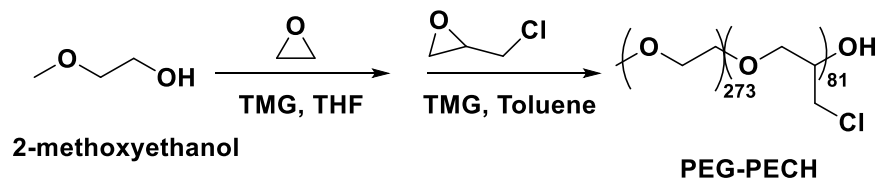
Scheme 2. *Synthesis scheme of PEG-PECH.*
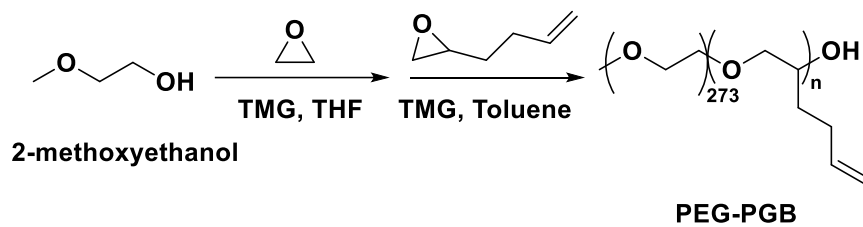
Scheme 3. *Synthesis scheme of PEG-PGB with TMG.*

Scheme 4. *Synthesis scheme of PEG-PGB with triisobutylalminum.*

Scheme 5. *Synthesis scheme of PEG-PBLG.*
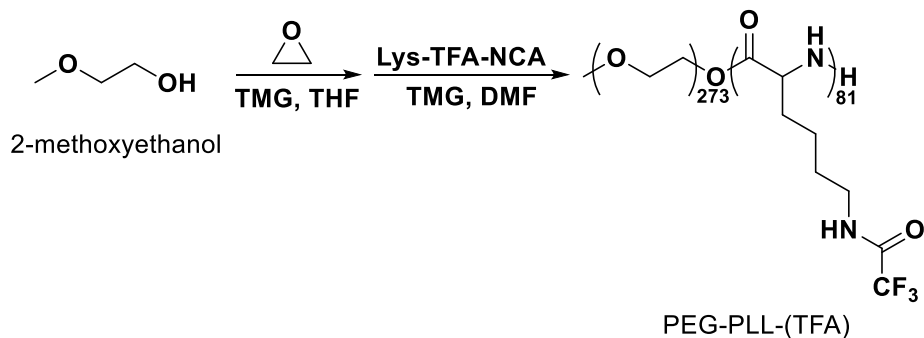
Scheme 6. *Synthesis scheme of PEG-PLL-(TFA).*

5.2. Materials and Method

5.2.1. Materials

Triisobutylaluminum, 2-methoxy-ethanol (purity >99.0%), 1,2-epoxy-5-hexene (purity >96.0%), epichlorohydrin (purity >99.0%) and 1, 1, 3, 3-tetramethylguanidine (purity >99.0%) were bought from Tokyo Chemical Industry Co., Ltd. (Tokyo, Japan) before the purification by distillation with CaH_2. Ethylene oxide (EO) was bought from 3M Japan Co., Ltd. (Tokyo, Japan). N, N-dimethylformamide (DMF) and tetrahydrofuran (THF) as dehydrated solvent were bought from Kanto Chemical, Co., Inc., (Tokyo, Japan). Lithium chloride (purity >99.0%) was bought from Nakalai Tesque Co., Inc. (Kyoto, Japan). Sodium dihydrogenphosphate (purity >99.0%) disodium hydrogenphosphate (purity >99.0%) were bought from FUJIFILM Wako Pure Chemical Co. (Tokyo, Japan). Toluene (purity >99.5%), thiourea (purity >99.0%) and methanol (purity >99.5%) were bought from Sigma-Aldrich (St. Louis, MO, USA). Diethyl ether (purity >99.5%) was bought from Showa ether (Tokyo, Japan). ε-trifluoroacetyl-L-lysine N-carboxyanhydride (Lys-(TFA)-NCA) and γ-benzyl-L-glutamate N-carboxyanhydride (BLG-NCA) were bought from Chuo Kaseihin Co. Inc. (Tokyo, Japan).

5.2.2. Measurements

Gel permeation chromatography (GPC) measurements were conducted with a Tosoh HLC-8220. The GPC system was equipped with a TSKgel G4000H$_{HR}$ column (linear, 7.8 mm × 300 mm; pore size, 20 nm; bead size, 5 µm; exclusion limit, 4×10^5 g/mol), a TSKgel G3000H$_{HR}$ column (linear, 7.8 mm × 300 mm; pore size, 7.5 nm; bead size, 5 µm; exclusion limit, 6×10^4 g/mol), a TSKgel guard column H$_{HR}$-L and a detector for refractive index (RI). DMF containing 10 mM lithium chloride was used as the eluent at a flow rate of 0.5 mL/min at 40 °C.

5.2.3. One-pot preparation of MeO-PEG-*b*-poly(epichlorohydrin) copolymer (PEG-PECH)

1, 1, 3, 3-tetramethylguanidine (1.0 mmol, 130 µL) and 2-methoxyethanol (0.10 mmol, 7.9 µL) were mixed in 60 mL of THF. After 30 min stirring, liquid EO in glass syringe cooled at 0 °C (27 mmol, 1.4 mL) was added to the solution. During the polymerization, ^{1}H-NMR monitor was performed to trace the growth of the PEG chains. The kinetics of EO polymerization with TMG was compared to that of the polymerization of EO using potassium naphthalene (0.13 mmol, 270 µL) prepared following the previous report [12]. The mixture was stirred to react for 2 days at room temperature and dried *in vacuo* to remove the unreacted EO and THF. Epichlorohydrin (100 mmol, 11 mL) in 11 mL of toluene was added to the crude PEG polymer to dissolve in reaction solution. After 30 min stirring, triisobutylaluminum (1.0 µmol, 2 mL) was added to the solution. The mixture was allowed to react for 1 day at room temperature and the polymerization was terminated by the excess amount of ethanol (3 mL). Then, the reaction solution was added for ether precipitation to the excess amount of diethyl ether (400 mL). The recovered polymer was dried under the reduced pressure to obtain PEG-PECH. The yield of PEG-PECH was calculated to be

110

81% based on the elemental analysis of chlorine, number-averaged molecular weight (Mn) = 19,494, molecular weight distribution (MWD) = 1.05.

5.2.4. One-pot preparation of MeO-PEG-b-poly(glycidyl butene) copolymer (PEG-PGB)

1, 1, 3, 3-tetramethylguanidine (1.0 mmol, 130 μL) and 2-methoxyethanol (0.10 mmol, 7.9 μL) were mixed in 60 mL of THF. After 30 min stirring, cooled EO at 0 °C (27 mmol, 1.4 mL) was added to the solution. The mixture was stirred to proceed the reaction for 2 days at room temperature and dried *in vacuo* to remove the unreacted EO and THF. 1, 2-epoxy-5-hexene (100 mmol, 11 mL) in 11 mL of toluene. After 30 min stirring, 1, 1, 3, 3-tetramethylguanidine (1.0 mmol, 130 μL) or triisobutylaluminum (1.0 mmol, 2 mL) was added to the solution. The mixture was allowed to react for 1 day at room temperature and the polymerization was terminated by the excess amount of ethanol (3 mL). Then, the reaction solution was added for ether precipitation to the excess amount of diethyl ether (400 mL). The recovered polymer was dried under the reduced pressure to obtain PEG-PGB. The yield of PEG-PGB of obtained polymer was calculated to be 94%; number-averaged molecular weight (Mn) = 21,212, molecular weight distribution (MWD) = 1.05. ^{1}H-NMR (toluene): δ (ppm) = 1.46-1.94 (-CH_2-CH_2-PGB side chain), 3.39 (-O-CH_3), 3.42-3.80 (-CH_2-CH_2-O-PEG backbone, -CH_2-CH-O-PGB backbone), 4.88-5.13 (-CH_2-CH-PGB side chain), 5.82 (-CH-PGB side chain).

5.2.5. One-pot preparation of MeO-PEG-b-poly(γ-benzyl-L-glutamate) copolymer (PEG-PBLG)

1, 1, 3, 3-tetramethylguanidine (1.0 mmol, 130 μL) and 2-methoxyethanol (0.10 mmol, 7.9 μL) were mixed in 60 mL of THF. After 30 min stirring, cool EO at 0 °C (27 mmol, 1.4 mL) was

added to the solution. During the polymerization, ^{1}H-NMR monitor was performed to trace the growth of the PEG chains. The reaction solution was stirred to react for 2 days at room temperature and dried *in vacuo* to remove the unreacted EO and THF. PEG-PBLG synthesis with conventional method was performed, as follow: macroinitiator PEG-NH$_2$ (0.1 mmol, 1.2 g) with a Mn of 12,000 was dissolved in 18 mL of DMF. Then, BLG-NCA (5.0 mmol, 130 mg) and 1, 1, 3, 3-tetramethylguanidine (1.0 mmol, 130 µL) in 2 mL of DMF with 1 M thiourea were added to the solution. During the polymerization, ^{1}H-NMR monitor was performed to trace the growth of the PBLG segments. After the reaction for 3 days at 35 °C, the ether precipitation was performed by adding the reaction solution to the excess amount of diethyl ether (1.0 L) to obtain the polymer. The recovered polymer was dried under the reduced pressure to obtain dried PEG-PBLG. The yield of PEG-PBLG was calculated to be 86%; number-averaged molecular weight (*Mn*) = 23, 320, molecular weight distribution (MWD) = 1.03. ^{1}H-NMR (DMSO): δ (ppm) = 1.70-2.70 (-C$\underline{H}_2$-C$\underline{H}_2$-PBLG side chain), 3.39 (-O-C$\underline{H}_3$), 3.42-3.80 (-C$\underline{H}_2$-C$\underline{H}_2$-O-PEG backbone), 3.80-4.13 (-C$\underline{H}$-PBLG backbone), 4.80-5.30 (-C$\underline{H}_2$-(CH$_2$)$_6$-PBLG side chain), 7.02-7.50 (-CH$_2$-(C$\underline{H}_2$)$_6$-PBLG side chain). The control polymer having no ester bonds between PEG and PBLG blocks was prepared as previously reported using PEG-NH2 (Mw = 12,000 Da) as the initiator [13].

5.2.6. One-pot reaction of MeO-PEG-*b*-poly(L-Lysine-TFA) copolymer (PEG-PLL(TFA))

Hydroxyl groups in 2-methoxyethanol (0.10 mmol, 7.9 µL) were activated by the addition of 1, 1, 3, 3-tetramethylguanidine (1.0 mmol, 130 µL) in 60 mL of THF. After 30 min stirring, EO cooled by liquid nitrogen at 0 °C (27 mmol, 1.4 mL) was added to the solution. During the polymerization, ^{1}H-NMR monitor was performed to trace the growth of the PEG chains. The reaction solution was stirred to react for 2 days at room temperature and dried *in vacuo* to remove

the unreacted EO and THF. PEG-PLL(TFA) synthesis with conventional method was performed, as follow: macroinitiator PEG-NH$_2$ (0.1 mmol, 1.2 g) with a Mn of 12,000 was dissolved in 18 mL of DMF. Then, Lys-(TFA)-NCA (10 mmol, 2.7 g) was dissolved in 41 mL of DMF with 1 M thiourea were added to the solution before the addition of 1, 1, 3, 3-tetramethylguanidine (1.0 mmol, 130 µL). During the polymerization, ^{1}H-NMR monitor was performed to trace the growth of the PLL(TFA) chains. After the reaction for 3 days at 35 °C, the ether precipitation was performed by adding the reaction solution to the excess amount of diethyl ether (1.0 L). The precipitation was dried under the reduced pressure to obtain PEG-PLL(TFA). The yield of PEG-PLL(TFA) was determined to be 81%; number-averaged molecular weight (*Mn*) = 33, 723, molecular weight distribution (MWD) = 1.03. ^{1}H-NMR (DMSO): δ (ppm) = 1.25-1.77 (-C_H_2-C_H_2-C_H_2-PLL(TFA) side chain), 3.02 (-C_H_2-NH-PLL(TFA) side chain), 3.21 (-C_H-PLL(TFA) backbone) 3.39 (-O-C_H_3), 3.42-3.80 (-C_H_2-C_H_2-O-PEG backbone). The control polymer having no ester bond between the PEG and PLL(TFA) blocks was prepared as previously reported by using PEG-NH$_2$ (M$_w$ = 12,000 Da) as the initiator [14].

5.2.7. Hydrolysis of ester bonds between PEG and PAA segments in physiological conditions

PEG-PBLG (0.43 µmol, 10 mg) was dissolved in 5 mL of DMF before the addition of 5 mL of 10 mM phosphate buffer (pH 7.4) and the solution was stirred at 37 °C. After different time points, the extraction of detached PEG was performed by adding the excess amount of water (100 mL) while removing the PEG-PBLG and the Homo-PBLG as precipitation. The solution was dried under the reduced pressure to obtain the PEG before the GPC measurement with a standard curve prepared by different concentration of PEG.

5.2.8. Preparation of micelles with PEG-PBLG and its stability in physiological conditions

PEG-PBLG (0.86 µmol, 20 mg) was dissolved in 20 mL of methanol before evaporating methanol to prepare the thin film on the bottom of the glass flask. After 20 mL of 10 mM phosphate buffer (pH 7.4) was added to the film, the solution was allowed to sonicate for 30 min. After 3 days incubation at 37 °C, the size and polydispersity index (PDI) of micelles were measured by dynamic light scattering (DLS) measurement. The measurement was performed with a detection angle of 173° at 25 °C.

5.2.9. Bioavailability and biodistribution of micelles prepared with PEG-PBLG in mice

For the preparation of fluorescence-labelled PEG-PBLG, CF647 succinimidyl ester (1.0 µmol), N-hydroxysuccinimide (0.12 mg, 1.0 µmol) and 1-(3-dimethylaminopropyl)-3-ethylcarbodiimide hydrochloride (0.19 mg, 1.0 µmol) were added to PEG-PBLG (20 mg, 1.0 µmol) prepared by one-pot reaction with TMG and the solution was stirred to react for 24 h. Then, the ether precipitation was performed by adding it to the excess amount of diethyl ether (300 mL) and was dried under the reduced pressure to obtain PEG-PBLG-CF647. After the preparation of micelles with PEG-NHCO-PBLG-CF647 or PEG-OCO-PBLG-CF647, the micelle solution (200 µL) was allow to administer in mice by intravenous injection, and the fluorescence in the vein and the tissue were observed by *in vivo* confocal laser scanning microscopy (IV-CLSM, Nikon, Japan) [15]. After 24 h incubation, the mice were sacrificed and the lungs, spleen, muscle, kidney, liver and heart were collects. The microdistribution of the micelles in these organs was examined *ex vivo* by detecting the fluorescence with IV-CLSM.

5.3. Results and Discussion

First, we tried to construct PEG-segments with 2-methoxyethanol, ethylene oxide (EO) and TMG (**Scheme 1**). To the 2-methoxyethanol, EO was added at 273 equivalent aiming to produce PEG with the molecular weight of 12,000 Da before the activation of initiator by TMG. After 48 h reaction, the reaction solution was added to the excess amount of ether to form precipitation as PEG-OH. By ^{1}H-NMR and GPC measurement, the degree of polymerization was calculated to be 273 and the narrow molecular weight distribution was confirmed (**Figure 1 and 2**), indicating initiator was activated by TMG to react with EO to produce PEG-OH with high yield. This is the first time performance of PEG synthesis with TMG.
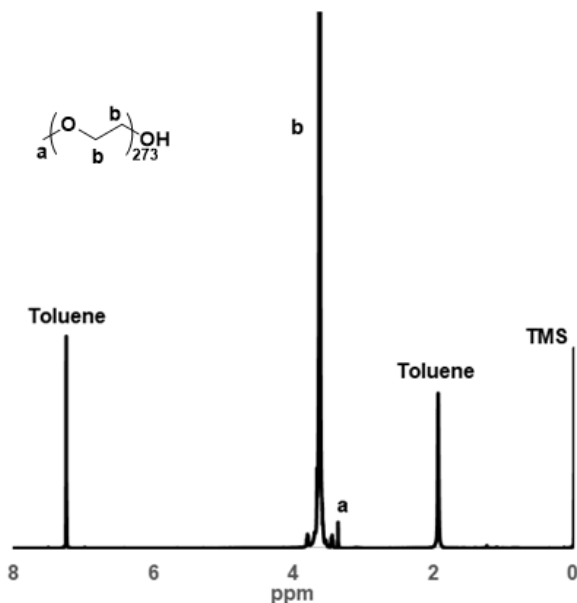

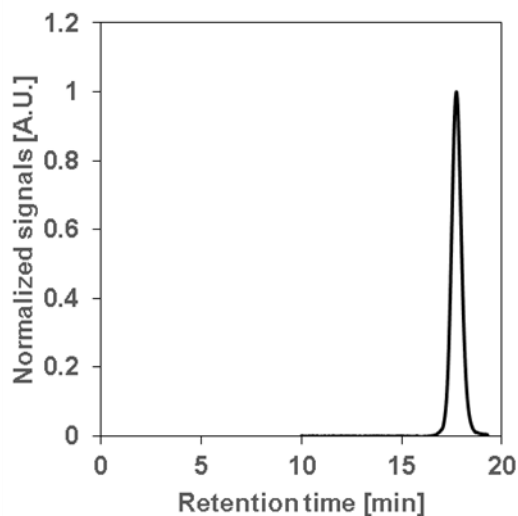**Figure 1.** ^{1}H-NMR spectrum of PEG-OH.

Figure 2. *GPC chromatogram of PEG-OH.*

This observation promoted us to investigate the utility of TMG on other kinds of epoxides including epichlorohydrin and 1, 2-epoxy-5-hexene. We tried to prepare PEG-PECH block copolymer in one-pot reaction with TMG (**Scheme 2**). To the 2-methoxyethanol, EO was added at 273 equivalent aiming to produce PEG with the molecular weight of 12,000 Da before the activation of initiator by TMG. After 48 h reaction, the reaction solution was dried under the reduced pressure before the addition of epichlorohydrin at 100 equivalent and the activation of hydroxyl groups in crude PEG by TMG. After 48 h reaction, the ether precipitation was performed to obtain PEG-PECH as powder. The residual ether in polymer was removed by dry under the reduced pressure. By elemental analysis of chlorine in PECH segments and GPC measurement, the degree of polymerization was calculated to be 81 and the narrow molecular weight distribution was confirmed (**Figure 3**), indicating initiator was activated by TMG to react with epichlorohydrin to produce PEG-PECH with relatively high yield. This is the first time performance of PEG-PECH synthesis with TMG and these observation indicates the broad applicability of TMG for the polymerization of various epoxides.

116

Next, we tried to prepare PEG-PGB block copolymer in one-pot reaction with TMG (**Scheme 3**). To the 2-methoxyethanol, EO was added at 273 equivalent aiming to produce PEG with the molecular weight of 12,000 Da before the activation of initiator by TMG. After 48 h reaction, the reaction solution was dried under the reduced pressure before the addition of 1, 2-epoxy-5-hexene at 100 equivalent and the activation of hydroxyl groups in crude PEG by TMG. After 48 h reaction, the ether precipitation was performed to obtain PEG-PGB as powder. The residual ether in polymer was removed by dry under the reduced pressure. By ^{1}H-NMR and GPC measurement, no elongation of PGB segments was confirmed, indicating the activation of alcohol initiators was not sufficient to react with 1, 2-epoxy-5-hexene as epoxides with relatively high steric hindrance because of long side chains. Therefore, instead of mild TMG, we hypothesized we can proceed the polymerization of 1, 2-epoxy-5-hexene with relatively strong organo metal catalyst, triisobutylalminum (**Scheme 4**). To the crude PEG polymer, 1, 2-epoxy-5-hexene was added at 100 equivalent and the activation of alcohol groups in PEG was performed by the addition of triisobutylaluminum. After 48 h reaction, the ether precipitation was performed by adding the reaction solution to the excess amount of ether before drying *in vacuo*. By ^{1}H-NMR and GPC measurement, the degree of polymerization was calculated to be 94 and the narrow molecular weight distribution was confirmed (**Figure 4 and 5**), indicating initiator was activated by TMG to react with 1, 2-epoxy-5-hexene to synthesize PEG-PGB with relatively high yield. This is the first time performance of PEG-PGB synthesis with triisobutylaluminum and these observation suggests careful selection of catalyst based on the chemical structure of monomers is important to prepare block copolymers with epoxides.
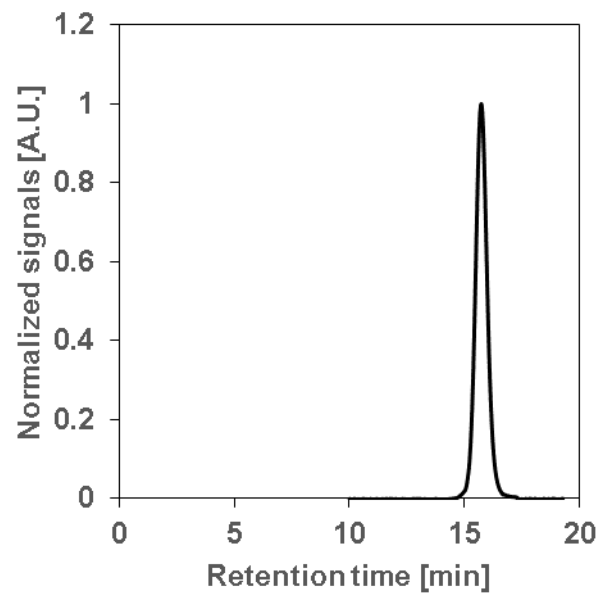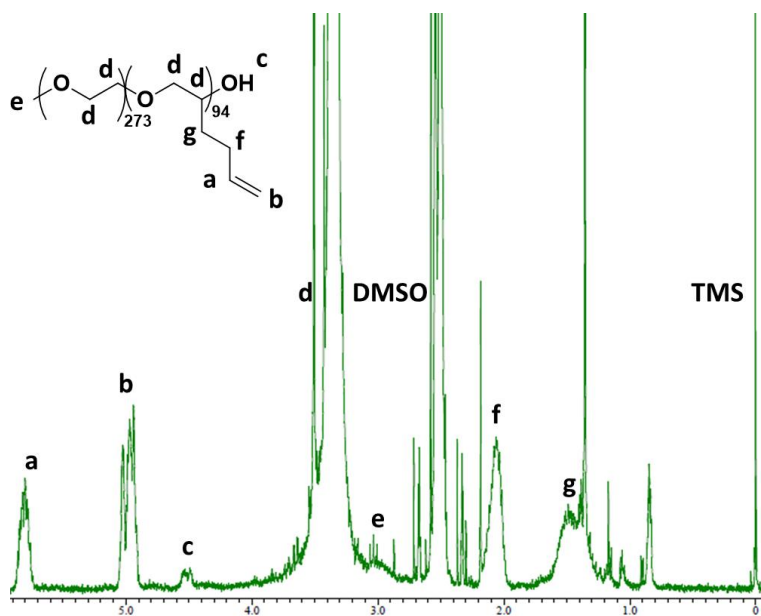
Figure 3. *GPC chromtogrum of PEG-PECH.*

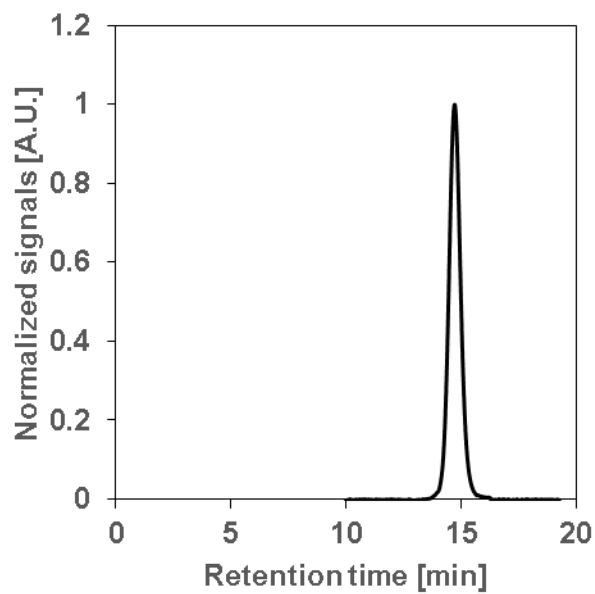***Figure 4.*** *¹H-NMR spectrum of PEG-PGB.*

Figure 5. *GPC chromatogram of PEG-PGB.*

Then, we examined the applicability of TMG on NCA polymerization. In this time, we tried to elongate PBLG and PLL-TFA chains by TMG. We tried to prepare PBLG segments by addition of BLG-NCA and TMG to the crude PEG polymer in one-pot manner (**Scheme 5**). To the 2-methoxyethanol, EO was added at 273 equivalent aiming to produce PEG with the molecular weight of 12,000 Da before the activation of initiator by TMG. After 48 h reaction, the reaction solution was dried under the reduced pressure before the addition of BLG-NCA at 50 equivalent to produce PEG-PBLG with 40 units of PBLG, and the activation of hydroxyl groups in crude PEG by TMG. After 48 h reaction, the ether precipitation was performed to obtain PEG-PBLG as powder. The residual ether in polymer was removed by dry under the reduced pressure. By ^{1}H-NMR and GPC measurement, the degree of polymerization was calculated to be 40 and the narrow molecular weight distribution was confirmed (**Figure 6 and 7**), indicating initiator was activated by TMG to react with BLG-NCA to synthesize PEG-PBLG with comparable yield with

conventional method. This is the first time performance of PEG-PBLG synthesis in one-pot reaction using TMG and these observation suggests TMG has high potential as catalyst to prepare the various block copolymers with epoxides and NCAs.
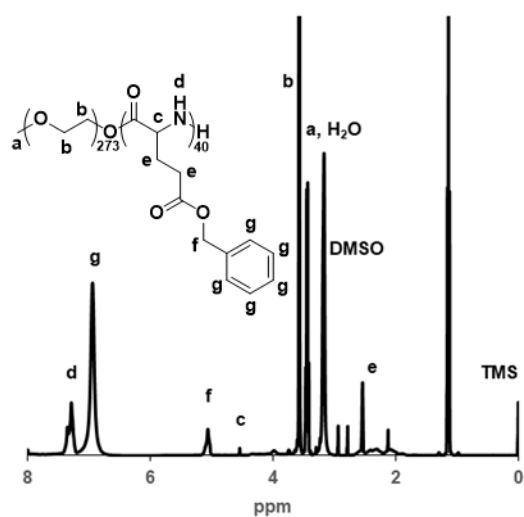

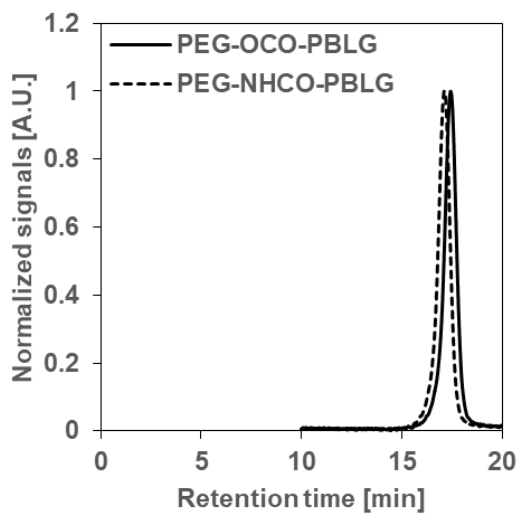**Figure 6.** *^{1}H-NMR spectrum of PEG-PBLG.*

Figure 7. *GPC chromatogram of PEG-PBLG.*

Next, we tried to prepare PEG-PLL-TFA in one-pot reaction using TMG (**Scheme 6**). To the 2-methoxyethanol, EO was added at 273 equivalent aiming to produce PEG with the molecular weight of 12,000 Da before the activation of initiator by TMG. After 48 h reaction, the reaction solution was dried under the reduced pressure before the addition of BLG-NCA at 100 equivalent to produce PEG-PLL-TFA with 80 units of PBLG, and the activation of hydroxyl groups in crude PEG by TMG. After 48 h reaction, the ether precipitation was performed to obtain PEG-PBLG as powder. The residual ether in polymer was removed by dry under the reduced pressure. By ^{1}H-NMR and GPC measurement, the degree of polymerization was calculated to be 81 and the narrow molecular weight distribution was confirmed (**Figure 8 and 9**), indicating initiator was activated by TMG to react with Lys-TFA-NCA to synthesize PEG-PLL-TFA with comparable yield with conventional method. This is the first time performance of PEG-PLL-TFA synthesis in one-pot reaction using TMG and these observation suggests TMG can activate several kinds of amino acid-NCA to prepare wide range of PEG-PAA by one-pot manner. Note that to prepare PEG-PGlu for platinum-based anticancer drug encapsulated polymeric micelle preparation and PEG-PLL for nucleic acid loaded polyion complex micelles, the deprotection of BLG and TFA groups are necessary and the potential problem is to cleave the ester bonds between PEG and PAA segments by strong base treatment. However, we can utilize the hydrogen reduction reaction for BLG deprotection and piperidine for TFA deprotection and we can achieve the orthogonal chemistry with these reactions to prepare block copolymers with no side reaction.
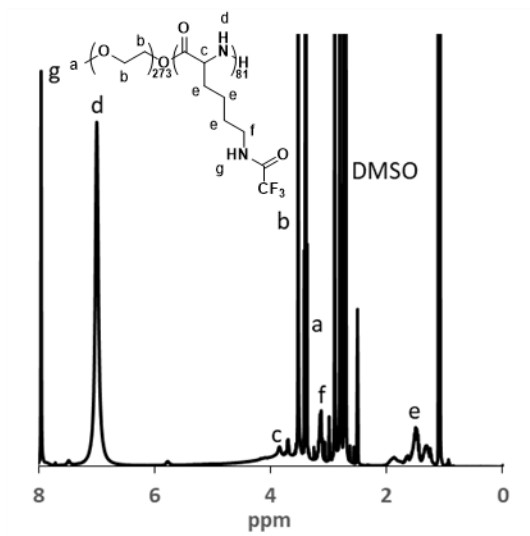
Figure 8. ^{1}H-NMR spectrum of PEG-PLL(TFA).
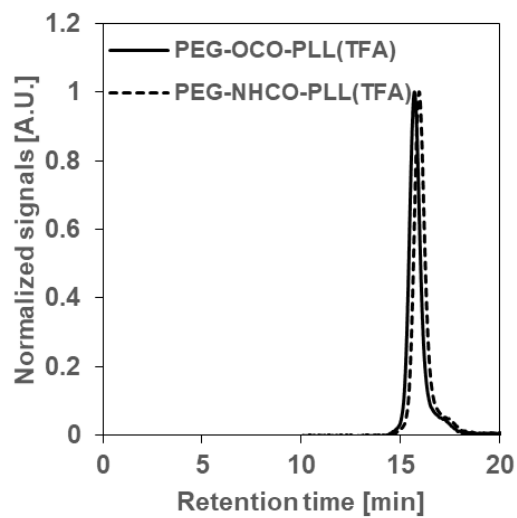
Figure 9. GPC chromatogram of PEG-PLL(TFA).

These observations motivated us to investigate the kinetics of ROP of EO and NCA. First, we compared the kinetics of EO polymerization using TMG with that of EO polymerization using potassium naphthalene, which is the gold standard for PEG synthesis [16]. During the polymerization, the elongation of PEG chain was monitored by ^{1}H-NMR. The reaction rate of EO polymerization with TMG (k_{obs} = 7.1 h^{-1}) was comparable with that of EO polymerization with potassium naphthalene (k_{obs} = 9.5 h^{-1}) (**Figure 10**), indicating that TMG can activate the hydroxyl groups in initiators as efficient as potassium naphthalene. Regarding the formation of radicals by potassium naphthalene [17], TMG as mild catalyst is promising catalyst to elongate the NCA without unfavourable side reactions, or degradation of NCA to induce the formation of homo polymers without PEG segments.
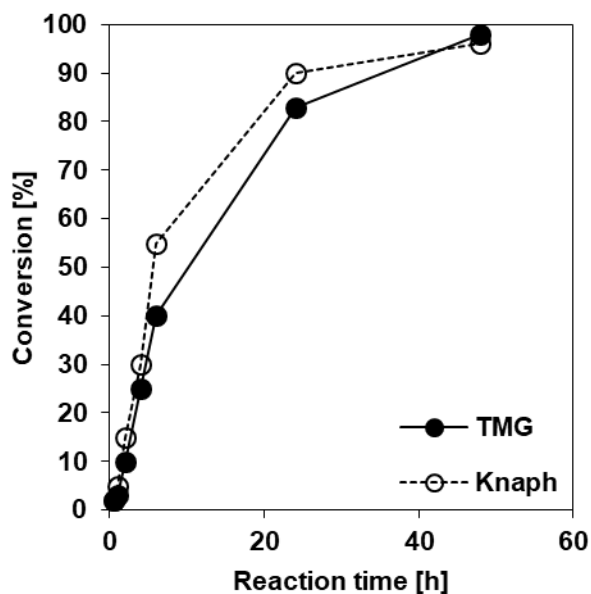
Figure 10. *The kinetics of EO polymerization.*

Next, we investigated the effect of TMG on the kinetics of NCA polymerization, in this case, polymerization of BLG-NCA. We performed the NCA polymerization with PEG-OH macroinitiators to elongate PBLG chains in the presence of TMG and compared the reaction rate with conventional method where PEG-NH$_2$ macroinitiators were adapted to polymerize BLG-NCA without catalyst. During the NCA polymerization, the elongation of PBLG chain was monitored by ^{1}H-NMR. The reaction rate of NCA polymerization using TMG (k_{obs} = 8.6 h^{-1}) was higher than that of NCA polymerization with conventional method (k_{obs} = 6.2 h^{-1}) (**Figure 11**), indicating alcohol initiators were activated efficiently to proceed rapid initiation reaction for PBLG elongation. However, there is a possibility to activate NCA by TMG so we also performed NCA polymerization with PEG-NH$_2$ macroinitiators using TMG. The reaction rate of NCA polymerization in the presence of TMG (k_{obs} = 7.7 h^{-1}) was faster than that of NCA polymerization with no TMG (k_{obs} = 6.2 h^{-1}) (**Figure 11**), indicating TMG can promote the NCA polymerization by activating not only initiators but NCA to increase the polarity of hydroxyl groups and carbonyl groups to promote the initiation reaction and the propagation reaction.
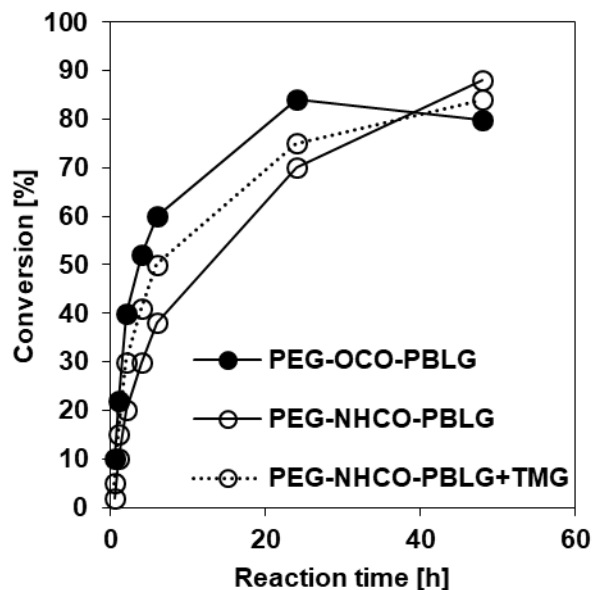
Figure 11. The kinetics of NCA polymerization.

Obtained block copolymers have degradable ester bonds between PEG and PAA segments. Therefore, we investigate the hydrolysis of ester bonds in physiological conditions. We dissolved PEG-OCO-PBLG in DMF before the addition of PBS solution before the incubation at 37°C. Then, extraction with excess amount of water was performed to check the amount of detached PEG from block copolymers by GPC measurement. Though PEG-NHCO-PBLG prepared by conventional method showed no detachment of PEG in physiological environment, PEG-OCO-PBLG showed detachment of PEG in physiological conditions (**Figure 12**), indicating the ester bonds between PEG and PBLG segments were degraded by hydrolysis to be PEG and Homo-PBLG. This observation is important in terms of biocompatibility of block copolymers and by detachment of PEG segments from block copolymers, the hydrodynamic diameter of block copolymers would decrease to promote renal clearance [17].
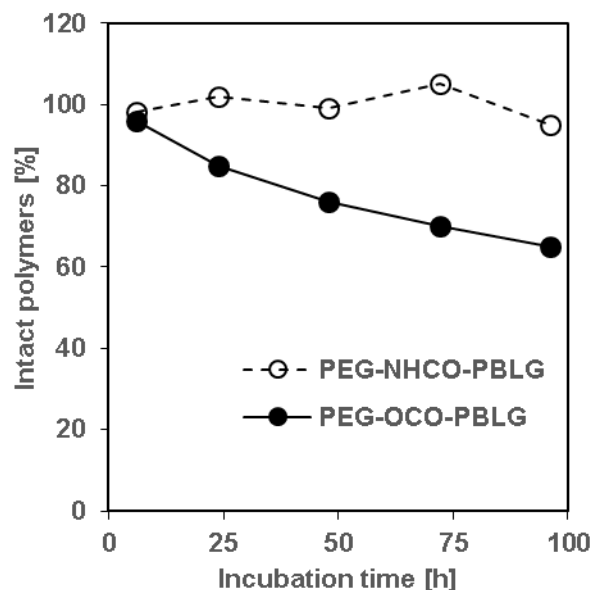
Figure 12. *The kinetics of the hydration of ester bonds in PEG-PBLG.*

This detachment of PEG is related to decrease of the accelerated blood clearance (ABC) phenomena, which is accelerated clearance of PEGylated bioactive agents [18]. In the case of PEGylated therapeutic agents, immune cells recognize the linkage between PEG and agents as exogenous substances to produce antibodies for activation of immune systems. By detaching the PEG in physiological conditions, PEG-OCO-PAA could increase its biocompatibility by decreasing the linkage of PEG and PAA segments not to get recognition by immune cells. Instead of block copolymers with stable amide bonds, new block copolymers can be building block of polymeric micelles with higher biocompatibility than existing PEGylated liposome, which can induce immune response by not only lipid compartments but also the linkage of PEG and lipid segments after second time injections [19, 20].

PEG detachment from block copolymers is important for also enhanced cellular uptake, which is hampered by PEG dilemma [21]. For prolonged bioavailability, PEGylation is a candidate

126

to protect nanomedicine by decreasing the protein absorption not to induce immune responses. However, by PEGylation itself, increased hydrophilicity on the surface of nanomedicine adversely decrease the efficacy of cellular uptake of targeted cells. By detaching PEG segments to decrease the density of PEG on the surface of nanomedicine, new PEG-OCO-PAA block copolyemrs could enhance the cellular uptake of build nanomedicine. Note that in physiological conditions, not only water but also esterase in macrophages could promote the PEG detachment to promote the functionalization of PEGylated nanomedicine.

With well-synthesized block copolymers, we investigate the utility on the construction of supramolecular architectures, in this case, polymeric micelles. We dissolved PEG-OCO-PBLG in methanol before the evaporation to prepare the thin film to form the aggregation in PBS, followed by sonication to compart it to polymeric micelles. By DLS measurement, the size of 83 nm and the sharp size distribution of PEG-OCO-PBLG micelles (**Figure 13a**), which was comparable with the micelles prepared from PEG-NHCO-PBLG, indicating the ester bonds between PEG and PBLG segments had no effect on the complexation to form polymeric micelles. Next, we investigated the stability of this micelles in physiological conditions by incubating in PBS for 3 days. No change in size and size distribution was observed in both formulations, indicating the ester bonds had no impact on the stability of micelles (**Figure 13b**). This observation indicated the PEG shell is rigid enough to keep its spherical morphology though the PEG is detachable in physiological conditions.
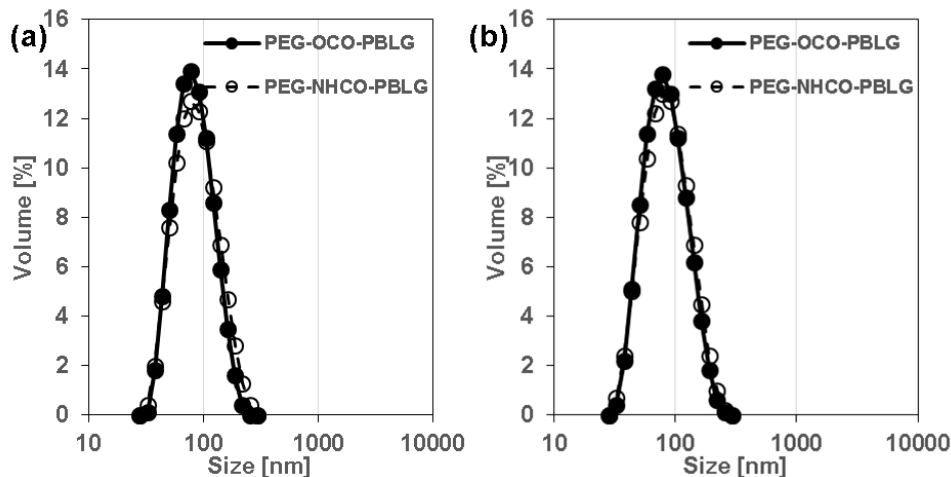
Figure 13. *Size distribution of polymeric micelles prepared by PEG-PBLG.*

(a) no incubation (b) 3 days incubation in 10 mM phosphate buffer (pH 7.4).

The advantage of novel PEG-PAA has been investigated in clinical trials [5, 23]. In the case of PEG-PBLG micelles, previous paper performed the encapsulation of MG132, which is protease inhibitor to promote the cell death, indicating with our new finding, we can construct the therapeutic agent-loaded polymeric micelles with various advantages, including efficient polymer synthesis, enhanced cellular uptake and reduced unfavorable secretion by ABC phenomenon.

Next, we examined the utility of prepared micelles in vivo harsh environments. To investigate the effect of ester bonds between PEG and PAA segments, we administrated PEG-OCO-PBLG micelles by intravenous injection to check its bioavailability in mice. The blood circulation profile of PEG-OCO-PBLG micelles was similar as that of PEG-NHCO-PBLG micelles (**Figure 14A and 14B**), indicating ester bonds between 2 segments had no effect on the bioavailability of prepared micelles. Note that this observation has good agreement with previous

reports [24] and we concluded we could functionalize polymeric micelles without unfavorable side effects, in this case, short blood circulation time *in vivo*.

Then, we finally observed the biodistribution of PEG-OCO-PBLG micelles in various organs, including heart, muscle, kidney, liver and spleen. We injected PEG-OCO-PBLG micelles intravenously to allow it circulate for 24 h. Mice were sacrificed to stain cell nucleus by Hoechst and check the fluorescence derived from polymer was detected by microscopy. The biodistribution of PEG-OCO-PBLG was comparable with that of PEG-NHCO-PBLG (**Figure 14C**), indicating the installation of ester bonds between PEG and PAA segments had no impact on the biodistribution of prepared micelles. Note that this result was comparable with also previous formulation with a diameter of 80 nm [25]. This observation also confirmed the high potential of our technology to functionalize polymeric micelles.
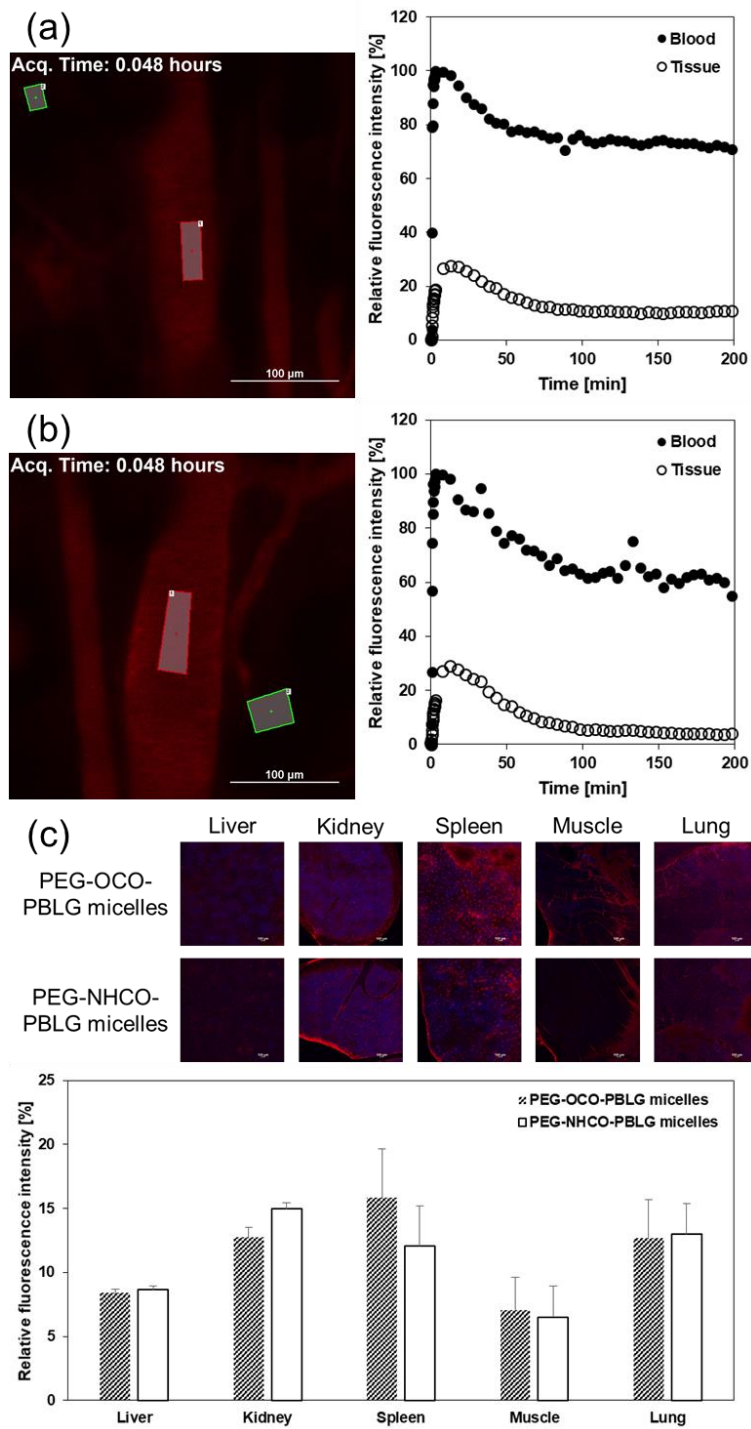
Figure 14. *Blood circulation and biodistribution of PEG-PBLG micelles in mice.*

5.4. Conclusion

We have developed a new method to polymerize PEG-polyether and PEG-PAA in one-pot reaction using TMG. Synthesized polymers showed controlled DP and sharp molecular weight distribution. Obtained PEG-PAA had ester bonds between PEG and PAA segments and it showed slow degradation in physiological conditions, which could be promoted by enzymes *in vivo* conditions. After complexation into polymeric micelles they showed comparable size with previous formulation with no ester bonds prepared from PEG-PAA with conventional method, and high stability in physiological conditions though it has an ability for degradation after decomposion, which could promote kidney secretion. Prepared polymeric micelles showed comparable bioavailability and biodistribution with conventional formulations, indicating without unfavorable side effects, we can functionalize the polymeric micelles. Our findings have an impact on polymer chemistry, biology and medicine to prepare the block copolymers by good manufacturing product (GMP) grade and to enhance the therapeutic outcome by encapsulating therapeutic agents to the core of polymeric micelles for medical applications.

5.5. References

[1] H- C. Kim, S- M. Park and W. D. Hinsburg, Block copolymer based nanostructures: materials, processes and applications to exectronics. *Chem. Rev.* **110** (2010) 146-177.

[2] K. Kataoka, A. Harada and Y. Nagasaki, Block copolymer micelles for drug delivery: design, characterization and biological significance *Adv. Drug Deliv. Rev.* **64** (2012) 37-48.

[3] H. Cabral, K. Miyata, K. Osada and K. Kataoka, Block copolymer micelles in nanomedicine applications. *Chem. Rev.* **118** (2018) 6844-6892.

[4] K. Letchford and H. Burt, A review of the formation and classification of amphiphilic block copolymer nnopticulate structures: micelles, nanospheres, nanocapsules and polymersomes. *Eur. J. Pharm. Biopharm.* **65** (2007) 259-269.

[5] H. Cabral and K. Kataoka, Progress of drug-loaded polymeric micelles into clinical studies. *J. Control. Release* **190** (2014) 465-476.

[6] S. Katayose and K. Kataoka, Water-soluble polyion complex associates of DNA and poly(ethylene glycol)-poly(L-lysine) block copolymer. *Bioconjugate Chem.* **8** (1997) 702-707.

[7] J. DeRouchey, C. Schmidt, G. F. Walker, C. Koch, C. Plank, E. Wagner and J. O. Radler, Monomolecular assembly of siRNA and poly(ethylene glycol)-peptide copolymers. *Biomacromolecules* **9** (2008) 724-732.

[8] M. Yuan and X. Deng, Synthesis and characterization of poly(ethylene glycol)-block-poly(amino acid) copolymer. *Eur. Polym. J.* **37** (2001) 1907-1912.

[9] Y. Xia and J. Zhao, Macromolecular architectures based on organocatalytic ring-opening. *Polymer* **143** (2018) 343-361.

[10] H. R. Kricheldorf, *α-Aminoacid-N-Carboxyanhydrides and Related Heterocycles*; Springer-Verlag: Germany, 1987.

[11] B. A. Chan, S. Xuan, M. Horton and D. Zhang, 1, 1, 3, 3-tetramethylguanidine-promoted ring-opening polymerization of N-butyl N-carboxyanhydride using alcohol initiators. *Macromolecules* **49** (2016) 2002-2012.

[12] Scott, N. D.; Walker, J. F.; Hansley, V. L. Sodium Naphthalene. I. A New Method for the Preparation of Addition Compounds of Alkali Metals and Polycyclic Aromatic Hydrocarbons. *J. Am. Chem. Soc.* **1936**, *58*, 2442-2444.

[13] Nishiyama, N.; Okazaki, S.; Cabral, H.; Miyamoto, M.; Kato, Y.; Sugiyama, Y.; Nishio, K.; Matsumura, Y.; Kataoka, K. Novel Cisplatin-Incorporated Polymeric Micelles Can Eradicate Solid Tumors in Mice. *Cancer Res.* **2003**, *63*, 8977-8983.

[14] Kataoka, K.; Togawa, H.; Harada, A.; Yasugi, K.; Matsumoto, T.; Katayose, S. Spotaneous Formation of Polyion Complex Micelles with Narrow Distribution from Antisense Oligonucleotide and Cationic Block Copolymer in Physiological Saline. *Macromolecules* **1996**, *29*, 8556-8557.

[15] Matsumoto, Y.; Nomoto, T.; Cabral, H.; Matsumoto, Y.; Watanabe, S.; Christie, R. J.; Miyata, K.; Oba, M.; Ogura, T.; Yamasaki, Y.; Nishiyama, N.; Yamasoba, T.; Kataoka, K.; Direct and Instantaneous Observation of Intravenously Injected Substances Using Intravital Conforcal Micro-Videography. *Biomed. Opt, Express* **2010**, *1* 1209-1216.

[16] Yokoyama, M.; Inoue, S.; Kataoka, K.; Yui, N.; Okano, T.; Sakurai, Y. Molecular Design for Missile Drug: Synthesis of Adriamycin Conjugated with Immunoglobulin G Using Poly(Ethylene Glycol)-Block-Poly(Aspartic Acid) as Intermediate Carrier. *Macromol. Chem.* **1989**, *190*, 2041-2054.

[17] T. Yamasoba, Y. Tanaka and Y. Ikeda, Distribution and tissue uptake of poly(ethylene glycol) with different molecular weights after intravenous administration to mice. *J. Pharm. Sci.* **83** (1994) 601-606.

[18] A. S. A. Lia, H. Kiwada and T. Ishida, The accelerated blood clearance (ABC) phenomenon: clinical challenge and approaches to manage. *J. Control. Release* **172** (2013) 38-47.

[19] H. Xu, K. Q. Wang, Y. H. Deng and D. W. Chen, Effects of cleavavle PEG-cholesterol derivatives on the accelerated blood clearance of PEGylated liposomes. *Biomaterials* **31** (2010 4753-4763.

[20] D. Chen, W. Liu, Y. Shen, H. Mu, Y. Zhang, R. Liang, A. Wang, K. Sun and F. Fu, Effects of a novel pH-sensitive liposome with cleavable esterase-catalyzed and pH-responsive double smart mPEG lipid derivative on ABC phenomenon. *Int. J. Nanomedicine* **6** (2011) 2053-2061.

[21] H. Hatakeyama, H. Akita and H. Harashima, The polyethyleneglycol dilemma: advantage and disadvantage of PEGylation of liposomes for systemic genes and nucleic acids delivery to tumors. *Biol. Pharm. Bull.* **36** (2013) 892-899.

[22] Y. Matsumoto, Y. Miyamoto, H. Cabral, Y. Matsumoto, K. Nagasaka, S. Nakagawa, T. Yano, D. Maeda, K. Oba, K. Kawana, N. Nishiyama, K. Kataoka and T. Fujii, Enhanced efficacy against cervical carcinomas through polymeric micelles physically incorporating the proteasome inhibitor MG132. Cancer Science 107 (2016) 773-781.

[23] H. Cabral, K. Miyata, K. Osada and K. Kataoka, Block copolymer micelles in nanomedicine applications. *Chem. Rev.* **118** (2018) 6844-6892.

[24] Quader, S.; Cabral, H.; Mochida, Y.; Ishii, T.; Liu, X.; Toh, K.; Kinoh, H.; Miura, Y.; Nishiyama, N.; Kataoka, K. Selective Intracellular Delivery of Proteasome Inhibitors through pH-Sensitive Polymeric Micelles directed to Efficient Antitumot Therapy. *J. Control. Release* **2014**, *188*, 67-77.

[25] Cabral, H.; Matsumoto, Y.; Mizuno, K.; Chen, Q.; Murakami, M.; Kimura, Y.; Terada, Y.; Kano, M. R.; Miyazono, K.; Uesaka, M.; Nishiyama, N.; Kataoka, K. Accumulation of sub-100 nm Polymeric Micelles in Poorly Permeable Tumors Depends on Size. *Nat. Nanotech.* **2011**, *6*, 815-823.

Chapter6

Conclusion and future perspectives

6.1. Conclusion and future perspectives

In this dissertation, we developed novel mRNA delivery systems based on PIC micelles with controlled rigidity of the backbone of the polycation segment by using a block copolymers consisting of poly(ethylene glycol) and the flexible block ionomers with poly(ether) backbones, which were synthesized by efficient one-pot reactions with optimized catalyst. These new formulations were compared to mRNA-loaded micelles prepared from the relatively more rigid block ionomer PEG-poly(L-lysine) (PEG-PLL). Moreover, for developing a safe and effective carrier for *in vivo* application, we prepared flexible block ionomers conjugating a set of amino acids based on the interaction between protein and oligonucleotides determined by bioinformatics. These amino acids were conjugated to a flexible segment poly(glycerol) *via* ester bonds, which can be gradually hydrolyzed to reduce the cytotoxicity. Furthermore, an active targeted system using phosphocoline (PC) as the ligand moiety, which is directed to the phospholipid transfer protein (PLTP) overexpressed in various kinds of cancer, *e.g.* pancreatic cancer, was developed for enhancing the intracellular delivery and the mRNA translation.

First, we report a new synthesis route for PEG-poly(amino acids) (PEG-PAAs), including PEG-poly(γ-benzyl-L-glutamate) (PEG-PBLG) and PEG-poly(ε-tetrafluoroaceticacids-L-lysine) (PEG-PLL-TFA), by doing one-pot polymerization of epoxides and N-carboxyanhydride (NCA) of the specific amino acids by using 1,1,3,3-tetramethylguanidine (TMG) as the catalyst. This catalyst proceeded the polymerization of both ethylene oxide and NCAs to show comparable molecular weight distribution to conventional NCA polymerization initiated with PEG macroinitiators. TMG also promoted faster polymerization kinetics than the conventional NCA polymerization. Besides, the obtained PEG-PAAs present an ester bond between the PEG and PAA segment that can be hydrolyzed in physiological conditions for improving the

biocompatibility. The ester bond did not affect the preparation of polymeric micelles based on the new PEG-PAAs, nor their stability in physiological conditions. Moreover, TMG catalyzed the co-polymerization of a different epoxy monomer, epichlorohydrin, to obtain flexible PEG-poly(epichlorohydrin) (PEG-PECH) with sharp molecular weight distribution. However, in the case of the precursor of the flexible poly(glycidyl butylamine) segment (PEG-PGBA), more reactive catalyst triisobutylalminum was adapted to polymerize the epoxy monomer, 1,2-epoxy-5-hexene. These results indicate that the careful selection of catalyst based on the reactivity was important to polymerize epoxides and NCAs without unfavorable side reactions.

Second, with the flexible poly(ether)-based block copolymers synthesized by one-pot reactions, we prepared block ionomers having primary amines to self-assemble mRNA-loaded PIC micelles. The micelles prepared from PEG-PGBA were approximately 50 nm in diameter, which is comparable to the size of the PEG-PLL formulation. Isothermal calorimetry (ITC) measurements clarified the loss of enthalpy and the gain of entropy in the case of PEG-PGBA formulations, indicating that the flexible PGBA chains decreased the contact area between block ionomers and nucleic acids and increased the release of free water during ionic pair formation to increase the free energy of the formulated PIC micelles. This high stability resulted in better protection of encapsulated mRNA against both polyanion exchange and enzymatic degradation to show high gene expression in cultured cells. These *in vitro* observations were correlated with the high gene expression in the lungs, as well as with the prolonged blood circulation time of intact mRNA in mice. These results indicated that the flexible polycation segment can enhance the stability of mRNA for *in vivo* applications.

Third, we synthesized hydrolysable polymers by conjugating functional amino acids *via* ester bonds. In this case, we used leucine with hydrophobic isobutyl groups, tryptophan with indole

groups and tyrosine with phenolic alcohols, which interact with bases in mRNA, based on the informatics of protein-nucleic acids interactions. The polymers showed the relatively rapid degradation of the ester bonds to reduce the number of primary amine in the block ionomers, resulting in low cytotoxicity against cultured cells. After preparing mRNA-loaded PIC micelles with these degradable block ionomers, the stability against polyanion exchange and enzymatic degradation were examined. All formulations showed better protection than PIC micelles prepared by control block ionomers, in this case, glycine-conjugated polymers. This enhanced stability resulted in high gene expression both *in vitro* and *in vivo* after pulmonary administration. For systemic delivery of mRNA, the bioavailability of mRNA-loaded PIC micelles in mice was investigated. Accordingly, the micelles prepared with the polymers having tryptophan moieties show the longest blood circulation. These results indicated that introducing bio-inspired ligands promoting the interaction with nucleic acids improved the stability of the PIC and biological performance of the micelles.

Finally, we functionalized the surface of PIC micelles with PC ligands for improving the cellular uptake of the micelles. To investigate the effect of ligands on the uptake by cancer cells, we prepared empty PIC micelles with irreversibly crosslinked core for stabilization in *in vitro* conditions. The PC-installed micelles showed comparable size (50 nm) with PIC micelles having no ligands. In cultured pancreatic cancer BxPC3 cells, PC micelles showed faster uptake than the control micelles without ligand. By doing a competition experiment with free PC molecules, we clarified that the PC molecules on the surface of PIC micelles promoted the cellular uptake, as free PC inhibited the cellular uptake of the PC-installed micelles. Moreover, an inhibition assay was conducted to check the interaction between PC micelles and PLTP by using the PLTP inhibitor thimersal. Thus, thimersal inhibited the uptake of PC, demonstrating that PLTP mediated the

uptake of PC micelles in the pancreatic cancer cells. After the installation of PC ligands on the mRNA-loaded PIC micelles prepared by tryptophan-conjugated polymers, the gene expression was examined *in vitro*. The PC-installed mRNA-loaded micelles showed higher gene expression than the micelles without ligands. These results indicate that the ligand/receptor pair of PC and PLTP is a promising target for enhancing the delivery against intractable pancreatic tumors, which can promote the internalization of several formulations, including our novel mRNA-loaded PIC micelles.

In summary, novel PIC micelles stably encapsulating mRNA were developed by engineering block ionomers with flexible poly(ether) backbone, which were prepared by one-pot polymerizations in the presence of catalyst. These micelles showed high resistant to degradation by nucleases and polyanions, which lead to enhanced *in vitro* translation, high gene expression in lungs and prolonged blood circulation in mice. Introducing amino acids, in this case leucine, tryptophan and tyrosine, to the poly(glycerol) backbone *via* ester bonds, further improved the stability against polyanions, significantly increasing the bioavailability. Also, in physiological conditions, leucine, tryptophan, tyrosine and glycine-bearing polymers were degraded to safe poly(glycerol) and amino acids. Moreover, PC was identified as a ligand molecule to promote cellular uptake, and by functionalizing micelles with PC ligands, the gene expression was augmented in cultured cells. In the future, we will investigate the possibility of our novel flexible block ionomers to encapsulate different type of nucleic acids, including small interfering RNA (siRNA) and the set of guide RNA and mRNA encoding Cas9 protein for genome editing. Moreover, to further functionalize the mRNA-loaded PIC micelles, we will conjugate more amino acids, including cysteine, histidine and other synthetic amino acids with various functionalities to construct polypeptide pendants in the side chain of poly(ether) segments. It is also worth noting

that this polymer could also be used for synthesizing polypeptides in liquid phase by cutting the degradable ester bonds between polymer backbone and polypeptides. In addition, the accumulation in tumors and the gene expression of PC-installed micelles with mRNA will be investigated to check the capability of our system for *in vivo* applications.

These findings will have great significance not only for the delivery of nucleic acids and other drugs by using novel poly(ether) polymers, but also for several materials and bioengineering applications. For example, the one-pot synthesis strategy developed in this work fits the good manufacturing practice (GMP) for PEG-PAAs, such as PEG-poly(glutamate), which is the building block of polymeric micelles under the clinical trials. Moreover, the effect of flexibility of ionizable segments on the high stability of complex may be extrapolated to lipidic materials toward the development of novel LNPs for siRNA and mRNA delivery. In addition, the possibility to use hydrophilic PC ligands with betain structure not only for nanomedicine delivery, but also for modifying low and middle molecular compounds for enhancing their selectivity. We expect that the systems developed in this thesis will make significant impact in various research and industry fields, including chemistry, biology and medicine.

6.2. Achievements

Original Articles

1. M. Suhara, Y. Miura, H. Cabral, D. Akagi, Y. Anraku, A. Kishimura, M. Sano, T. Miyazaki, N. Nakamura, A. Nishiyama, K. Kataoka, H. Koyama and K. Hoshina, Targeting ability of self-assembled nanomedicines in rat acute limb ischemia model is affected by size. *J. Control. Release* 286 (2018) 394-401.

2. K. Suzuki, Y. Miura, Y. Mochida, T. Miyazaki, K. Toh, Y. Anraku, V. Melo, X. Liu, T. Ishii, O. Nagano, H. Saya, H. Cabral, K. Kataoka, Glucose transporter 1-mediated vascular transportation of nanomedicines enhances accumulation and efficacy in solid tumors. *J. Control. Release under revision*.

3. T. Miyazaki, K. Igarashi, Y. Matsumoto, H. Cabral, One-pot synthesis of PEG-poly(amino acid) copolymers with PEG-detachable functionality. *ACS Biomater. Sci. Eng. in press*.

4. T. Miyazaki, S. Uchida, S. Fukushima, S. Nagatoishi, K. Tsumoto, K. Kataoka, H. Cabral, Flexible polyether segments in block ionomers enhanced in vivo transfection of mRNA by polymeric micelles. *in preparation*.

Proceedings

International conferences

1. T. Miyazaki, S. Uchida and H. Cabral. CRS Annual Meeting, New York, USA, July 2018 (oral and poster presentation)

2. T. Miyazaki, S. Uchida and H. Cabral. Biomaterials International 2018. Tokyo, Japan, July 2018. (poster presentation)

Domestic conferences

1. T. Miyazaki, S. Uchida and H. Cabral. 67th SPSJ Annual Meeting. Nagoya, Japan, May 2018. (oral presentation)

2. T. Miyazaki, S. Uchida and H. Cabral. 34th DDS Annual Meeting. Nagasaki, Japan, June 2018. (oral presentation)

3. T. Miyazaki, S. Uchida and H. Cabral. 1st KKLab Annual Meeting. Kanagawa, Japan, October 2017. (poster presentation)

4. G. Huang, T. Miyazaki and H. Cabral. 1st KKLab Annual Meeting. Kanagawa, Japan, October 2017. (poster presentation)

5. K. Koji, T. Miyazaki, Y. Mochida, L. Hespel, K. Toh, S. Fukushima, Y. Matsumoto, A. Matsumoto, H. Cabral and K. Kataoka. 34th DDS Annual Meeting. Nagasaki, Japan, June 2018. (poster presentation)

6. T. Miyazaki, K. Igarashi, Y. Matsumoto, K. Kataoka, H. Cabral. 1st Glowing Polymer Symposium-KANTO. Tokyo, Japan, December 2018. (oral presentation)

7. Y. Tachihara, T. Miyazaki, K. Kataoka, H. Cabral. 1st Glowing Polymer Symposium-KANTO. Tokyo, Japan, December 2018. (oral presentation)

8. G. Huang, T. Miyazaki, H. Cabral. 1st Glowing Polymer Symposium-KANTO. Tokyo, Japan, December 2018. (oral presentation)

9. T. Miyazaki, S. Uchida, H. Cabral. 2nd KKLab Annual Meeting. Tokyo, Japan, November 2018. (poster presentation)

10. Y. Tachihara, T. Miyazaki, K. Kataoka, H. Cabral. 2nd KKLab Annual Meeting. Tokyo, Japan, November 2018. (poster presentation)

Patent

1. H. Cabral, <u>T. Miyazaki</u> and S. Uchida. 生体内でのメッセンジャーRNA(mRNA)の輸送担体の安定性を向上させるためのポリマー設計. PCT/JP2018/016798.

2. H. Cabral, K. Kataoka, L. Hespel, <u>T. Miyazaki</u>, K. Koji, G. Huang, A. Matsumoto, Y. Mochida and K. Toh. pH およびグルコースに応答して PEG が脱離する高分子ミセルの構築. PCT/JP2018/001089

3. H. Cabral and <u>T. Miyazaki</u>. ミトコンドリアを指向するホスホコリンリガンドの開発. JP2018/229599.

4. H. Cabral, <u>T. Miyazaki</u>, G. Huang, A. Tao and Y. Tachihara. ホストゲスト相互作用を介した環状薬物の送達. JP2018/229598

5. H. Cabral, G. Huang and <u>T. Miyazaki</u>. がん免疫療法に向けたインドールアミン-2,3-ジオキゲナーゼ(IDO)を阻害するブロック共重合体および高分子ミセルの開発. JP2018/229602.

6. <u>T. Miyazaki</u> and H. Cabral. One-pot synthesis of PEG-poly(amino acid) copolymers with PEG-detachable functionality. PCT2019/13B18Y002-1